RDFZ SCIENCE JOURNAL

Volume 1 , 2025

Editorial Board

Tailai Cong (丛泰来)

Editor

Email: tailai.cong.ai@outlook.com

Runbo Li (李润博)

Editor

Email: runbo.li.rdfz@gmail.com

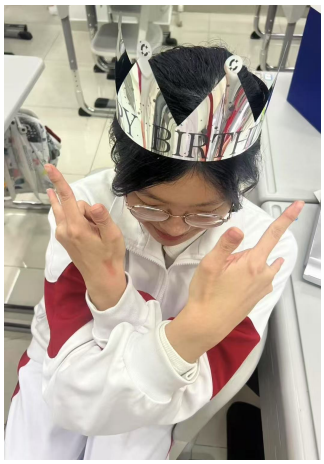

Yijing Wang (王奕静)

Editor

Email: 2022926409@qq.com

Yicheng Zhou (周奕成)

Editor

Email: monosarccharides0903@gmail.com

On anti-sociable numbers of special form

Tailai Cong (从泰来)

High School Affiliated to Renmin University of China, Beijing, China

Abstract

A positive integer n is called an anti-sociable number if there is no positive integer m such that $\sigma(n) = \sigma(m) = n + m$. By applying an elementary approach, we show that any number of the form p^k is an anti-sociable number, where p is a prime and $k \leq 32$ is a positive integer.

1 Introduction

Let n, m and k denote positive integers, p, q refer to primes, and $\sigma(n)$ means the sum of divisors of n. If there is no m such that $\sigma(n) = \sigma(m) = n + m$, n is an anti-sociable number. All prime numbers are anti-sociable numbers since $\sigma(p) = p + 1$. It is interesting to determine whether all prime powers p^k are anti-sociable numbers. In 2005, Le [2] considered the case $p = 2$ and proved that 2^k is anti-sociable for all k. When p is an odd prime, he also showed in 2006 [4] that p^k is anti-sociable for all even k, and in 2008 [3] that p^k is anti-sociable for all prime k. Hence, it only left the case when k is an odd composite number.

Recently, Jiang [1] first made a progress toward this case. She proved p^9 is anti-sociable for all p. In this paper, we further extend Jiang's method to larger k and prove the following.

Theorem 1.1. *Any number of the form p^k is an anti-sociable number, where p is a prime and $k \leq 32$ is a positive integer.*

2 Proof of Theorem 1.1

Before proving Theorem 1.1, we first state the following two lemmas which will help us calculate.

Lemma 2.1. *Let $q_1^{r_1} \cdots q_s^{r_s}$ is the unique-prime-factorization of n, then*

$$\sigma(n) = \prod_{1 \leq i \leq s} \frac{q_i^{r_i+1} - 1}{q_i - 1}.$$

Lemma 2.2. *[5]. For prime p, if $p \geq 2k^2$, then p^k is an anti-sociable number.*

By the discussions in [1]-[3], we only need to prove Theorem 1.1 with $k = 15, 21, 25, 27$. By Lemma 2.2, we only need to show that $\sigma(p^k) \neq \sigma(\sigma(p^k) - p^k)$ for all $p < 2k^2$. Let

$$A_{p,k} = \frac{p^{k+1} - 1}{p - 1}, \quad B_{p,k} = \prod_{\substack{\frac{p^{k+1}-1}{p-1} - p^k = q_1^{r_1} \cdots q_s^{r_s} \\ 1 \leq i \leq s}} \frac{q_i^{r_i+1} - 1}{q_i - 1},$$

where $q_1^{r_1} \cdots q_s^{r_s}$ is the unique-prime-factorization of $\frac{p^{k+1}-1}{p-1} - p^k$. By Lemma 2.1 we know that if $A_{p,k} \neq B_{p,k}$ for all $p < 2k^2$, then Theorem 1.1 holds.

For $k = 15, 21, 25, 27$, by a simple calculation we know that $A_{p,k}$ never equals to $B_{p,k}$ if $p < 2k^2$. One can find values of $A_{p,k}$ and $B_{p,k}$ on the appendix of this paper. Now Theorem 1.1 is valid when $k = 15, 21, 25, 27$. By [4], [3] and [1] we know that Theorem 1.1 is also valid when k is even, k is prime or $k = 9$. Combining the above cases, Theorem 1.1 is proved.

Appendix: Values of $A_{p,k}$ and $B_{p,k}$

$\boldsymbol{k = 15}$:

$\boldsymbol{p}$	$\boldsymbol{A_{p,k}}$	$\boldsymbol{B_{p,k}}$
2	65535	38912
3	21523360	8494444
5	38146972656	8765632512
7	5538821761600	1146781040640
11	4594972986357216	603218536439040
13	55451384098598320	5782021649858304
17	3041324492229179280	179486204158025072
19	16024522975978953760	1184572000639647744
23	278755018894590847680	14026560413024565760
29	8937374060012405313840	338725097139457380352
31	24247437391572842127616	1369998379251329937408
37	342708664283810176729840	16021963747285222293504
41	15939757728663263586608 16	48188073779291086147584
43	32527148983169546062456 00	10101924608656827317 4912
47	12325595054099071896078720	308296720033627976957952
53	74543635579202247026882160	1771561371992645128135680
59	37170995529442073106479088 0	7363090165816592712400896
61	61252823094395774386522321 6	17614816588337012293100544
67	24983478599430934075115636 80	59891645287861206825664512
71	59571089016624289732082924 16	11410564560442833931311513 6
73	90330261085806884866961504 80	16778459555404926106564934 4
79	29507937706360279997609626240	59374973078058577642124083 2
83	61863662182364192103394590240	80582556675650616408707072 0
89	17609922074066973221703781512 0	19997302359982795888824875 52
97	63984755569029760881456007912 0	99074255622750847262529945 60
101	11725786449236985205186256120 16	14428236720573341819140571 136
103	15732416069595956058216220009 60	23335587417712123999757402 112
107	27850601401560446013176291064 00	33566527623371893850559741 952
109	36762091491290711746509604952 80	53433390514668539942837157 888
113	63101120774981528287467370999 20	68158548235147320626936020 992
127	36348708964895034906955626972160	38168419626533649880145224 7040
131	57862524567501709233543846899616	55622479403538857696170243 2768
137	11323747222252418732879133566664 0	11072135553606796912181567 81568
139	14072061279235277846106112175152 0	14921118457218385304918954 88000
149	39876641984338029086018394924120 0	32063823131059608001963614 53568
151	48701226380719833302063745511801 6	59128119014186200013767962 53184
157	87351394023476477433965097981880 0	83548475742199716031052374 42560

p	$A_{p,k}$	$B_{p,k}$
163	153280410888719856394290886189072O	172632258645978176225404806758 40
167	220473019641125087111086794601248O	135238294941407662551266955755 52
173	374290843770249269689685886463608O	223365659281472287989031143997 44
179	624063084581112903244976676961104O	441963484322239832047455255920 64
181	737198924243098222522193099848561 6	726810461622729589266262499328 00
191	165112622352725198915850689440988 16	144943331076308846161986764931 072
193	193025957492472806696305562209060 00	157681521617473924793819986526 208
197	262544876303771419152884378435599 20	140973437000398561686008448286 720
199	305480879498866400064601876137616 00	210981513173093887630324710703 104
211	735021410771658126234700228306212 16	63684867115429869115941090376089 6
223	168470876094797401134698774233818 880	113199867061162160902005016785715 2
227	219940534398514001974787032622604 960	102260183449719942759113553412096 0
229	250860839006023866622336281583283 440	161872040707935135813274119183667 2
233	325242096257183744026203430512914 640	164697429246933470690833444898816 0
239	476200073514059734593375119809384 320	213255430527977687112734454691840 0
241	539586952290548318879964116706844 816	366235729820156398477114074567475 2
251	992749175453391901604517090972530 016	534186310950906555674666407967539 2
257	141478357102625383052210240848032 3600	630659515379006448369779599422259 2
263	199981897366821965328914372178755 2320	966927476989958438813808184723488 0
269	280479862606370326075313083656099 5760	130083108476087214943710443442135 04
271	313433122914438056214558595419239 6416	185797647859991493770365833060065 28
277	435278506689660594824215158685506 1360	253360556361652967441934973465804 80
281	539688404534349057875730549102505 7616	241519527343545038106869770695475 20
283	600252337651029157388326616713880 9440	303969898943023409600335410395873 28
293	101041334663448732115212728821664 79600	356001271857623561192394339815260 16
307	203466343836340209070718633121921 16000	938086496415080304158445082289111 04
311	247061190952706821550995203661315 53216	110088802224456774492421528985272 320
313	271991170954038731159518865810144 23120	127099478596619390691403094454669 312
317	329049407301146452081492101803868 85680	136225059210441081254989720857083 904
331	629120678985760465885184898424700 43616	348744322874814019223589983875547 136
337	823643236617551645166818211889930 60240	333828765958454634941233666208980 992
347	127701352767473963555801240399972 481120	463592033468166039922663641487245 312
349	139196266675217298449141803415897 642800	578722432894734902151089535729008 640
353	165140130222804175044976084943498 994960	492633365799671704921965847564191 680
359	212631768154975837196538325054171 817280	719060222475434392570738119540736 000
367	295921106790783650791299136885841 630080	127598610812945719412588056705577 7792
373	377396935263210511917557088832517 127280	171357257830537402823612432511048 6144
379	479441429578900212659890048882507 020640	198016127071366666218219865583360 4096
383	561199170698430203139971044093928 279040	160482186572606384093867183142164 8896
389	708535958247820079539657648136775 233520	228368097217772581494364942822506 0864
397	961508044833087882009630802472820 441520	333537809798876791807503343604244 4800

p	$A_{p,k}$	$B_{p,k}$
401	1117506275365417564403548353857369648016	41902374151104815423664762384914841 60
409	1502840066377136609546069322000843641680	498079581904733909401393250589598924 8
419	2158977347737535860495800003187866060960	573304256453194848316345239085632716 8
421	2318805079080656948166684945761365874416	1003193059068221224625182160511093964 8
431	3297371401970450783123887561198648415616	1123367944549693371517054634565618892 8
433	3534456124399854254213049446848677853840	1220788182194566998893077863509532057 6
439	4344684187945133979756127553814315689920	1406547038348181158347472434753375641 6
443	4977798932342758994412526737813048540000	1477076788752090368209263484081274880 0
449	6090647175881218973167896223939052163600	1520303525648835800519937690421385011 2

$k = 21$:

p	$A_{p,k}$
2	4194303
3	15690529804
5	596046447753906
7	651636841430498008
11	8140274938683976111332
13	267653239829571258763114
17	73410179782571778685878918
19	75388780100967171710007622O
23	41265747035272553427579116424
29	53161585193958322299763773O6330
31	21519689939837935767891101337952
37	879296670546086841578707817614738
41	75715510787435895623648292808732O2
43	20561591767152589138131280609343044
47	13286024314619130006688483384902964O
53	16522120588460116848320827655937963O4
59	15678924273990919706286225465197244660
61	31557683764913767374901251218007037882
67	22599650550583563004874548265359060346O
71	76310734165127362036647876076302104719O
73	13670060171903949960610922027276178329O4
79	71730094947112933227200360049405509768O0
83	20225728811875834333419868785404350396284
89	875180180609241501129616259976980926449O0
97	532975101312267181806958652071719946774198
101	12447158597509209576548523482927707304231O2
103	18785327537850795224444447921700510490629O4
107	41796242840570060682995424578541696155671O8
109	61653707714790635656225039161212157860352IO
113	13137348898906497313769400342168624542546214
127	15251456342971631429599230446326643635863692O
131	29243217347297917294134139384091881080775105O
137	74870988851765955934955702775655557253757383O
139	10149543732151403418378142343782780007246055IO
149	43635121509798854071718472282292761539731516IO
151	57730003176375532353943039039115554684978096O2
157	13081807514727886023064528048914383550161901658
163	28748307552870158616800105384207299744047062764
167	47824922750907936360934244914570027899471152568

p	$A_{p,k}$
173	10034270905096073436359485299767006726223601607 4
179	20528001900998457160011663518981319689443191798 0
181	25921262017144611227787889680443390337706525760 2
191	80164202883162833193277727629216776419199406291 2
193	99760718751623396577772766762313655528557949269 4
197	15346201778661927433406943135078704979818176132 98
199	18971535846379135215788723804433990081657156022 00
211	64862655043742568837846823644791222759887540175 32
223	20718295003635226470079262677744063135712037982 624
227	30092648968253308638922010026636704955291213466 028
229	36178100800919107884766260593913993779384461688 530
233	52040597912883120313703218503384018148341159245 934
239	88751737453750519840001157995737242436674402626 640
241	10572159215541485863194242213127828976347729835 9462
251	24824577392665699526774361282656575753755189318 2772
257	40765122148109422551427449236142174926234111842 0758
263	66179758109101936436638306668156128644006033759 5864
269	10627114651461328303997128400494935510505790722289 70
271	12415397679833157855250630012356428506596866815133 92
277	19662821530074009850832733699006515936206753431805 78
281	26569354694252838192695091348477802417583307451207 02
283	30835604959876826554094613583947038749968708388624 84
293	63930013529269468476715815827578588299762696916757 94
307	17034242830782103186914209869344696568448751311105 308
311	22354598017830288380201659666514985413587227609670 632
313	25575305611308086613038977214869789738029138246112 414
317	33390020536905405283864658011846748189835045338476 218
331	82737410287238504735840862676267929571145669309977 252
337	12064755963971050954884364463449371372542086873989 2038
347	22293196630463226633304156035235461015380804118099 6948
349	25152441591044975976313294734075113908215945345465 3850
353	31952206556627358861120229946429561234684311589914 5654
359	45519223200225552708677098153389242867176395326798 7960
367	72305665573628641299504300093746677621435445167165 0768
373	10163688821182900123060733595778982840790451542503 82274
379	14209239009516588292725069811305184480689195088432 00180
383	17713715467543414368199693726793055362239924102805 95584
389	24550452633936542869843134032488120417680097246236 58290
397	37644017172547202896727663795798912090255453115156 91498
401	46463958449576725804772559895112060056809357388064 92422
409	70348139006303647225996505937520800524989320045507 28510

p	$A_{p,k}$
419	116824040694442119735598526428438554335401949806079206 20
421	129109089372813225852077222972958088734120954079077130 42
431	211364228116560706564058681170508190478468570672457903 52
433	232943165548397128608284245411735931457322457803652121 34
439	310989219811491881785996995125425746439852962569300688 40
443	376235444737169957708924538833338162598410047712830754 44
449	499047044683354150416122133108396014159184394110696049 50
457	723088673662022816131234443984115898516771032939418589 58
461	868285456697751096276127200688613258570070174010546502 82
463	950910902687841182455369489184737983797372889767596620 64
467	113916191176721763013305235398453404360699204940651599 868
479	194067762414174228569628878378730365946398804921953541 280
487	27478997050235261933528140063214030439349551638887060 5688
491	32628472791757063911553630814733541998525936190967534 2212
499	45812359593578394348607086437478907371054720008934750 5500
503	54174131062050344278965240830157449695288637163641319 5304
509	69490830030643566616539669859824311781055748633519255 9610
521	11335131661012482044133278258471149661229527619206990 96142
523	12284759313482556248124101767507639251897601347002587 81924
541	25000349065674773040157455399484717330388368000984605 88762
547	31515814575802759928427745917436478863761636376715379 75148
557	46104095082624474852026033429262013007336423933000687 78058
563	57736223192967341014626206502927739540331806190078711 95164
569	72130928887176145529637865712030238720575312558864791 62270
571	77646078334719359546437685283557019745239249790509407 12692
577	96704215472753320465512964353002014547887343850435024 17878
587	13872048911958082550540831139344103570596375010450137 914788
593	17174398959316879212776874084948695552376818645037452 225094
599	21217240958544432052715018768729529393382444446394400 406600
601	22755539355168687727334153274098474076199378185346994 538622
607	28033581100548208096584941386721090630843528596139117 912608
613	34465058283331909760145041939026962141135247302448991 461714
617	39508714258887664174543023738906598543836043954419274 273518
619	42286895582146570174510288962095771345085369934284096 642820
631	63285665863977574652062626661049544415432289397160336 816552
641	88043373632609224424006965759691181390746094634762870 931862
643	93995351496006495954076464656102893505213461000988733 941644
647	10706848479959751211328490529510618927571983906799314 7164248
653	12996978254746970469170098022572954952204199663748540 6494954
659	15749008864842898337234019350438991276749108068978751 4931260
661	16783717970882034404262313811964415531164668650526789 5256482

p	$A_{p,k}$
673	244884975121534214584924659624850957318837553998707566931574
677	27733457446195533829768129431544599748344669150514148109697 8
683	33378829745272082748876309020661845684429942883960087579488 4
691	42625349357598400364056727430248979614376253741327507852841 2
701	57636600200927463602175568517884214521656758858821319976172 2
709	73144877403844543384852800842654693036441801096208379662181 0
719	98154709981865329937029595500610470013412975295900278970392 0
727	12382844470880262096783221869891195382368650128651380046115 28
733	14715545336393049438635462892984200875185235026811423741614 34
739	17463097664782273568828787487908340564600001817461429997321 40
743	19559150906467167703129115813068930367721428940727929028747 44
751	24491610874592106221380326186187349918588004477484150070482 72
757	28945933064774783614068723928970493924339582756343224030162 58
761	32333212510124441819108140304228411516686504347792839197595 82
769	40273396292093107128694537489365540513000126564626521877844 70
773	44908811928409104859554638184307063021078941323870663111146 74
787	65466868229201252780030605103837631615985931313101657899329 88
797	85343412228683031310269769138825274720405253657976527774478 98
809	11680356943017481137678930305427686583000076005477450338852910
811	12301944794206048648021154610865492833488662891158776554936132
821	15912396953670578839234977320574962136566098689225841658045442
823	16746519408930179828224145096980891681287098702435607678581224
827	18541341922216448295941643951268901089725030827220719576240628
829	19506050099248705030200760464447831154845696588924608350035130
839	25091066392205927183368936079560633735536698887698754790553240
853	35517230266239900200522529529981164984679857119092859168061154
857	39183598489755523696328107410672280978712674659519774870335358
859	41149287181177208125486650387042811998202234520953815421893460
863	45365974038170379907344501393344965235772356328732602687794464
877	63604368914366625808254190901329777718245624724803915506855178
881	69982155175153953123907470309037589754978732107176200865099302
883	73395070769576904222373702173039721296175611517259541064261084

p	$B_{p,k}$
2	2466048
3	5637666440
5	123385987840000
7	135187870559760000
11	927927227106191769600
13	28687601469635766102016
17	443339018560016401399808O
19	53397797666374632774131712
23	22372455422569924988110080O0
29	22902141850300076359360894412 8
31	95011523702391649817825978777 6
37	37938198058723178521448161075200
41	18907634940758654292210877360096O
43	73339375075971753263489401487360O
47	30432138178086623814596248017305 60
53	38480146926545205795599176523788800
59	27338821345790669731387639938919603 2
61	75641354125636176827200936457555148 8
67	55399690212939025182807044596400128O0
71	12299734676636644062722911994669248000
73	25298049713243186029122586014040195072
79	14579190453692676204386962859800166400O
83	27231720459121523162117098503662284800O
89	98369855468396847282814490765396384153 6
97	75072781472194920288223508623923937280O0
101	12849989532780033063381957971247200894976
103	26111772569678413609670603418814173511680
107	52207236276476522884346874782542493122560
109	91262919767713943159496776542564395515904
113	14324704376005941169164659364969106217369 6
127	18728816448704051492778564976580766960640O0
131	22507641325418374707961861489611494785024O0
137	66195003798761652769966666445404830230208O0
139	11124591293090138752117552780818592197120000
149	35591267208868092696178367642827567391318016
151	59469540741399681275435858252145600000000000
157	11129765125839701016247403248560218754539520O
163	29289205328189648766054880038669910121349120O
167	29347470023275953146148536574528282327622809 6

p	$B_{p,k}$
173	583361508281664450034515805970154859038556160
179	135954838496646848206092337448590746812650291 2
181	207105790213132355105030401287575808953548800 0
191	552875060979775442781119100365328787550502912 0
193	82160027419835949717494330727244616669848535 04
197	99249098957795634921240325255240472635637760 00
199	13227846486496809989293986179595084976477962240
211	53505918653089856780311261237206873404761702400
223	12868259215464380470935505019892569530555760640 0
227	14050538476065966818579633215469715456000000000 0
229	21981411760588208808374547422736863287676056371 2
233	26484643127775289176071684100634331323910257920 0
239	47430756139469657835737449397294321817128140800 0
241	58495885989715372707291000091333056356518723584 0
251	10149028975760181602243457479609368629343269683 20
257	16693726824297598519335540423848524925895298258 0
263	32037144160336384186514121271678938437148672000 00
269	45313864979914256916991419927445685894575217049 60
271	62508576512666742627722254041530421535150983741 44
277	12052377786325852357951559128807618202413503283 200
281	11572141869047307266369531432854059910410613555 200
283	15174259007760930990690908821728373996696633344 000
293	22328721633446304699931840336784340275271661568 000
307	75920318658620848480733501058416317318025276160 000
311	78040015981754602708796802509488092514991308800 000
313	11333818699390325516744694490594551022874856652 8000
317	12563325363858475957888516992683857834186534233 9072
331	38777065224366515950334790744205552970655408843 5712
337	56118809875433385372118408624873592752952007720 9600
347	80551836902572161170827424182509021761665009188 8640
349	10119823818087757577611128468302168265557300693 40160
353	97827217995920981726212981174866618828495059025 9200
359	15662117567510510821858197582917925429116928000 00000
367	29235679248153483223587559028761603519520180754 43200
373	47850299062791783052119842369080250529528854937 60000
379	59494025069100501139931336959951060299090628431 13472
383	46614399300537351522204996623305509068508008415 23200
389	74772548063100143572962078019897432430454343965 08160
397	13931651355368665710099654487382614096820601618 432000
401	14310857803983479775157127060233893554255239682 457600
409	22939073913419723442837891237444859971885436642 631680

p	$B_{p,k}$
419	3026902302392986424874793829873339645743633598513 1520
421	4673191026635317070251904899721066970149137727085 8752
431	6070910405385523539824115126062658075454106212761 6000
433	7382553817130665188948078888543843772806343790860 8000
439	1013811586978713905591333479233949739336487562895032 32
443	1010961170838562551858473215900576156669100330188800 00
449	1287344156656625668108405524962173852803247457461862 40
457	2474202400090794291605823540842817122122212405411840 00
461	1935853544540340737465984978540898297809047895583948 80
463	3341606291628251400541185562139674866170665295462400 00
467	2573671098497745545890577823776106304109548781568000 00
479	4146794630903197862129665058184555294546941235221216 00
487	9264899757417177591291777383597913582872288165549568 00
491	7821173638244329491071578339738483950002463369515520 00
499	1437589874380736548914520346470860014175728523883315200
503	1169191807305275814915076414138236540527828117618688000
509	1446060283046912125171668253189948645702756430624256000
521	2256070825310771221274315341773696523374073889716102464
523	3390439137887537866473262909541470441038314395858731008
541	7334773909538938083186871888038549263883993015922575360
547	9365770506840981505076662442425853000970988771049472000
557	9878908491927000607552143971173904087184725197312000000
563	1083353137490749608718159674751782258126982244571545 6000
569	1525089810021829530184948950649537675261383805488332 8000
571	2220168027926966911001170992427305417901835169573663 1296
577	2356084489568997258685554177340643953244532410287226 8800
587	2453099047967124892746060058477596697354165887375835 3920
593	2965390889479468783730978450104975396113329632659861 8112
599	4216778121008555797629856663333717759164893317327257 6000
601	5471723408547296803385542763935933728725041632945392 8448
607	6663797830421568323383064797755333608006150494448844 8000
613	9049538863644668717154158322495687966563815124849079 0912
617	7567436036595163551473484988552003976190030858179051 5200
619	9828452272444016584923025353964619129967136965918720 0000
631	1536812656921508594794609702560556326763302909368995 92192
641	1608328578206373577238332077894626499795644964491231 23200
643	2032282827508702876434062118217787655507525816216426 90560
647	1663524856957950171335004993005022211932098894750436 64960
653	2659711895620548172230354625129000088406435128039648 83968
659	3058846954096433166880683481955962215456026358605414 40000
661	3587173667153493573864009112745795727504197879377428 48000

p	$B_{p,k}$
673	559868786193086660625843209239123364826537249255012171776
677	40989409501133465107312423089750584343884053098586767360 0
683	60181724687319364756560992129614189005564633741656217600 0
691	89999292756064118834151768449245533317740508306964480000 0
701	96405491772721141559390806810940172934243282446426806272 0
709	16374107358448401188693299713953071304819071841845248000 00
719	14497780974162743691316188184682291944017542851001843712 00
727	23089276994493600135778235829126400288644266932358086656 00
733	28196811340266744316112777466626860768931036803681628160 00
739	36666163878656471604280316330782342178721967266690416640 00
743	30255721610986526764409505704772763389752546451638403072 00
751	50583985819117697385616856972222999142670473400010145792 00
757	63247510287109558669125640144088315633541185760032949534 72
761	44139403597673921099080889976876754264526058552453599232 00
769	74143045238816797904828798988619892607768654923059062374 40
773	58369292806120013300989933608775422317172598498670592000 00
787	11939721622389513103156332596043629441732803383611719680000
797	11059447525005352090460027146614957936228827211351152640000
809	19687139507489569409083901622257780753757376869789037363200
811	21863676466492008234890628833774854942356150388521112829952
821	23431741110870367843991580065959143779237939119187847321600
823	32674171136756991097225532371817328389952359752743360921600
827	26221182062896432849446151028004476797347588592277199896576
829	31994878329387428568493039804442437317208394911368452505600
839	29910383849160145822787562863972487760498638201156482989568
853	56839996313331132957776328457752905783072722606186718822400
857	48428415783283318238271506976557215107515588417227407360000
859	63935222325597854172270493328981566455768271126562078720000
863	61365867557339643898242752503376857994166246053538481280000
877	12305990253559946559648773315193681958108480881372954624000 0
881	85704087871038497605598978707379856459008756764128438784000
883	12998652818690261264846403629143458483211335757049561088000 0

$k = 25$:

p	$A_{p,k}$
2	67108863
3	1270932914164
5	372529029846191406
7	1564580056274625717608
11	11918176537727209424601 3276
13	76444441827728472153330 1334
17	61312916256201775276232931 15498
19	98247412115381427844199033073860
23	11547847916097706623727167519221304
29	37600179137568036154499221175984 13990
31	19873885572929070278298557798726799776
37	16479435273673246610999926221686550 36878
41	21395393747821564385337602353549709773026
43	70295990495133038898032360278502608251644
47	64831560413584990930167665292126684 1888368
53	13036747858295337124945537252345303849258014
59	18998718551961088480308416328918794975075 1180
61	43694267173727740178387011506558178339537 9526
67	45540829280252599872235061191559053349469929 48
71	19391840334800178484468061361785207447529412776
73	38820566324622979983336947096279748576693793154
79	27938930083277394653470454271535086073410562 6640
83	95987913041295195793826116059559977590332385 7924
89	54910765810208557091076155620994391739722907355 70
97	47183902510077170085266330264638527321278019213818
101	12952563149674059497286795495913738760889297603 2526
103	21143051642586678490618153491460124868279697072 1864
107	54786348348410301668728277385808386939485990660 0508
109	87029239998513586292537547301496907344089972615 5830
113	21420100685029601727636896883430912486619924146970 34
127	39675846350695279314374085783359144773866950885967488
131	86121251985650662065870378120180476350296631003932276
137	26375204626182827614496612714302763443223550984819 5778
139	37888352408871440656915190685802916545789400239907 2220
149	21507070727919423819625370251492970678146406210957 41950
151	30012997397081902639524621570617052655848203485147 98776
157	79481556665890763549964751362331965885136106586021 61958
163	20293768410416174273534686576751356551375111342617124884
167	37198048967765392311236783817465526997076020313024787848

p	$A_{p,k}$
173	898814840329038940919083805057869473042843579698869968 54
179	21074573931181835661846300028117053752453325290435941194 0
181	27820852998019723846891828162229974645474903949974949852 6
191	10668760048097197849388795919906200086284126678591167717 76
193	13841680023901316202252417718728181604432146744445993911 94
197	23113505036033373597083761988320818533750483457117028047 18
199	29751906217468473753879470803875240862899943115873697626 00
211	12856552955707885109277696572643916101853476835517041478276
223	51235793286792913512526197766923609930043048555012382628704
227	79903140276435792771517926470507196956841443169806325314388
229	99491892934040485233455425648949275577577481826161518984590
233	15337902113880236869708161081830804003158861222548902836547 4
239	28957993586786053399219771575849771578789313619371410250552 0
241	35664148973007399412644752322219726089181440255117022343802 6
251	98531875593066214692573513027159925177855895311851500633127 6
257	17783663876427689398980414759160029754346067130757926560248 58
263	31662716283612614879681682346188281491353843690506213379405 84
269	55644787217425584710242005560707355314530816754410032276171 10
271	66963446589800807544671621397598421608052840589862946512777 76
277	11576170471534868584383007980001088378722505940963227265907838
281	16565566269519446713023356904219458570437775060667930767131026
283	19778721500666722314067896921813065227609322659679214024641324
293	47116744741933328309166364828941405258911529252127208627250894
307	15131303276827498689513947826585961205510732992233200303532630 8
311	20912618788171640710792842404851980884892598134117430826221077 6
313	24546986411197724836443674747650901529145151691768209957332843 4
317	33717373363266420683282542667291454467759022236474153592408019 8
331	99314783062649237940815812385246382420453623067330223436419727 6
337	15561023022983289420083905411432088235019553001203032061810735 78
347	32321406088814227436491942861633508169790747294916195100080410 68
349	37314863474905808955003484846565100828754467633936399888491445 50
353	49613478414168274162357913735757284477900309690674111334023411 14
359	75608850668197983609988569367943198416324258702886961040359790 80
367	13117062418174443376093616224850706584031952766985886865594537648
373	19673729105652574774651058568592532070760219501983775005727644254
379	29317548976259682124860137188901619058122478779929502000006422540
383	38115775496636001279966631758863248624975916592481708747570353024
389	56215737018881604376949548368051293862147059947358534298672055470
397	93509985556468648710172737039233907657239279914560859607839746518
401	12014167894611648938373099037463851244809254325606804012521613 0026
409	19685472577445041167348538420698830156338297480744038281911000373 0

p	$A_{p,k}$
419	360071141363655502263115494983899072127569987769264426106696183060
421	40558809725966376026350421492177064007122899318988436721123917652 6
431	729357693846322127105509645014532095619238730790623212436047329776
433	818844730143907244583553639184641162439927890835722222010156788874
439	1155056998343174164426911101482604358706651810238740243081078412120
443	144902077612868359298526457012382955315548452648946284900668969044 4
449	202827506726333654326130706930461629476068062860145006603254816585 0
457	315396129304714672431021111003113344176550960166659952405910871065 8
461	392162649846227367734613667991334338343159162008677313841552830952 6
463	436982244371550918044968868464352016283501873891136745540448141198 4
467	541817437569509688754937113182127076589009752864644601170953449254 8
479	102163426897711028737760909626500742963085210883186720170719036478 40
487	154566980268000532520610538789578104432612287945077635021619997219 28
491	189636842312818779505427763190817945522986040183702045851058517692 76
499	284043492176234398964195196688778268684611338789558263836527110065 00
503	346787866853174168024621039460047324181439614597954005464547467526 64
509	466443052146136266602463493645162711736601980669303719458130421130 30
521	835174954624036784654865338100364979132341407612539627586037336090 26
523	919122520825422899539834888737255868385634812854874559581499683398 04
541	214158409574739201483156793428553512891139244298334752272377433935526
547	282148562507095200654310010295736111244333795852440487805866751742868
557	443772394613906681750742289205898756724717140495376301186894875533558
563	580072064019197103954008611686588152618903488917482562696929840067684
569	756084944983237727349740731389206012967924702935520253229212853129010
571	825399038658973605373985021096005483835622643810875654713818199075276
577	107188614815112485377382233247584976414239236071896780756503764384853 8
587	164699779000556149565378975960323566022939725720768821502123228822 0828
593	212373498187788175065774768325126015102016356437669103316256914090999 4
599	273146851037948540116346202618837512558783105960654951574876949584780 0
601	296882789303378483178443324785235738569171652318469766801311813619502 6
607	380568942790343554793164942804650688044417736112374693190120840581500 8
613	486654692474979297841604784474614645643540264966955690366711482087553 4
617	572576543773424433668319494008752623847078638146505739974888679952489 8
619	620823859585268242506332692693860621242062086458058943951926471541766 0
631	100328146937397125054051506077146111800614813025681419370072559195947 76
641	148637637374542022411922002180787547027117607246692418090492635547680 26
643	160675724908699188679769314924490330818160409111518793157339003484898 44
647	187619847830466969497636459441245602127982695169113209645493318454737 68
653	236317083092445581249653052770534683939897139089758124089050398957442 14
659	297026286655804403771578463029841544442087452427777242018962290979269 80
661	320401109333753756347486982763867207500613814180950324415161665867745 26

p	$A_{p,k}$
673	502368496232704064185243903359062211066345199182823699469957737442153 54
677	582584183531074266277533341256862722818935268313765883061548585987354 38
683	726363346864220018178931763582628168597625816109108817582566179647681 24
691	971807264038957776812562593074846314278515448827424630036111442184342 76
701	139177947367630643804853548270157470471578794211889282755255007124227526
709	184828465151779962020869950226754680916802250507477186652587663144571630
719	262317162388013873546608297305165290580299047526252426161316716113954960
727	345905973230716357952659258222318440482954905970083473523392681048848888
733	424807582142217100749681227004495910128257758015163001783197264731023974
739	520833651313208818869342661731591277107779007556310308820266914844872020
743	596080963659312944214599223256738620280186435527469139151195668140409544
751	779071107932580877136660606175076960522006538945743680741903495993993776
757	950541475664894458094688993137746686225847414407685229798152037910139358
761	108439494335676859771503945316952669760385684994817333985188677201400 7026
769	140839221175124794458813990839596927623957805813141894828467523970320 3610
773	160342828911622928410873431011580012919402992874440693135291753184989 9054
787	251142663172814263474185656050234976257986218172340515911648650606577 8628
797	344352538257041641981877032297191255448312706347379071557041763882467 0118
809	500322692582871321797374327269510200674777737005807197932698773205892 0930
811	532178335221589250298906195634191948572869806017690722198667669859587 3276
821	722949951162923061744383842476206191244457613485672647545564789320890 6526
823	768287731185058622398909868198361623559502737409603946245921141609477 0904
827	867287727636918222464910141231299130075588160320987108403028153824691 5788
829	921271120861677249955433007335098142603747855286533902094928838266821 6390
839	124327431881359403109773096819150514335980004813195673045099004262823 85320
853	188033493782109182906713581725310746589899351143080750090081845717870 79614
857	211362338510391155955872866776807487518159041809918384521383636549459222 58
859	224044853248224844254040025011964196811915062916920144859127587634196255 80
863	251636376467050578958232152177166527766807415300787323897744224290797147 84
877	376257634980104134758636359087424751008271372606468598699557339485358692 38
881	421590626698388772400827007730416173694846930699237352139189039988649260 26
883	446179598025206605022873868689379423639840729748183127054137778751721115 24
887	499551645364407504317142783247353235493012858177683893254953372519628375 28
907	872290747505535219251012280811608265551384631749206707639862229150051837 08
911	973725198402672343829694782836123247627245421438196536800688434338086057 76
919	121160376674551738275084818095849869686574751031687739289638920694748869560
929	158803689282751595689480226628134839599015241002319239200596565477908101690
937	196767566398387978910157508419032934920368310904210272398860620723840186978
941	218878122882300878913020088466543015655850024460463013419986634776069265526
947	256571443557262042946724254052751793211139948196164093704334831016142186468
953	300454330677449848790997882594585134211307758495110972114394540962285467314

p	$A_{p,k}$
967	432624589026491703959534467485713089626389538002968637803905285090745067048
971	47965419083632473565829190798906087515026480029317501573563096426181080527 6
977	55951127033237706590398064009223636182861405821673183441943077352184611613 8
983	65204861361124097537424445168294971956601957512226246942968380503810310322 4
991	79850901210127576190143934145811650818747253213583225724270320030258343177 6
997	92857027623681651636350044167810416888540868297618899790230654334557665191 8
1009	12523040642476175942691338357683829167128321647204598630319225034374738595 30
1013	13824997672569435728801958932533596610818713821380357274331237928104248583 34
1019	16024371548909339710455607750851770551373668143389635474875460322536092468 60
1021	16829418975163857980351608687869814521860753149649219668988366835471857715 26
1031	21472770018377790936262254402993492841793344833262999081066307931500881247 76
1033	22538689582736408321791112644658142993148146847405421331321867513847151790 74
1039	26049949335282399916251927023699871824262493719891406607505739964731824519 20
1049	33097973993806373781840465043975869728706673946683054069629370580101707736 50
1051	34712134321597441126453461146049560646746892325667516135557883172886105912 76
1061	43983938592888702565938322404134123699991988629149199506729541366546877045 26
1063	46104186232643958515095407366241058614247616759440568788507037484094222546 184
1069	53069999401999362303166035989246203130927556549074633421735453832348679155 10
1087	80563499174447620336596094887142249574552515807856871304026888729257935153 28
1091	88311450362060154501507125190144217669292369648687450424103514094882557642 76
1093	92448862584721245950130968876241496203245357215862799569008619532747106084 94
1097	10128887856282500393381972751802374907376507958819038001703402135894021522 818
1103	11608650306998654044163752351538892627263937046325526627523200000643365198 864
1109	13294758093744961145265501074135387766620052490743508599961789533605118448 830
1117	15911763179533917812285572329864214026015283929299321828478396613209672999 398
1123	18192015018507753782615189228284915290892997041801743284600884959814677922 004
1129	20784203712288696546519918192973341645470742067421415435296260951265697312 290
1151	33671353483265416005884947993459891860459949008082823962376125469681020123 776
1153	35164910027870596679849196953225678900426993019454032675983943986513527682 714
1163	43638162469792652477988811851913520654729238050816787794051285989382492881 884
1171	51795664621407185574833821304192843737237848795009710669004864342441508670 276
1181	64064188696018907618110025094989600864828202868236089399733485849991265823 526
1187	72716673563025708472802483174551900514546356505987314570962888202242535134 228
1193	82485057223098573508328154398229737694776562523963760264144910557237023588 194
1201	97484809293754640065035822509399006933997872982232346975625617540845344390 026
1213	12499084459284182007918111211080584550808668818609508280952253621034908252 9734
1217	13571300254950183857265655869211039330091942008509719498888846612413027585 4298
1223	15346759136779688178993211604162447253123576198019981861833161118310614446 5704
1229	17344052850805949437002077393947995423755542709002953981256433138820075063 7590
1231	18063598215488637096731246775929139613832512875498197265861852474818118438 9776
1237	20398288017943271053991196869850943927071503837902535241266883463374018926 3678
1249	25966224784742994472237005334150852877313579261950963080744767001215210001 6250

p	$B_{p,k}$
2	34713728
3	465711829632
5	83779964055373824
7	223678882089578222208
11	13444241339675294203337856
13	588951830411268202894931136
17	360877102821398499990218307072
19	526657065995747594461919315558 4
23	50215870238285235885109194130444 8
29	13051461591305402315821510635546 3936
31	87603792285900280529702896132372 0704
37	50295762033621835961803172401427447808
41	64712367888976542475918284001322126 0544
43	16347909436871718590737055779018346 02404
47	15535365008247256888176482298536243232768
53	27079479106551243562639561236425477549 2608
59	36424917368487881998276131315232783241748 48
61	89505078848920106674585747669625366630154 24
67	68064285339399683087503352842256385874407936
71	37505816431552123345890139518113795023984 2432
73	53206857663726669623626077994103178783978 3696
79	35731135209074931587050156641986520456313405 44
83	11570736672395587806566208194801751393713596928
89	62347245449920930769001825033180938210368407552
97	55319649850808497894408315489511589312596217 1392
101	16460472188570183682323960733254460473915270568 96
103	22425293871658834062674128991967418010014138859 52
107	51451927019080754593009839372025031159888986840 32
109	82871355405749201883099320024784950267212885524 48
113	20761845479135980303484423361806452864222319628288
127	31449207234107307280035471076173585557899393373 1456
131	82855825068368706880794641342983766732068941301 5552
137	21219018550824267463053406708476849810071406651 31008
139	27923019975049060703656901000032495522047035176619 52
149	14522920285026945709888095420705745061358419602096128
151	24646435184064376145510050235176193186071248095001724
157	57669446692174617575647208067208476010307541835235328
163	14053025432302134682946203574756395737584187751435 4688
167	22628734110263498395607295818928360183918864942784 4736

p	$B_{p,k}$
173	52090246022084364964238261336705546741287617154396339 2
179	12988261972648451200651446017204009417936364240712826 88
181	21000183376543382235009539098108732672765485728179928 64
191	75630302418791572450820961226173518353101301690509557 76
193	72525076967069466814453554493361388595583660136145720 32
197	11776777092556966015659325331237334590889043108723830 784
199	15161368829929210525569807439111355516824200198191480 832
211	75912109230394308360084085557355891163025644833500669 312
223	26002931351826489996614497017568154721931761849665794 8672
227	35548136224782528320763184176712993846167870115746616 6656
229	47709780091084587540143667705013821158506712281263245 1072
233	68638402663752454364458949974725419907547163728400665 8048
239	12246909828031955018529377554278965811972580397540585 96352
241	18725146350694945336138967423926720252056198514631744 41536
251	53504591193513073764312774290715223211557593422294391 67488
257	75495688248541888375651636736434690464914634797208049 33632
263	12059087330213181978755059690529574889207271524624412 790272
269	22737278780631912856335430360954463777580355574781879 302144
271	30762552694779421629469821892042253096971161742528179 953664
277	41792848910796156267574472019748766170779565030483071 194256
281	76487640253059667082928869925204595765700313713602058 846208
283	74635316989448910455483433021345228622913082073205687 451648
293	16081737019235019400922654922111536240760956932641670 1654016
307	49374418685481257043577394861952467726692261426112914 6174464
311	91596724425575119327576465846164290727614950982411352 1410048
313	85554411057475503025844657290887218699503822173348935 2954368
317	11651730425832121060116173616861078419107412851459224 57305088
331	37696499987333838779647236696812491558502373066304392 48887808
337	46175191814273391786692490115031921996990039542918183 93016352
347	93454304401853515005664989591661381972843362009773303 84928768
349	11058188808452235692984737045050318380187736701167624 749842432
353	14058159128477814356026570770092025083853765514787701 884478752
359	21269485558397079624442356763090138074112574018547028 000316328
367	39129287981000741235235353659795378899388958022862961 713283072
373	52744582055405412383759352045696490055381925374525642 574346248
379	86592457648762615196972421318834565170726092789950026 161746944
383	11038338969466549575443937212937353930132321830963825 5402811392
389	15766996674549883924600556784266844098602705584720271 4335838208
397	23561398478593228532243569808810762926189463851319704 4827365696
401	40561440157854523700643374480983773388420644097368670 0943376384
409	49298534201170293412158025008957182514075597561014037 9762983424

p	$B_{p,k}$
419	887079570036050683636198978634639750557442958883409477469008896
421	131751325506998078357390541015619381838823248741792712028638412 8
431	213908614676252746728917876728425931066972302130281570436802150 4
433	206416111139834798827674274556546841652468922311230291420339302 4
439	263112081277967761394507727730730228814146935526268760219150195 2
443	357150642479986325793029534976696438986002391593713967425549926 4
449	492798189343582129932933763748415956080357478021131895321473843 2
457	690144872204303345623327764422122521326448124871498517421714881 6
461	110571831402593728627502401831833157292881802947083070523362836 48
463	944877828701800223809246690187871172812531933604708477890705254 4
467	133852337564234425483566624400406051748831652880128566934115450 88
479	213306893479444615000072281022566313582433389547140674682878589 44
487	350789845900298155181867519958241165575969157034485660715211692 8
491	486194781192282098251089396403606834960917385909942987581822074 88
499	627956511353874294161834693972611286588084350346648376305200496 64
503	694004920970919953928459000660150030868098944219368821602218138 88
509	999699343930900524357368109268291697902219134264136229394707537 28
521	220794715468358464696291020994129952066595281174502738620317581 312
523	175869561153629151483496053744005225456379879858040420493287661 568
541	495722183020096277223317035040414036446477162617923460137459300 568
547	520572190990350420925112830726673168143942166083048161381661507 584
557	805590319584823281862593783513762726870428400421223057018308204 032
563	104770704483278189255824309757755930562349593956366365658630073 5488
569	136006968260992612598112396387231234709764578691879790701426721 9968
571	180105210440642225686368821628339308084379340616310273911345391 2064
577	205556250958517261486605320995582512601958702253364482659889088 1024
587	306096687454286144600636867085629973525587867231779650385557675 1104
593	380181394266710632634677004919685353099913364496855902187439993 6512
599	498132791109292000223713475412607243995743316408730902860652448 9728
601	616625967493572197631109073159871663907439344087852751799787449 7536
607	637245103978150249076350068654106581421171352482984588527275753 2032
613	805510124327392176904885427430238597781344578147871988617778390 6304
617	929902090002688312644095092782280256707285309410078180811990443 4944
619	111506690437928319453203349158028014690945454211052128760681192 07936
631	222675172811791475896397111607179139775210918209896865039061383 90528
641	313752889041345611068146164825440759335152216542385795038734604 06272
643	275374932722315728852121680538383216770201968150322400852627470 70464
647	316346518772898120069612807599478842956783071826468190302384811 95392
653	407810108226408429579581377795698726304020768048174215355723835 88352
659	465339039275518601814545878666073419970447264329388482336856681 34912
661	601077888869652391006804604773707105939166841648916338848212740 87424

p	$B_{p,k}$
673	748533938962710173720166585680927344276423831009730193422224819537 92
677	871062044437424454053103130268377163145543650920796965589283200040 96
683	106441350685563076011929085361643140737469790322027220444985795149824
691	193413713279918325457403090282761171870631048006347628308149205106688
701	248629635454938345276045114771463857942146294659633284805942896843696
709	284865175111654926099083328353035666221244177723776726069923227803648
719	398995560856595762229393588326716282716954785999569301114077439275392
727	478983687611410404975157438569071279622606483573861548669237402677248
733	579649246695293815036406471131994404303651044356524416826509085043856
739	705160658701527349706931760697161736218632950935185088016934699975552
743	813994399928845389781261666597129678619771956433941929781272568971264
751	140892251645091882667538650904862098999669238915826679534130182418739 2
757	138330073235178830397809052548482853961762808015738596889014557383065 6
761	178889559594453347009807860438376652769052898918323320270410981767884 8
769	184216602051819605312605328956367612371937658415458079980171118270156 8
773	227758778143871603038853050796618551019475843828936739532795156302233 6
787	322274517709827826621133423787613580332854916177427202697303153542657 6
797	482835242679356444463232843246044015694360246995428369068081499917516 8
809	619225963896932809687982702973926798429143747778699840474787846884044 8
811	813808436984326772827219725808163045295972503127028624395189066433971 2
821	110167587118470151273453474033600533301575711783773269400175437879992 32
823	103057606177255985972559595704484781680921014471921787772030382619033 6
827	108629220997443090561920235599307443243044802981903191360842332126484 48
829	121542724195194713666273283302240937248271642460558382749456107727165 44
839	170934598561581818917720442547923701988818227910935629744914112855408 64
853	230816047386315354117134334130588327543663579015158503104328018661212 16
857	256780092201470236337848961104082035650514212294476655296475133320913 92
859	262677231929263997988578359862089495186046433172639918154982026682082 56
863	323305469420956458666198687624017749039628507618153168234250106710589 44
877	446053315456267907065344093403897396079857777743615619535809036569738 24
881	593427306459597354885820481501764351363664109663346300506605991473345 76
883	551335029586440242570338936470943227771967854313329905403848616357396 48
887	569078436383531734235683632016562429554775555123116138159816030949015 04
907	108300590458293235298198698785758152824338544146337855526329383225336832
911	144792943338210771483811289944409298147444509347965858161065922067431424
919	131841750366238812812862009751951132784127557516848218230843290270360992
929	187398920283803322575819117307784046091615070091864291590465877104459776
937	210044302922622879977752000572046513812590695225651070692938000224354304
941	288426006775542651480202331783258149367362733191067638641890109901107768
947	272427849525106068919552860888269138157020126492526335885481965867707392
953	323368495184921305167765625984935636589047212949268303919375986810749504

p	$B_{p,k}$
967	45181803815106921654784131573555179881440265668895591919094683851323187 2
971	67379239272532645023155148583891556690360501388607125373605666614928998 4
977	66545991919960258554960516375544736647386083888954107068124289404408627 2
983	72363433047134594438685229466659788279948441254776143629043072412579891 2
991	99914351715468048440260923981982334103730096599431394690613738528375416 8
997	95004139894179922711064216800503146068244189105895372064131870022882713 6
1009	12461009491610953634662421366965334971572561514580783481946531530657300 48
1013	13654487843519514180709158355859404043705401015241154375700383469148221 44
1019	15960061139831603284669900679570050367576093960835314379671658300940615 68
1021	22889899800829129861586681361706900771709613505711218385916465849161482 24
1031	26836241743817480029449320227459948190189542305461285208216277748306411 52
1033	21999712271496973621852071097088153786536409716476274803983554666284042 24
1039	28233725039225838716230536396890378317352631050494899023541262885727093 76
1049	34681229270684913014211447950901055287633890244804749429196783300252625 92
1051	41723507056694756201836520616795804483918899477506063311549916140224839 68
1061	56078738874817921322742723888216385558220486838651423821519087020879380 48
1063	43432471965257372725958329859261913502479816184095251424079989429966397 44
1069	49653202037881151019887183900299079558341181552704123716093217155297361 92
1087	83461391735810186370731516366813318863807414121184592692626262034502123 52
1091	10155957030528672034070050271601941085655207931379631709774900719965437952
1093	95263082656072823014678171707629456227723227686269256558056795979201249 28
1097	93253766920663308471569612846887629683542918463452099425272718928793763 84
1103	11767638359068644573439840606362790132467726362713590924779145258572335104
1109	13177714547660864060099718209546618208885628710108262896178506357703130112
1117	14731606375244932211265731195050792258295960847259032768016387952592101376
1123	16636829767677796338427741797041574818624169363708329097373610401365278592
1129	18605138546839648951136113361647859990607625105186360198736069571992190336
1151	37733557574882585735644962952311752876034858548777893635021602650226294784
1153	33412236162827963646013200474864189124210759649995477797396807107948740608
1163	39129664710128368397662636831859978720032378403962099354742619579816050688
1171	59970505259925326476315110557904970136319217343513793780716541136076537856
1181	73917343297318855257661699185985561051593928985138637779528314383677423616
1187	61444961391836228333123769059454735810921340789035009413104086993189547008
1193	77775730332577863690362093912025044024502999656206595140115434250808803328
1201	10078444945513036063532958204179956524332112058840857211287391682209142169 6
1213	11697696612487710243530642575982040910668576211323130779560307054467191603 2
1217	11921629245221616407871247611295016896268765968353210754014479160873635020 8
1223	12610434861053624669293132232255830255307883233523413162274991756725280819 2
1229	14372565304295644677551096269015637664317267956804002499530228148486097817 6
1231	18381427831687842063139582808201395100282035557508131664022677918045736140 8
1237	18566855940187083802190234565440901592913418892714005135390288951855282585 6
1249	20996264502854936832947655821721416591241737385883230021620532745438652006 4

$k = 27$:

p	$A_{p,k}$
2	268435455
3	11438396227480
5	9313225746154785156
7	76664422757456660162800
11	144209936106499234037676064 08
13	12919110668885330179391279254 60
17	17719432798042313054831317103789 40
19	35467315773652695451755850939663480
23	61088115476156868039516716176680698 40
29	31621750654694718405933845009002661656 20
31	19098804035584836537444914044576454584768
37	22560346889658674610458898997488887454860 20
41	35965656890088049731752509556317062128456748
43	12997728642550098892246183415495132265728980 0
47	14321291695360924496474037263030784537314049 60
53	36620224733951601983972014141837958512565761380
59	66134539279376548999953597240966325308236485764 0
61	16258636815344092120377806981590298160142072163 08
67	20443278263905392082646318968890859048577051343640
71	97754267127727699740203497324759230742995769803888
73	20687479794391586033120259107607478016520122371774 0
79	17436686264973422003230910510865047218415532158603 20
83	66126073294148260382366811353430868561979980572385 20
89	43494817598266198071841422867389657697034514916450060
97	44395333871731609333227090145998390356590488278281366 0
101	13212909668982508093182260085381604909983172485077978 28
103	22430663487620207210696799039090046472757930623882552 80
107	62724890224094954380527004779012022207017510706692162 00
109	10339944004223399187416385994890847561551329646457416340
113	27351326564714298446019553630452932154164981143266427260
127	63993172579036416006153962959979964605770005083976961408 0
131	14779268053257510117124015589204171546474404846584817885 68
137	49503621562882549149648692403474856706586282843407865574 20
139	73204085689180510493225839924039815058119700203524743627 60
149	47747847723053912821950284495339544202552836428946567032100
151	68432635365086446208380089643163941760599488766485926891728
157	19591408902575414307430811563301206271027198912388469010290 0
163	53918513289634733427354308765770679221348533326199439104316 0
167	10374163876620090261680826638852960824214531305099483082930 40

p	$A_{p,k}$
173	269006293562078064627672592015769754586992654968074792884354 0
179	675250423328997196441217299200898519282356995630857991796972 0
181	911438965068124172948023182422816199360403328305129332121046 8
191	389207035314633874743552663954098085347731225361684389511604 48
193	515588739210300127217700307604906036583493034083868827225855 00
197	897012016943419195929223719004742646476322512487254741483010 60
199	117820523811796902912738092330426341341170064733171429968722 800
211	572386594141070752950152329110679788770618642194054203654326 008
223	254790476435892479606441528875134419821111076159221077574282 1440
227	411732891530445996572354723309876535198908272509695013712509 9480
229	521745435735401708612763597645654896056374072444573621707088 4420
233	832679367860444179419586356971512518527491416910957386093321 8220
239	165410955167080615621683257218411480235202438325211432492178 08160
241	207140943650124276528581985962684391098574723145745177475039 88348
251	620760669423876459184682389422410244613009926054195639138767 19528
257	117459321537417245711325741442776080524480338791943029137785 846300
263	219007842262120095861270228620349724247545401422862427324012 254960
269	402651244784013273521782176437834493791476443116586434553601 696980
271	491786248100156110688822854706102568131700866576012465484491 147488
277	888227984110398931611123819297503510210999158344167464885842 502180
281	130803367820752503190703728451407266818033715656540048130343 2944268
283	158405802626689712341138379657108658101400304249104857201949 8998120
293	404492541935023430201362325419979070007229587476586873344086 1999300
307	142611020253771492398800006870790025765818107378498689540764 69203000
311	202268940181074926118859451023968844316769698412997202694292 88465808
313	240484371171862990450155037135261117190882136609083976130994 13350860
317	338822513190127934804237943009345096801063638552105122034748 95017140
331	108810269471269131580337212207399789043673193968797666099175 817756168
337	176724982369718919614950905367093082876293561479362714822778 345180220
347	389178818574803231140055834802642908521633409103356413580558 216957160
349	454498768610700243652837945779647584604312291228108744281814 655334900
353	618228593171109447509725727269897946150667969024521033922132 323874780
359	974454428296802432563893680870988735509428678588677442584261 019809840
367	176672402004149760388267307570891681909667968623256211604006 2681271840
373	273718625674033707582242712758971039447279857909150063277188 1417415140
379	421120205249891700009703496595101746312777097442785359678292 2540068520
383	559116499182603839175702524607589107754909222903454937447234 7514737920
389	850662154143418325592438260860188983851395525829424076860935 4105776260
397	147380153135694672545616149120166169519498256680540225219320 14608955860
401	193189021162144776093933269832322474401657290481189969201748 78924311228
409	329300553822758393151523085555292100738242674087634346783635 40533958540

p	$A_{p,k}$
419	6321444964894472363281481941486830500178831462275983191171768859419708 0
421	7188683994640006453286375055694955001686469798196829512888724288664518 8
431	1354862145665866446532465771675444966143254058703969585653325880265199 68
433	1535243796099510253797258882570891869046996403248987236824622861891978 20
439	2226037397776948681425187343888289946143046435210202583868285126621789 60
443	2843688782944780264397651866222314259772106828390305946547138450599450 00
449	4089022818353559104580227664788799496400479754066809347622277427835263 00
457	6587016620916035462254632801188921881792849147984676440002207951122131 00
461	8334279850797008641832783133518636491902652826924611141492064918687755 08
463	9367544674368499875038193136383467737867801320416909300476032758055985 60
467	1181644231420967985108754800767769120062205479924974764247720667945301 240
479	2344047883083771614462060086561395696619323387024924426268994644864057 920
487	3665849614318141829738068087418544945017822371964611762044259312049942 320
491	4571783958161666418194803057780558112462699755352707291581903850388827 848
499	7072711359537454157648356817070247768073690796993879725355908693329507 000
503	8774045140465474307774134457274711344382185544981374496857969021144766 480
509	1208465323930731300876328443970824005194305777537838769409318876368592 5940
521	2267007248581031688635013022393011703006618840237553690515815605456762 6988
523	2514066639988571002882314972814128604236543047253809834077680269001824 8840
541	6268009747274424422929181345746247070649152516048091362983169974168368 5748
547	8442138923918544789257544387057690610930587072321286591590558492223179 1960
557	1376799416565699341064860444838408833750867681215500020669329482394108 36500
563	1838648620601008868431981556376861601474612199786855304154831544764137 30360
569	2447908178727180298444794089353007279645082697471069727057431825419014 07180
571	2691139279634104132697394502631627239552502424107417093385479994447020 62888
577	3568619834178058464420648953288521861261625462618052332048204177288499 08380
587	5675043815044263189959306836767273082095831835187959205616509883199624 83720
593	7468092826423752397370463150676223808460894972494990251205842758318584 80700
599	9800536329926697414228513384584151834360393720178895728001742438796864 88400
601	1072343603791696115025369073557519340069233699890835982384006283911779 586828
607	1402202464021592924199868300114307413592776704528683433312068335914133 883200
613	1828697471366304957706419882572414707788274818263679728134088069125578 536260
617	2179735918725611742287588798546980276197205196773551236453003966824333 895340
619	2378754908625509650669689408652723294957297511093563230235640987624146 023880
631	3994675531274097670864620171118257302064459456911833961780746024201775 607568
641	6107238108208920071063292417804416811004910958312822743743970458646641 291548
643	6643121778777677086046194348621560278643760298674833351210865365182777 512600
647	7853935688046394763443610065024038026119270804204731157649031254501928 549360
653	1007677310843666278550833085788309240441275991821246719346878915690439 4548180
659	1289928727951693922743248665030626157618541809277875284412369626887682 6802040
661	1399899730912130249771003599961716241683756883057549966937968502126011 2675108

p	$A_{p,k}$
673	22753726063018241908735833590451668819606866472067715537722848806193716072540
677	26701522625361373738871557876491663488687978259098000341771650186699814563780
683	33884051131534313206027169946189663174093786933092206320527371457766717397320
691	46401950424058559823023919950397069298801983502156753977427252752562216539448
701	68392182514401065996348838473503651147204291054516605435215065755852530504628
709	92909757690961903088612927449935269757939072087349139663709419097176411540740
719	13560774258527004008252817198317555378368197590821898048078045087898627007728 0
727	18282133812565728595236104508898374303001567349746224817784521032206705392648 0
733	22824444100160968384469547677601860305690148254620891406509227517006713996722 0
739	28443819448882091336974428376751835984537737938565974216323298780199635243516 0
743	32906589990716005154072528659965929858705664154650381079927841740124494835640 0
751	43939688394508354728595371854334958081137220997193838168211431364410848365852 8
757	54470684208829210431670343282859260079503563497890961325060122717236744896330 0
761	62799588399171518707733136315898947064304318279883609274836451929552376290490 8
769	83286822673342973575958700436894878716631312003465404067657383442612619001398 0
773	95809490216733136790420790358918393539717950929271672928437745988873833183834 0
787	15554998014668279755374289560217798700993266596318437299968191307754552430465 20
797	21873583147371716436166612780846656018206726588621231266467694179401798809854 60
809	32745169616433020556126734708567630564782920809329770071019062578656546291881 40
811	35002486682027890329584688189871636260729650168376155949522989848771763669648 08
821	48729790803180782346124622956650449735260545425149627702426003615864245636923 88
823	52038356067584457165083122211692808012393442962690963130680352092520550816362 40
827	59316322827498984297220352798218118273346693490017239206297464221716748679718 80
829	63313528637209993493662173539398018262114227981497284540962098973932877000808 20
839	87516690177358392396434588086033249201897380968109511365579136179691229568405 60
853	13681486237730668046557096248557162701553007698586584149229436168093425210863780
857	15523485815661827410063487113135948240022439009825274759334569048011377656466700
859	16531844035965339630301530769585315350777269854019995340879792349110836742596840
863	18741097246498879264014360174483613771835739188615207443199906818083270099965760
877	28939065853461251306277522422855191131824075254144058684919183696103444571154580
881	32722220240884812797539829114704754779116608857845076247370510446662999849267068
883	34788132460467531266367950380455355343832377873663115414971363057715068462036920
887	39303174847170952776409411043273685773560223341559817901230640994389549719067920
907	71758911114468104258162600179738872804758101592385314883322502294806099372203400
911	80811499038354423426348412386613824179405114740540950801816414611429871914224608
919	10232732888463609062934390905584906179236325830607322878219673650087780002446408 0
929	13705409480227521989544470426937212010237371260988259851892206046661928599064022 0
937	17275582350322629545577207750914992683910084555625858864775526031628924512088862 0
941	19381241912794266456077994095544297604595773550927524958614318534814858930722894 8
947	23009557972514461547300883155279428291788920580185372471089081546875545810418156 0
953	27287532721023604972062339595334557015691760803508624087304215165281632198378158 0

p	$A_{p,k}$
967	40454249432819310096381712566674796726565096670165794 055541598913021971400084824O
971	45223763694231125009279960082031414458755081457321742 501119803397556996145723008 8
977	53406973335909354834026073640660228221990514837555882 11765448368190342513910899 80
983	63006740279779243085340329697226580156972948922531587 93227397342864636095112167 20
991	78420052911343300152392744989852851847726121183249027 90251712016563614392620068 48
997	92300721171188174861396671053201064680961619955647864 96158738248443933021963602 60
1009	12749469740332787679911140446529110482299168830907704 97815402694222126824384162940
1013	14186784036662905292388977395839068300527228743372059 84384321209344480866451743460
1019	16639082465897050891088395319782195321494913427038205 28132715785596889951178797480
1021	17543676345888787276895711312191697319983045374073482 20095990211233611882855335988
1031	22824717091504875031400262202460366144605495617310070 76620932374517610823200022768
1033	24050787728152611219691756600875613148415462871251003 64301892028348364335722896620
1039	28121467356373391639992196512551509331599671482990891 15234120391246726393679131360
1049	36421043680758527515911029574856091025338552717603979 38127422901571449929495234700
1051	38343058283770855065721619635387490739957264009824663 99085337331065316547734061928
1061	49513643336725263141230654235104269865678681431594466 01791508603669051697426714308
1063	52096301213114461159343842366224042761282765262048300 07338050863886220791288989360
1069	60646325586628193264928322453106980336101905449577077 16365582895690860893996124180
1087	95191333156052900313491511239705780687554441550573635 56982774688894056918112590720
1091	10511544144840332276020840247845004955162299103780934 71782523548603709055935820264 8
1093	11044394123797465175307801183703302719771086275257327 76423165783161767975372674970 0

p	$A_{p,k}$
1097	12189194806241067515899406447273744184911056066214459 70259188946095408854675288 7660
1103	14123188441347325498016018584653380620362951185993052 62478437282958272389122473 3280
1109	16350970379093146558300279726558704841798436777368117 10042960567337979668296549 0340
1117	19852931889709494381292773454675951333904983590463541 55285238219193896369494589 2340
1123	22942477708275665020115710976277726935888594466330390 70676542944848612495309898 3640
1129	26492398204035376454752695045409733168324472139560100 39186146135518225968783463 9020
1151	44607842765983506390012384986683658196629200905857133 26817985339835888514099856 9728
1153	46748547875241422061561641072390796561337748362999366 12574713899116696232314913 7180
1163	59023625773604978169500849257730818718446470781155211 84981215383937308901475696 1160
1171	71024338951123010554820703958982699239093765019517910 66747689918579383679053793 3688
1181	89354231889848027608342756711512790691828649060703836 28726167645761966791128694 8468
1187	10245553883342276944121604191596521671607986537988444 06237350096274254624855380 9120
1193	11739677520771782164715453741912607594435304783566889 78321839798056770365848735 23500
1201	14061218641012098658444773542337963700060546598744491 95099893663665328659351789 3628
1213	18390765401772507596808463374536428609938800230968653 58983643645812851192126921 7060
1217	20100303523303912858973732985673909030366544297441651 94288978294033219861347663 71740
1223	22954592696896346220277337399482293067467273503088229 45021785224632961703555429 79440
1229	26197168532024189073574854780992204155852745684929130 81440294812663253299937920 78420
1231	27372872255421076599539758845618756934356850543527823 70699368262809285877580753 50368
1237	31212827978128237125414655723142949017943075956139484 44759410580226755916654129 02820
1249	40507336630423856119684200558280664639462060962222764 35692491726666272881774500 17500

p	$A_{p,k}$
1259	5023886299674279133430888521254563065250994979218176664842180424882606597538729064 40
1277	7370457546008196630905173052318852284673610006325384316813057464733315028701854561 80
1279	7688549089620109764727945768610596239210800482153234348668459304326743831648305331 20
1283	8364853771145743543178284747619182262116181736513860062608273830345189089961421961 20
1289	9487806587874882658568090021440303903790029565128989746373755076844465186182903948 60
1291	9893388718479702447980480045571370358753668940637954170427484294361804090230721542 48
1297	1121280653215972362858595626017172890442327851964677572251937226458563895319633622 460
1301	1218487144061264331792412837528093600050780748264513308772085825256046850697111931 428
1303	1270084616259888026482065367832164703690833090776475622756374150956709126441866108 880
1307	1379663819097641552334500079293579549093703834824778597298779633200063591277946737 000
1319	1765789235781650551420252973748032567770583126473167140789819758366048608913294357 680
1321	1839521897505522212531273779701456242521076347856066379434991949852154567992734201 388
1327	2078941726821518232538670718710850702020857278012179980812977874607985145331349598 880
1361	4116125400128019818540102697385270485958685212647979749287508854867575780960210203 708
1367	4635191789246744382679053410657213097007276483086790594598367453675598989974967765 840
1373	5217001135622418867201165665056985405089248428485378631779927488018360271441506673 140
1381	6103007642466600162018509130866826113854130986230757051580055308896632656496506336 068
1399	8657426922744317373960446699372924602232114846763813677513953145079406353262211299 600
1409	1049313238859696329715006530455777274913958403226853124952745972146118971193018883 2540
1423	1370369253544875859004730337711545868349316502913784637369587848550584780539263629 1040
1427	1478263050291766845048603169423283566322576779302214701468793706161345426024412620 4280

p	$A_{p,k}$
1429	153523265241091143036466460761561481299506397000078111555214421441474165754197878372220
1433	165558054065866944689725543593596585636668669130928354209229491450171741164827234958220
1439	185328983699453977231041051484167791455935780380541427736845224129192368320439536329600
1447	215253676748768084628211068611167428827037370795626617625007474525087662565496547685600
1451	231910037446448118007270896513565154357423142648572687120504145925806708312692352131280
1453	240696948253454849253109170405262825038026351082885323048954221338216456126806159705800

p	$B_{p,k}$
2	155493536
3	4159324584800
5	2053064358625280000
7	17747733012127483904000
11	157714304796270200904152896O
13	14964020167697016647044656640O
17	11033400025711084089689257111552O
19	27984311011523161595762022809600O0
23	32363449028353635988634067862814720O
29	11919436926643609020980301015047694233 6
31	91574705062872730037294036197234786304O
37	10706205805062597252107286133259873812480O
41	88132571679675203922043560342533201612800O
43	47727656583761122299130995635457425408000O0
47	33482526839878870378700601936227748869120000
53	82235645707684514718367669148608434316574720O
59	11220350384319327676835804415562304539570995200
61	45621306882371506207040721497925327158067200000
67	54279898226081331947760327088403228258293923840O
71	14143124403443128761515860154296243704274336768O0
73	44872346830182692233012352195097813450772480000O0
79	39123080204434412206264375051335806955335993548800
83	86685049072377835490150887909865303345174831104000
89	50000778318254208246791978380490295366216245735680O
97	68508039190446313880165541269661294414673094917120O0
101	13771975370775178329135774130089759157554410738892800
103	32542893559425768112672673544695963391393334742220800
107	74879902542101030953361350039325486738072022974464000
109	160971184330423488581112986451232476982486622535680000
113	26105402688082608461959773440125576809484044837191680O
127	76716263881691702897171640320683938062396231494515200O0
131	11985650879980841047490626093896280243738468794200000000
137	45313361825407687043482976629015355522159310672370073600
139	88828377523010654161263089021772823009775179897241600000
149	40502645018780097536186969048749374459849949570001797120O
151	77005185177192315740801664090176501120328885832220672000O
157	20179334108394989283816702125284432634719030538963200000O0
163	59834130350377131582917595330967471513821891858714951680O0
167	62123507306280704909260468476174088573410057764111411200O0

p	$B_{p,k}$
173	155692451716575634512253619917398921247809681483287756800000
179	434732428381057652892733896756485820272174373196662308864000
181	781675055878763010759864282015138493479729053732700160000000
191	260951404495914282952914419858946597112737286824354314649600
193	45404536227118201416400938416609049275932421387415348838400 0
197	49446261388381640278088521072355690162093500643781756236800 0
199	93016376421589821690551268622187626895529306461757010124800 0
211	46054314195813055726381890841894198900384552429873922048000 00
223	17317193573717125621671328368538101604635442580208922624000000
227	18708385926973641541083329351153017237847080572066811346944000
229	35229010603663515925421089108348701262110393943541688583168000
233	43394634975248752571548044885093804724914455696785796003840000
239	73743400107303593364524378278320580550617786862860197969920000
241	12738887818482756529869746196201648084769786048564015833186304 0
251	27103597105221091827578168395541841783238391313858350546944000 0
257	46730409358684531301681414984540473859482446132579103539200000 0
263	11081791092871848452284725445489584491066251437368476808808096 00
269	16708907124181947131381896887741502692440792891227616843710545 92
271	29143222459185097834449698994867950077459274775141053308928000 00
277	57473689152145505050430581390022027502794097389501328688414720 00
281	47086952519175563008726950309952692102939095786348808881360076 80
283	88725396250320089609905256902154343822249876625658206869340160 00
293	14318715122824438041890209191700908937378822612514248333459456000
307	71164213697465352254625858342367899600934857122580221807112601600
311	68490786301295710860538097162012550805277004313247589376542638080
313	12125059500783860524304911386984205306859854251462333102433075200 0
317	12233056790784812315417286725879493413992036570359016986568818688 0
331	55669025966454027852244695332162563807924485601053798111309365248 0
337	79665495776030432573114898446848438315502289751395526280037056000 0
347	14843244137799228360854581639728213620473477927433849929333735424 00
349	21097577807324105142402814672881935679046595474843801925110988800 00
353	18814885552627399778989974141833478525143542847344379322989019136 00
359	33739234868079982938055167508784065769892278342704606299959296000 00
367	84293233977693394211030919072060580586201450883490027701272576000 00
373	13825044253299760023026510648862953843478372573129334939412641075200
379	17399543108146910065039752173233363163165524565392690727712849920000
383	14598442792945164925274822370804051717197787485196783742535223352832
389	26388109943029814596042552000400588741345361218805590547977854924800
397	60837788462320120889387519708495458277397539617390513554980864000000
401	55408501381068200341978338117076577270789915330567376323333761126400
409	11928801848583225179999326559028735575179601100852746669526559907840 0

p	$B_{p,k}$
419	16688448073426462924990045240430266852054530344467791517614175616000
421	252971724434589115197791250044441463686974398938573851813632320312320
431	367198777047823231043381977983179943267574238461827072982923594956800
433	544374891873190469739178336189696995365044013787239772976369715118080
439	795046185673441957311616691422851039593560444071202624996482179788800
443	780947010048273052036222711418771947092193368780016871502939422720000
449	933173121243633648500523419755174616039226501621717083501212016312320
457	24630351761654073470809369617355829373121588416507717483102208000000000
461	19412286845796569266511301583799609294125930568399950817589081113600000
463	319339906298738665129737327394664898687542016432067306181552128000000
467	26680375194676099821521412148276604242442510379256214711560587469619200
479	52726509986945793112849291916074415460493055210415341607952961116160000
487	12746084041153890485711602818928875726633232507569935178574879680102400
491	10067671392086768138429872543872291110663102335499532575269896588800000
499	25581620734490709855601274994859013921652645152367943417494263876812800
503	19784834944819636311434502377981432184173092969606635757543123187200000
509	24611516023943235604994788425746685509401691867031818668443505563729920
521	45155958594336713878029462847922782363427243003592803349526450494504960
523	76709366980877862512493509876379008320703725813569413292394110746624000
541	208407307534481177267684767988147321140956429621088052665406480384000000
547	23188069592108943264428278997012090662019677022166654432278589983948800
557	30271864562940790720254551906661656954524927265038452047629397772546048
563	33750710841905011825629589258043799686179668208600195274767321275564032
569	50145269939917108977048492080384585470689134192075044110556514300928000
571	84062277348783308551958177009625622638280896821768127494152017202380800
577	96469725317796573622469803414806315137344879205432667400458068242923520
587	10225833141564957957511803475379810790155532932198323260840745360582246
593	13500421494006932583450434939242655711783038867112981351498629943449600
599	19247624266703046821403310046723799996846624765742636746474357984497868
601	29239442538268043021646476292269396510733983780007542509726541300079846
607	37218357668276346214037049552808892538355824366317953380711626919116800
613	53311070756532934082322337055321421877375940012128566966775568728064000
617	37721731260529597721083734631409341225383454881166378938102112403845120
619	60170097058951366632915778907420631706426164046509504115881717077647360
631	99528799779528013214418267573336750673941276514178545488009176154112000
641	11195915126229894656968309745440067408205049621369272789763268562808238080
643	16288957621377917232734830395168869792077040884885463296699343661667942400
647	12310910562860333462491693416924227009578848040544853581406154246505758720
653	20196726201022181966514290097301842387338437302659599136646285837058867200
659	21638362418936798278195994189011820867673374001251342967971070165567488000
661	32117340669150378702994042560037954469633095926742487649422790962315264000

p	$B_{p,k}$
673	526746004005074674273960940363858287933766465349793133258816839574896640000
677	396836511842429796322699682406468162945108198106928539475237219277581516800
683	56845849243300260406189612295516556513362144446728799856774256299638784000
691	1047327667823285245532084809361235176129115325034812118684631605516615680000
701	10307134973026084213776334343944152036996060533798862501230086109077176320000
709	2342233018964888841813196029820693816760923528432729805238763330023587840000
719	2045135353431989367961236550289573453710698952794880390006921820617932800000
727	3958116796877644738168876103206546476529324424940616695161248153600000000000
733	4856593819927279694026125051891226827481424119379193060925121390182400000000
739	6860341445958683874365588814933937992379606121769155558237006143037440000000
743	4471338986724339821816717810109211367821054377161394311063087275378442240000
751	1000568201497145355125795810201766033811814115867018906320040256731086848000
757	1208783117737885829522403299779070271892748784764640470093225142820126720000
761	8252267857432536840067037363911995974606576400774140532058782050501722585600
769	1747986719103964180579332257904143912513797943906853942645096629697249280000
773	1275027437477176664772216103907157385469242305591251046522740453493557362688
787	3053267419356748957671939255612145705491628741145294321366574696930213888000
797	27779156285913100328176974969362334785840201598895332065381077668354227901440
809	5261061147344549410458484291187009327723778371609041650291371352072886681600
811	7006675467684829762959232614690806854538781955663023149825099665033605939200
821	7450608572234608340035529166013366758366488992069689664884684251379943342080
823	1186579393269108884544510891655912602967049282099146254906371570964889600000
827	7172480030182721153251181285628374962743068495220181715178647615558772224000
829	1148691249339608011887534485134134091906204450733381630024559168644157931520
839	1048849599966814979416405203141908284224349073726398108895795294162860564480
853	2580388433196099546394636389624694178205531105421275124094280156513773158400
857	1814664900763458757589613270212920588666563098098442432579231363507467136000
859	3001252405317440531333525844590084768452237917468326460769255151209125959680
863	2596103060399333513686584482398628174636779810363635285974604845118146327654
877	5798971655985476840049685725941358611464847636765068412544822603142438912000
881	3945760584899501396326846955853762764822569731126977785989457139361689600000
883	6158097334820817823117214259320320753475925812988765936240595303357656596480
887	4821711158993292237413739439020642751648512989112148367455458612310487859200
907	13553181230564038771975808306753785073140145086627689611456449023164416000000
911	894678021710420280991005838952594937374188392805251155720649302000898441216
919	215814805534783280791150834342589690574499650598154140453024824940078412595200
929	156385620968731062958483450482185907880117306510169886150778390355177848832000
937	295472418157116615608878196758122105873584456545956134488796906418765578240000
941	215197908009850377410199664152022391686009034917416598980461504657338295910400
947	299554379186698568751746029861411212941834421507058813180919324818721996800000
953	295766371481421167008599070565916637879098326295154108303699993455645246095360

p	$B_{p,k}$
967	669992156239766755945484745508068359052216514658682029028439760890005789327360
971	528425765183210389056649269353428369983252574370000835142758145982464000000000
977	630812371017976280967055643171568039639489106758682841651878064714623254673920
983	648115102923620536730242540101932546780580898425334377893226373317624843468800
991	146505840350588713767981527422478111656639878518615892989892918591113134080000
997	162642773038184014190548760299770109425509252047636331394814336162141831168000
1009	193303450863037407440247256242666560095928937662489793049648836033191873085440
1013	149806077865888599236007865722251659088510351282684915941223969096920103649280
1019	189492739428584984092620840864698877759436697581059159132651454205494116515840
1021	254561540183006505354133193156191505206512205184330899693036273356404411417600
1031	270907552622184672684789283663185322617612365206689564205092768412361031680000
1033	426584883474275253035411522398726727226077325637609256441615377777307836805120
1039	403518252093113368158806437976829223683980660585474409129044605172446285219840
1049	396799171249587565490536314535540186052638576245821540770917634842758041600000
1051	572084602590174582037319933094384232604808347520389891451726870466546538905600
1061	568652087274905526638016843404570716434944794949121640201156365510604882739200
1063	730511821236453883466607941707423036676237960264298622240716924689020537937920
1069	991697308623468882847891693854545085072103172531006737990833981665033807462400
1087	157670198995413509614592334722096575339720958879286301516364864944439296000000
1091	963823941310348268569094478639725658262071387305049491661291264732205146147596
1093	152001940218362347190791433663604820258830487291566139193538512606061112626688

p	$B_{p,k}$
1097	114181963273184849506874564349528211915602939192324548606877912326999265357824000
1103	14847234180078245095214588671274105688933604882779173359893996310714445505372160
1109	15863569488025792447896703703601215663133870870478880676873418840788884342702080
1117	31257206301451474956681764923662491164543568568942172982312222329573337989120000
1123	30623029545768180597081362576677578259090321474508249235829586080338168103567360
1129	40508542803789179164971466219018355197660941068713893090745068183033234595840000
1151	41140039862395257406084804209206164270582561477330830740028800679320722456414080
1153	65529158304959048127515218992689481536453288577089719096901874965570733973504000
1163	55730262785702705358998332765099284403115673593300804798352195093434749566976000
1171	10363637624204544078391005782289304568846812518790370618619765269847031808000000
1181	78184603875296370144161204889046843156752175887293793618421751373826503062026240
1187	10486323858084795585354363985688220217380786477949688699678901128954847428608000
1193	10107020889092897747563477654244870133316221501140877798201290782346956977647104
1201	20914765355823688585366342211235973033723864884577004295378654455848533753856000
1213	27030614683264512979506742902222280634771948244603035148437947423662927000371200
1217	16967874463978401231924970356689820719927209005111381906170940995104831009172864
1223	20028107217441003841133616374015657376517030099124460188951562947949856107520000
1229	24416729556842661142261617916031268750014235262815067125096736154263676560998400
1231	36476836847101302973918079786443857656054169189889927562051711696282559137382400
1237	39065815730080111885501021349471940727201788868328942847971223944732785049600000
1249	48712915021635494101989254226314503036217734439671272468046602463628597526092800

p	$B_{p,k}$
1259	420736472921810494701052321547788208589876374360731623627055727533472491512908800
1277	664340331066946111554153060780611622833116144722016226443025574417198601748480000
1279	950583978118973081325199015780761351443271848615053648152112010912244499742720000
1283	824957488861791837228580045394565025843120824290761490231985622730449990338150400
1289	781142796210143368887246349861056013616996105886727559538221988101965187425239040
1291	11788446282607814494884379910265779956959370013340018326469091636020556475924480000
1297	154081851206896162222953372711428099904024470972613363333054391445717825070694400 0
1301	991084435886250920917205332939069667628244575145493810925927066607078969180160000
1303	16378956520629890648612826367567463653412005115769221104436264687807095953448960 00
1307	113006835902396415278288066046293925090899381317492810352020900157250634489266176 0
1319	135585463270840503520393414145029873992380416789775621817190582521259026961776640 0
1321	213069956015175443990946831622160437289084006295146491461249338059640801739407360 0
1327	288333181643044793258651516752940946122867091536279022960902012157389588880424960 0
1361	325912938162888723672313988632906213659690760912968101032702141222194909148610560 0
1367	389028108564682457919293807679344217171528707227200453369309880682686884452761600 0
1373	403400509308102908741137371569097064513370010455435145776207840253749399388160000 0
1381	840406714632297401562901862419792116431729770964866462095973203466856123983462400 0
1399	922105369826058254444823098810888379434712080814938449570234226719162493293465600 0
1409	851115443859009023196219357681136781712508295882835472509799105738409162544002560 0
1423	171633467512702460356521636693180378331598828950968496370250648351486248837120000 00
1427	10362221942952320573500967865891394511750104815281419544440211189181044104692549632

p	$B_{p,k}$
1429	167946542146535168826488685961381167709258752446126116623077130255000419252568064 00
1433	125573599931602062823588620929842158210820816712186219436998543410821932243476480 00
1439	168345725486476796463005769714870808244022095099947080311119788195891736657920000 00
1447	221040744603236246891905914093802087944040321686477883798204785314129226544307200 00
1451	205817058614606419217970066722633241665697130399427227778091238779404472684380160 00
1453	303366312850296422050574640573722400912575535035612430761825238165528598229811200 00

References

[1] L. Jiang. “All Nine Power of Prime Anti-sociable Number”. In: *Jiangxi Science* 42.3 (2024), pp. 464–469.

[2] M. Le. “Powers of 2 are anti-sociable numbers”. In: *Journal of Sichuan University of Science and Engineering (Nartural Science Edition)* 18.3 (2005), p. 5.

[3] M. Le. “The anti-sociable numbers in power of primes”. In: *Journal of Hubei University for Nationalities (Nartural Science Edition)* 26.4 (2008), pp. 361–363.

[4] M. Le. “The anti-sociable numbers with the form p^{2^r}”. In: *Journal of Shangqiu Normal University* 22.5 (2006), pp. 25–26.

[5] W. X. Li. “All prime cubes are Anti-Sociable numbers”. In: *Journal of Mathematical Research and Exposition* 28.3 (2008), pp. 498–500.

Gaussian Integers and Their Properties

Yicheng Zhou (周奕成)

High School Affiliated to Renmin University of China, Beijing, China

Abstract

This article explores the fundamental properties of Gaussian integers, the ring $\mathbb{Z}[i] = \{a + bi \mid a, b \in \mathbb{Z}\}$, as introduced by Carl Friedrich Gauss. We establish that $\mathbb{Z}[i]$ is a Euclidean domain and a principal ideal domain (PID), leveraging its norm function $N(a + bi) = a^2 + b^2$ to derive key results. The paper classifies Gaussian primes into three distinct cases based on their norms and rational prime analogs, and constructs a complete residue system for modular arithmetic in $\mathbb{Z}[i]$.

1 Introduction

The Gaussian integers were discovered by *Carolus Fridericus Gauss* and are defined as

$$\mathbb{Z}[i] = \{a + bi : a, b \in \mathbb{Z}\}.$$

These numbers played an essential role in Gauss's work, bridging the gap in the study of binary quadratic forms and quadratic residues. Gauss's profound understanding of the ring $\mathbb{Z}[i]$ allowed him to provide his first proof of the famous quadratic reciprocity law. However, since quadratic residues are relatively prevalent, we can hardly provide any insightful arguments about them here. Instead, this article focuses on the primary attributes of the ring $\mathbb{Z}[i]$ discovered by Gauss and explores its relation to quadratic forms.

2 Basic Properties

To study $\mathbb{Z}[i]$, we first define its Euclidean function and show that it is a Euclidean ring. The fractional field of $\mathbb{Z}[i]$ is $\mathbb{Q}[i]$. The Euclidean function of a ring measures the "magnitude" of its elements, and for complex numbers, this can be represented using their conjugates: $\overline{a + bi} = a - bi$. We define the *Norm*, which quantifies the "distance" of an element.

Definition 2.1 (Norm)**.** For $a, b \in \mathbb{Q}$, the norm $N(a + bi)$ is defined as:

$$N(a + bi) := a^2 + b^2.$$

The norm is a completely multiplicative function. We immediately derive some properties of $N(\alpha)$ in $\mathbb{Z}[i]$:

Lemma 2.1. *For $\alpha, \beta \in \mathbb{Z}[i]$, $N(\alpha\beta) = N(\alpha)N(\beta)$, and thus $\alpha \mid \beta \iff N(\alpha) \mid N(\beta)$.*

Lemma 2.2. *An element $\alpha \in \mathbb{Z}[i]$ is a unit if and only if $N(\alpha) = 1$. Therefore, the only units in $\mathbb{Z}[i]$ are $1, i, -1, -i$.*

The proofs of these lemmas are left to the reader. The ring $\mathbb{Z}[i]$ is generated by its units $\{1, i, -1, -i\}$, so the concept of associated elements ($\sim$) is clear. We define $D := \{\alpha \in \mathbb{Z}[i] \mid \forall a, b \in D, a \nsim b\}$. Since $N(\alpha)$ has a finite number of factors, α must also have a finite number of factors. Therefore, every $\alpha \in \mathbb{Z}[i]$ can be factorized, and $\mathbb{Z}[i]$ is a unique factorization domain (UFD).

3 Principal Ideals in $\mathbb{Z}[i]$

We now determine the structure of principal ideals for Gaussian integers to prepare for modular arithmetic in $\mathbb{Z}[i]$, which involves the set of multiples of a given Gaussian integer.

Theorem 3.1. *If $\mu = a + bi \in \mathbb{Z}[i] \setminus \{0\}$ and $C, C' \in \mathbb{Z}$, then*

$$\theta \in \langle \mu \rangle \iff \theta = \frac{CN(\mu)}{(a, b)} + C'\theta_0,$$

where

$$\theta_0 = ax_0 - by_0 + (a, b)i, \quad ay_0 + bx_0 = (a, b).$$

Proof. If $\mu \mid \theta$, there exists $\delta = x + yi$ such that $\theta = \mu\delta$. Expanding these numbers:

$$\theta = (ax - by) + (ay + bx)i,$$

and we define

$$C' = \frac{ay + bx}{(a, b)}.$$

For the same θ_0 as in the theorem, the subtraction yields:

$$\theta - C'\theta_0 = ax - by + (ay + bx)i - \frac{(ax_0 - by_0)(ay + bx)}{(a, b)} - (ay + bx)i = \frac{(xy_0 - yx_0)N(\mu)}{(a, b)},$$

since

$$ax - by - \frac{(ax_0 - by_0)(ay + bx)}{ay_0 + bx_0} = \frac{(xy_0 - yx_0)(a^2 + b^2)}{ay_0 + bx_0}.$$

Let $C = xy_0 - yx_0$, so θ takes the form given in the theorem. The construction confirms that $\theta \in \langle \mu \rangle$. $\square$

4 Modular System in $\mathbb{Z}[i]$

We first prove that $\mathbb{Z}[i]$ is a Euclidean domain.

Theorem 4.1. *For all $\alpha, \beta \in \mathbb{Z}[i]$, there exist $\gamma, \delta \in \mathbb{Z}[i]$ such that*

$$\beta = \delta\alpha + \gamma, \quad 0 \leq N(\gamma) \leq N(\alpha),$$

and $\gamma = 0 \iff \alpha \mid \beta$.

Proof. Rewrite the equation as:

$$\frac{\beta}{\alpha} = \delta + \frac{\gamma}{\alpha}, \quad 0 \leq N\left(\frac{\gamma}{\alpha}\right) < 1.$$

Since α and β are arbitrary, it suffices to show that for all $\eta = a + bi \in \mathbb{Q}[i]$, there exists $\delta \in \mathbb{Z}[i]$ such that $0 \leq N(\eta - \delta) < 1$. Choose the nearest integers c, d to a, b satisfying $\max(|a - c|, |b - d|) \leq \frac{1}{2}$, and let $\delta = c + di$. Then:

$$N(\eta - \delta) = (a - c)^2 + (b - d)^2 \leq \frac{1}{2} < 1.$$

□

This theorem justifies the use of the Euclidean algorithm in $\mathbb{Z}[i]$. Using the Euclidean algorithm, we can further prove:

Theorem 4.2. *$\mathbb{Z}[i]$ is a principal ideal domain (PID).*

Proof. Let S be a non-zero ideal in $\mathbb{Z}[i]$. There exists $\alpha_0 \in S$ such that $N(\alpha_0) = n_0 = \min\{N(\alpha) \mid \alpha \in S\}$. For any $\alpha \in S$, we can write $\alpha = \beta\alpha_0 + \gamma$ for some $\beta, \gamma \in \mathbb{Z}[i]$, with $N(\gamma) < N(\alpha_0)$. By the definition of an ideal, $\gamma \in S$, which contradicts the minimality of n_0 unless $\gamma = 0$. Therefore, $S = \langle\alpha_0\rangle$. □

The fact that $\mathbb{Z}[i]$ is a PID implies it is also a UFD. With these properties established, we can explore number-theoretic identities, such as the classification of Gaussian primes.

Theorem 4.3. *An element $\pi \in \mathbb{Z}[i]$ is a Gaussian prime if and only if it satisfies one of the following conditions:*

1. $N(\pi) = 2$,
2. $N(\pi) = p \equiv 1 \pmod 4$, *where p is a rational prime,*
3. $\pi \sim p \equiv 3 \pmod 4$, *where p is a rational prime.*

Proof. *Sufficiency:* If $N(\pi)$ is prime, π cannot be factored further due to Lemma 2.2. If $\pi \sim p \equiv 3 \pmod 4$ and $\pi = \alpha\beta$ for non-units α, β, then $N(\pi) = N(\alpha)N(\beta) = p^2$. This implies $N(\alpha) = N(\beta) = p$, but for $p = 4n + 3$, p cannot be expressed as $a^2 + b^2$, leading to a contradiction.

Necessity: Let π be a Gaussian prime. Factorize its norm:

$$N(\pi) = \pi\overline{\pi} = \prod_{i=1}^{r} p_i^{\alpha_i}.$$

There exists a prime p_1 such that $\pi \mid p_1$. Then $N(\pi) \mid N(p_1) = p_1^2$, so $N(\pi)$ divides either p_1 or p_1^2. If $N(\pi) \mid p_1$, π falls into the first or second case. Otherwise, $N(\pi) = p_1^2$ and $\pi \sim p_1$, which corresponds to the third case. □

Theorem 4.4. *For $\mu = a + bi$, the set*

$$S = \left\{ m + ni \mid 0 \le m \le \frac{N(\mu)}{(a,b)} - 1, 0 \le n \le (a,b) - 1 \right\}$$

forms a complete system of residues modulo μ in $\mathbb{Z}[i]$.

Proof. The theorem is equivalent to:

1. For all $\alpha, \beta \in S$, $\alpha \not\equiv \beta \pmod \mu$,
2. For all $\alpha \in \mathbb{Z}[i]$, there exists $\beta \in S$ such that $\alpha \equiv \beta \pmod \mu$.

(1) If $m+ni \equiv m'+n'i \pmod \mu$, then $\mu \mid (m-m')+(n-n')i$. By Theorem 2.4, $(a,b) \mid (n-n')$, so $n = n'$. Similarly, $m - m' \mid \theta = \frac{CN(\mu)}{(a,b)}$ implies $m = m'$.

(2) Let $\alpha = c + di \in \mathbb{Z}[i]$. Write:

$$d = q(a,b) + r, \quad q \in \mathbb{Z},$$

and

$$c - q(ax_0 - by_0) = \frac{q'N(\mu)}{(a,b)} + r', \quad 0 \leq r' \leq \frac{N(\mu)}{(a,b)} - 1,$$

where $ax_0 - by_0$ is as defined in Theorem 2.4. Combining these:

$$c + di = \frac{q'N(\mu)}{(a,b)} + q(ax_0 - by_0) + q(a,b)i + r' + ri.$$

Thus, $\alpha \equiv r' + ri \pmod{\mu}$, where $r' + ri \in S$. □

5 Conclusion

The Gaussian integers $\mathbb{Z}[i]$ form a rich algebraic structure with properties that generalize many concepts from ordinary integers. As a Euclidean domain and a principal ideal domain, $\mathbb{Z}[i]$ shares similarities with $\mathbb{Z}$ but also exhibits unique features, such as its classification of primes and modular arithmetic. These properties make Gaussian integers a powerful tool in number theory, particularly in the study of quadratic forms and Diophantine equations. Further exploration could delve into applications of $\mathbb{Z}[i]$ in cryptography or algorithmic number theory, where its structure provides elegant solutions to complex problems.

中秋科普

Weiling Luo (罗玮凌)

High School Affiliated to Renmin University of China, Beijing, China

摘　　要

本文转载微信公众号 RDFZPhysics 发布的推文《中秋节到了，你对月亮的认知有多少呢？》。

1　引言

又是一年中秋节，物理社先在这里祝大家中秋快乐！关于月亮的知识你又知道多少呢?

2　超级月亮

非常巧的是，今年中秋的月亮正是超级月亮！那么超级月亮到底超级在哪呢?

2.1　月亮在椭圆轨道的近地点

我们都知道，月亮绕着地球转，然而月亮的轨道并不是一个完美的圆，而是一个椭圆形。

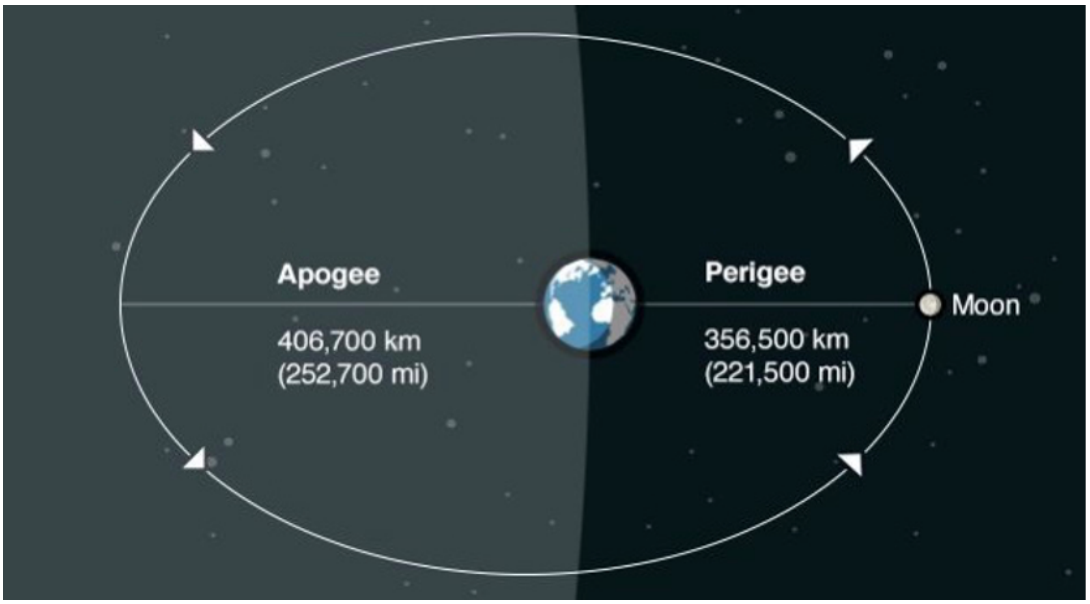

当我们站在地球表面观测月球时，近地点的月球所占视角为 $0.5482°$，而远地点的月球所占视角为 $0.4911°$。

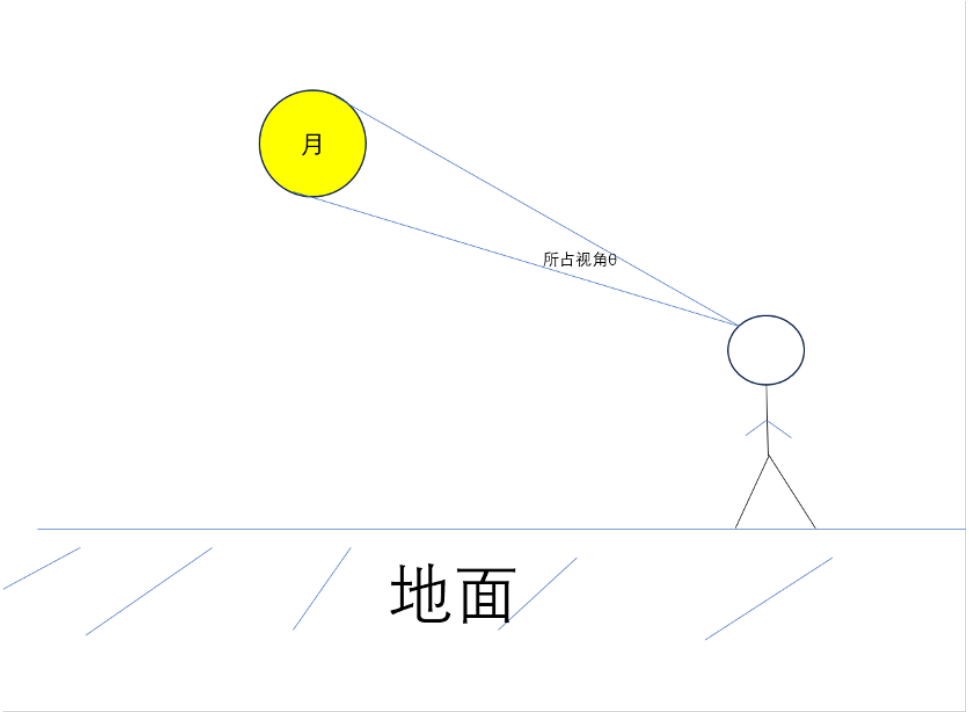

这是什么概念呢？请看下方对比图：

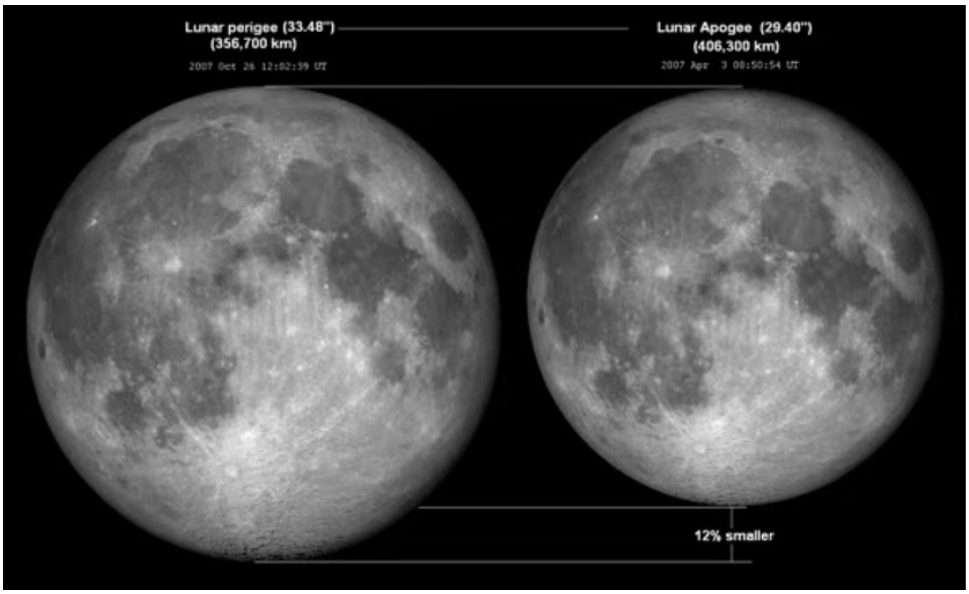

是的，远地点的月亮要比近地点的月亮视觉上小 12%！这就是为什么超级月亮看上去非常非常大。而今晚的月亮距离地球约为 358400km 左右，月球的位置非常接近近地点，也就意味着我们能看见非常非常大的月亮！

2.2 满月

说完了轨道，我们再来看看月相。

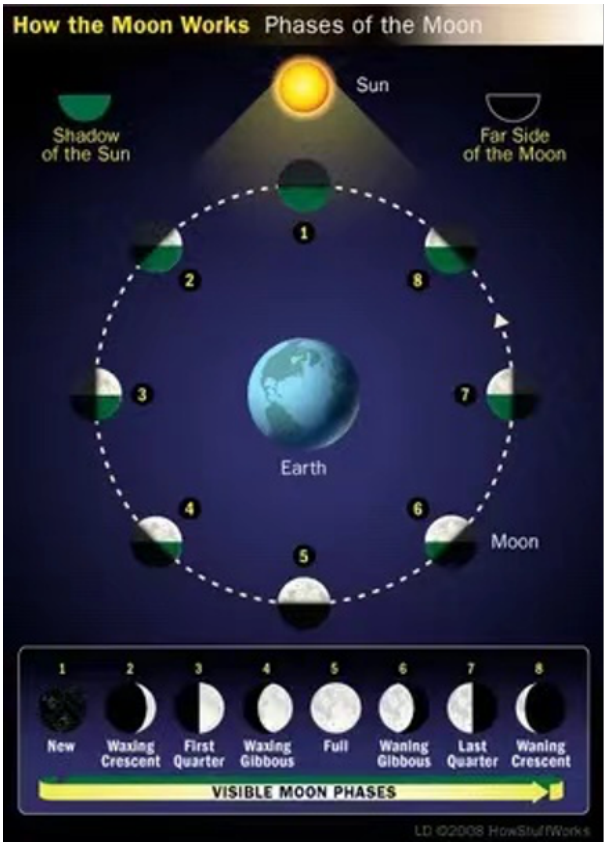

想要一个又大又圆的月亮，那必然是要在满月的时候，月亮对着地球的整个面都被太阳照亮，地球上的人们也可以看到圆圆的月亮。月亮绕地球转一圈的时间约为 27.32 天，但同时地球也绕着太阳转了一定角度，因此月亮绕到和太阳与地球在同一角度的时间间隔大约为 29.54 天。因此，月相变化的一个周期为 29.54 天，而我们的老祖宗正是靠着月相变化周期制定的农历历法。

3 十五的月亮十六圆

又是近地点又是满月，是不是觉得今晚能看到超级无敌宇宙第一好看的月亮了？然而，当你打开一款天文软件时，你会发现.....

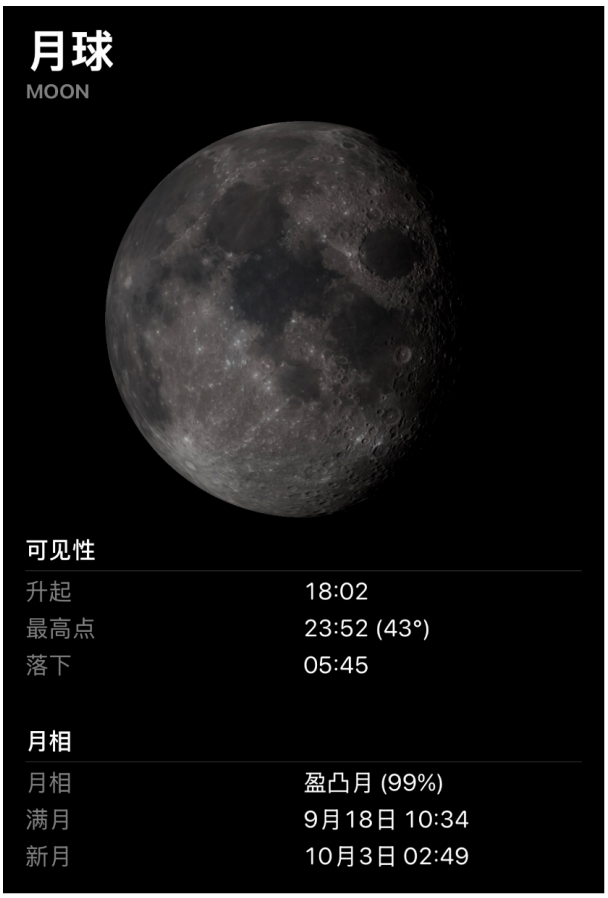

什么？今天不是中秋吗？为什么满月是 9 月 18 日？我的超级月亮呢?

大家肯定听过一句话叫：十五的月亮十六圆。

那么为什么“十六圆”呢？这还是要从月球的轨道说起。

月球绕地球转的轨道是椭圆的，地月系可近似看作二体系统，且地球质量远大于月球质量，则可使用以下方程：

$$\frac{GMm}{r^2} = \frac{mv^2}{r}$$

其中 G 为万有引力常数，a 为椭圆轨道半长轴，M 为地球质量，m 为月球质量，r 为地月距离，v 为月球速度。当月球绕着地球转时，由于地月间距离不断变化，月球的公转速度度也在不断变化，有时靠近近地点转得更快，有时靠近远地点转的更慢。再加上地球和月球都不是完美的质量分布均匀的球体和其他天体引力的干扰，每次满月的时间都不是固定的，最早可能出现在十四的晚上，最晚可能出现在十七的早上，所以说除了“十六圆”，还有可能是“十四圆”和“十七圆”！总的来说，满月通常会在十五和十六出现，并且这句话使用了互文的修辞手法，想说的实际意思是十五十六的月亮都很圆。今年中秋的满月会出现在北京时间 9 月 18 日上午 10：34，也就是农历八月十六，而那时候我们都要硬撑开被 502 粘上的眼皮听老师念经。。。那么，古人为什么不把十五和十六都定为中秋节呢？这样还能多一天假期（bushi）。

总之，虽然中秋之夜看不到满月，但有家人的地方就是团团圆圆的中秋节。

4 日食

月球在围绕地球转的时候，地球也在围绕太阳转，在远日点时太阳所占视角约为 $0.532°$，而在近日点时太阳所占视角约为 $0.542°$。

看到这两个数字的你有没有觉得 amazing！竟然和月球所占视角这么接近！这难道是上帝的安排？站在地球之上竟然觉得月球和太阳差不多大！

当月球所占视角大于太阳所占视角且二者重合时，就会出现日全食，而当月球所占视角小于太阳所占视角且二者重合时，就会出现日环食。

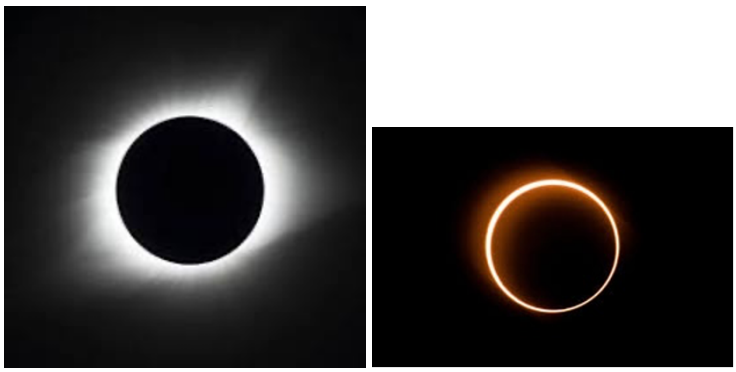

也正是因为月球和太阳的大小和到地球的距离使得他们在地球上观测有相似的大小，月球被用来研究太阳。1905 年，年轻的爱因斯坦发表了狭义相对论，其中有提到大质量的物体会弯曲周围的时空，而光在穿过这些区域时会发生偏折，俗称引力透镜效应。

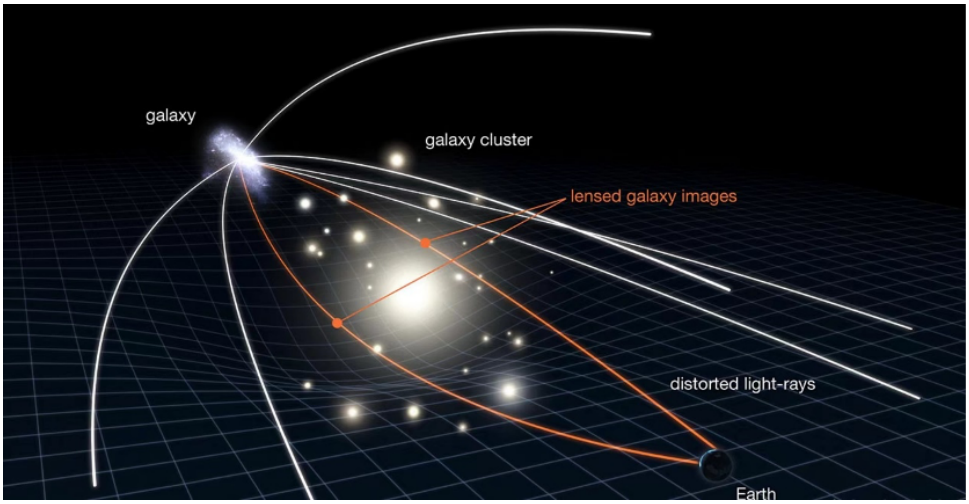

那么这个理论对不对呢？做个实验不就知道了！我们身边质量最大的物体就是太阳，科学家们决定测定太阳后方的星星的位置是否会与平时出现偏折，但太阳的光线太过耀眼，且大量蓝光在大气中散射使得我们在白天几乎看不到除太阳外的恒星，于是科学家们等了一个时机——日全食。1919 年 5 月 29 日，英国科学家爱丁顿和他的助手在西非日全食时，记录下了太阳背后的恒星，并对比于平时的位置再稍加处理后，得到了这张图片。

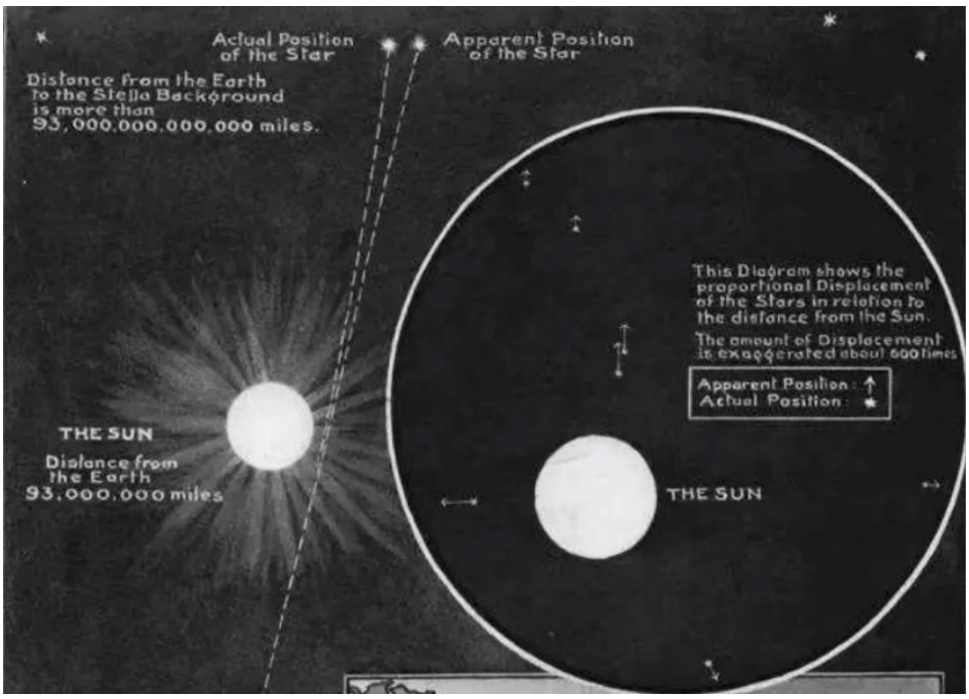

太阳周围的星星无不因为引力透镜效应向外偏移，且偏移程度几乎完全与爱因斯坦的理论计算吻合度极高，自此，爱因斯坦和他的相对论登顶神坛。

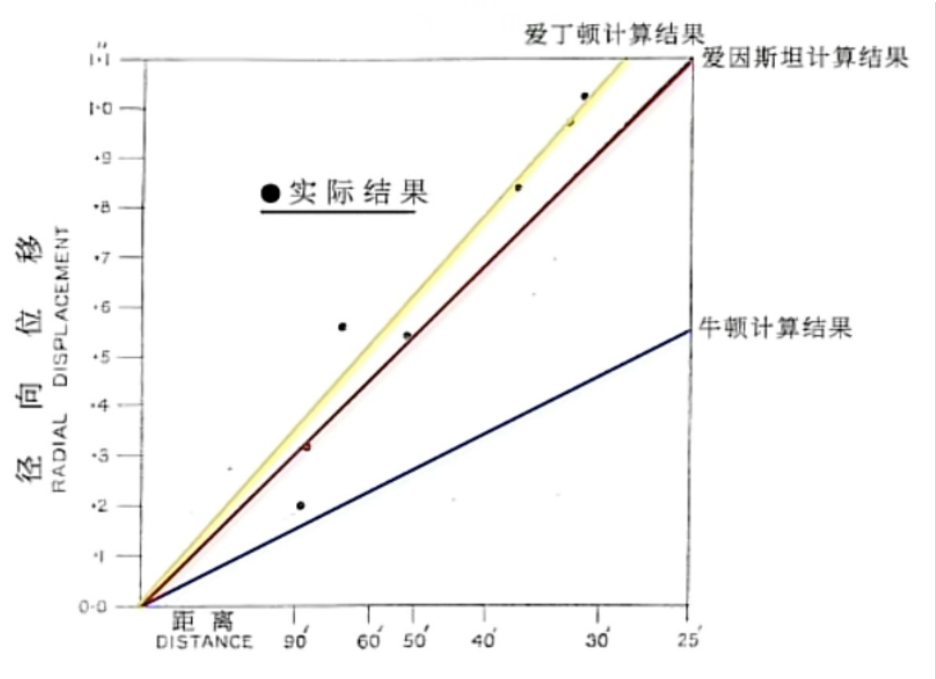

5 正在远离我们的玉轮

怎么样？听完刚才的故事有没有觉得月亮非常厉害？但有个不好的消息是，月亮正在以每年 3.8cm 的速度原地我们！这就意味着，大约在 6.5 亿年到 14 亿年之后，我们将永远也看不到日全食了。14 亿年？好小众的数字。。。这是为什么？我们不得不请出一位新的朋友——潮汐能。地球和月球都不是完美的质量分布均匀的球体，因此，地球会被月球拉成长轴与月球共线的椭

球体。由于椭球体两边受力不均，地球的公转速度会越来越慢直到最后只有一面朝向月球，但那大概率会发生在被太阳吞噬之后，也不用担心黑心老板堆出月景房啦 然而因为角动量守恒，地球的角速度变慢的同时月球必须远离地球以获得更大的角动量，这也就是为什么月球在远离我们的原因。事实上，月球早已被地球潮汐锁定了。

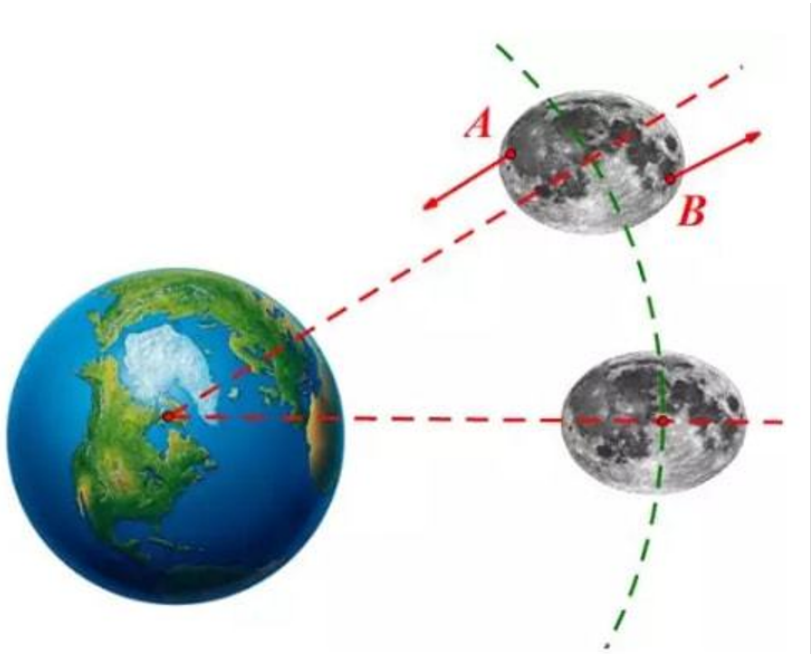

引潮力对月球的作用

当月球的长轴不对向地球时，椭球体的两边会因受力大小不一样而产生力矩修正月球的朝向。这也就是为什么我们在地面上永远只能看到月球的一面，直到 1959 年，前苏联的月球 3 号探测器才拍下了第一张月球背面的照片，人类也第一次看到了这颗美丽的卫星背面的样子。

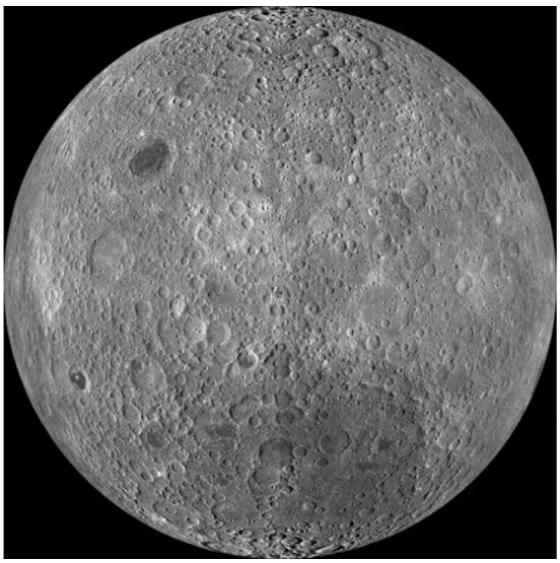

这就是今天全部的内容啦，祝各位中秋节快乐！让我们用北宋文学家苏轼的一句诗作为结尾：

但愿人长久，千里共婵娟

一道数之谜原创二试模拟题的进一步改进

Runbo Li (李润博)

High School Affiliated to Renmin University of China, Beijing, China

摘　　要

在本文中，我们证明了在任意 1400 个互不相同的实数中，都能找到三个数 x,y,z 满足

$$\left|\frac{(x-y)(y-z)(z-x)}{x^4+y^4+z^4+1}\right|<\frac{1}{1500000}.$$

这一结果改进了龚固的上界 $\frac{1}{1000000}$。

1　引言

数之谜原创题目二试模拟 4 的第二题为如下形式的一道不等式：求证在任意 1400 个互不相同的实数中，都能找到三个数 x,y,z 满足

$$\left|\frac{(x-y)(y-z)(z-x)}{x^4+y^4+z^4+1}\right|<\frac{1}{500}.$$

原题的证明较为简单，可以用三角函数证明。在 2022 年龚固将上面的上界改进为 $\frac{1}{15000}$，2024 年龚固 [1] 又改进到 $\frac{1}{100000}$。最近，他 [2] 进一步优化了证明，得到上界 $\frac{1}{1000000}$。在本文中，我们进一步改进了龚固的结论。

定理 1. 在任意 1400 个互不相同的实数中，都能找到三个数 x,y,z 满足

$$\left|\frac{(x-y)(y-z)(z-x)}{x^4+y^4+z^4+1}\right|<\frac{1}{1500000}.$$

2　定理 1 的证明

首先，在 1400 个实数中显然有至少 700 个数正负性相同，因此我们可以将问题简化为在 700 个正实数中找到三个数 x,y,z 满足

$$0<\frac{(x-y)(y-z)(z-x)}{x^4+y^4+z^4+1}<\frac{1}{1500000}.$$

不妨设这 700 个正实数为 $a_1>a_2>\cdots>a_{700}$。首先我们需要一个引理：

引理 1. 对于任意 $a>b>c>0$，我们有

$$(a-b)(a-c)(b-c)\leqslant\frac{(a-c)^3}{4}.$$

证明. 用均值不等式即得。

下面我们分类讨论 a_i 的大小情况。

1. $a_1\geqslant 2149$. 此时我们有

$$a_1>a_2>a_2-a_{700}=(a_2-a_3)+(a_3-a_4)+\cdots+(a_{699}-a_{700}).$$

若等号右边的 698 个括号中的值均不小于 $\frac{a_1}{698}$，则我们有

$$a_1 > a_2 > a_2 - a_{700} > 698 \times \frac{a_1}{698} = a_1$$

矛盾。因此必存在 $k \in \{2, 3, \cdots, 699\}$ 使得

$$a_k - a_{k+1} < \frac{a_1}{698}.$$

取 $\{x, y, z\} = \{a_1, a_k, a_{k+1}\}$，我们有

$$\frac{(a_1 - a_k)(a_1 - a_{k+1})(a_k - a_{k+1})}{a_1^4 + a_k^4 + a_{k+1}^4 + 1} < \frac{a_1^2(\frac{a_1}{648})}{a_1^4} < \frac{1}{698a_1} = \frac{1}{1500002} < \frac{1}{1500000}.$$

2. $a_1 < 2149, a_{21} \geqslant 769$. 此时我们有

$$1380 > a_1 - a_{21} = (a_1 - a_3) + (a_3 - a_5) + \cdots + (a_{19} - a_{21}).$$

若等号右边的 10 个括号中的值均不小于 138，则我们有

$$1380 > a_1 - a_{21} > 10 \times 138 = 1380$$

矛盾。因此必存在 $k \in \{1, 3, \cdots, 19\}$ 使得

$$a_k - a_{k+2} < 138.$$

取 $\{x, y, z\} = \{a_k, a_{k+1}, a_{k+2}\}$ 并用引理 1，我们有

$$\frac{(a_k - a_{k+1})(a_k - a_{k+2})(a_{k+1} - a_{k+2})}{a_k^4 + a_{k+1}^4 + a_{k+2}^4 + 1} < \frac{138^3}{4 \times 3 \times 769^4} = \frac{219006}{349707832321} < \frac{1}{1500000}.$$

3. $a_{21} < 769, a_{79} \geqslant 189$. 此时我们有

$$580 > a_{21} - a_{79} = (a_{21} - a_{23}) + (a_{23} - a_{25}) + \cdots + (a_{77} - a_{79}).$$

若等号右边的 29 个括号中的值均不小于 20，则我们有

$$580 > a_{21} - a_{79} > 29 \times 20 = 580$$

矛盾。因此必存在 $k \in \{21, 23, \cdots, 77\}$ 使得

$$a_k - a_{k+2} < 20.$$

取 $\{x, y, z\} = \{a_k, a_{k+1}, a_{k+2}\}$ 并用引理 1，我们有

$$\frac{(a_k - a_{k+1})(a_k - a_{k+2})(a_{k+1} - a_{k+2})}{a_k^4 + a_{k+1}^4 + a_{k+2}^4 + 1} < \frac{20^3}{4 \times 3 \times 189^4} = \frac{2000}{3827969523} < \frac{1}{1500000}.$$

4. $a_{79} < 189, a_{129} \geqslant 64$. 此时我们有

$$125 > a_{79} - a_{129} = (a_{79} - a_{81}) + (a_{81} - a_{83}) + \cdots + (a_{127} - a_{129}).$$

若等号右边的 25 个括号中的值均不小于 5，则我们有

$$125 > a_{79} - a_{129} > 25 \times 5 = 125$$

矛盾。因此必存在 $k \in \{79, 81, \cdots, 127\}$ 使得

$$a_k - a_{k+2} < 5.$$

取 $\{x, y, z\} = \{a_k, a_{k+1}, a_{k+2}\}$ 并用引理 1，我们有

$$\frac{(a_k - a_{k+1})(a_k - a_{k+2})(a_{k+1} - a_{k+2})}{a_k^4 + a_{k+1}^4 + a_{k+2}^4 + 1} < \frac{5^3}{4 \times 3 \times 64^4} = \frac{125}{201326592} < \frac{1}{1500000}.$$

5. $a_{129} < 64, a_{177} \geqslant 28$. 此时我们有

$$36 > a_{129} - a_{177} = (a_{129} - a_{131}) + (a_{131} - a_{133}) + \cdots + (a_{175} - a_{177}).$$

若等号右边的 24 个括号中的值均不小于 1.5，则我们有

$$36 > a_{129} - a_{177} > 24 \times 1.5 = 36$$

矛盾。因此必存在 $k \in \{129, 131, \cdots, 175\}$ 使得

$$a_k - a_{k+2} < 1.5.$$

取 $\{x, y, z\} = \{a_k, a_{k+1}, a_{k+2}\}$ 并用引理 1，我们有

$$\frac{(a_k - a_{k+1})(a_k - a_{k+2})(a_{k+1} - a_{k+2})}{a_k^4 + a_{k+1}^4 + a_{k+2}^4 + 1} < \frac{1.5^3}{4 \times 3 \times 28^4} = \frac{9}{19668992} < \frac{1}{1500000}.$$

6. $a_{177} < 28, a_{195} \geqslant 19$. 此时我们有

$$9 > a_{177} - a_{195} = (a_{177} - a_{179}) + (a_{179} - a_{181}) + \cdots + (a_{193} - a_{195}).$$

若等号右边的 9 个括号中的值均不小于 1，则我们有

$$9 > a_{177} - a_{195} > 9 \times 1 = 9$$

矛盾。因此必存在 $k \in \{177, 179, \cdots, 193\}$ 使得

$$a_k - a_{k+2} < 1.$$

取 $\{x, y, z\} = \{a_k, a_{k+1}, a_{k+2}\}$ 并用引理 1，我们有

$$\frac{(a_k - a_{k+1})(a_k - a_{k+2})(a_{k+1} - a_{k+2})}{a_k^4 + a_{k+1}^4 + a_{k+2}^4 + 1} < \frac{1^3}{4 \times 3 \times 19^4} = \frac{1}{1563852} < \frac{1}{1500000}.$$

7. $a_{195} < 19, a_{291} \geqslant 7$. 此时我们有

$$12 > a_{195} - a_{291} = (a_{195} - a_{197}) + (a_{197} - a_{199}) + \cdots + (a_{289} - a_{291}).$$

若等号右边的 48 个括号中的值均不小于 $\frac{1}{4}$，则我们有

$$12 > a_{195} - a_{291} > 48 \times \frac{1}{4} = 12$$

矛盾。因此必存在 $k \in \{195, 197, \cdots, 289\}$ 使得

$$a_k - a_{k+2} < \frac{1}{4}.$$

取 $\{x, y, z\} = \{a_k, a_{k+1}, a_{k+2}\}$ 并用引理 1，我们有

$$\frac{(a_k - a_{k+1})(a_k - a_{k+2})(a_{k+1} - a_{k+2})}{a_k^4 + a_{k+1}^4 + a_{k+2}^4 + 1} < \frac{(\frac{1}{4})^3}{4 \times 3 \times 7^4} = \frac{1}{1843968} < \frac{1}{1500000}.$$

8. $a_{291} < 7, a_{301} \geqslant 6$. 此时我们有

$$1 > a_{291} - a_{301} = (a_{291} - a_{293}) + (a_{293} - a_{295}) + \cdots + (a_{299} - a_{301}).$$

若等号右边的 5 个括号中的值均不小于 $\frac{1}{5}$，则我们有

$$1 > a_{291} - a_{301} > 5 \times \frac{1}{5} = 1$$

矛盾。因此必存在 $k \in \{291, 293, \cdots, 299\}$ 使得

$$a_k - a_{k+2} < \frac{1}{5}.$$

取 $\{x, y, z\} = \{a_k, a_{k+1}, a_{k+2}\}$ 并用引理 1，我们有

$$\frac{(a_k - a_{k+1})(a_k - a_{k+2})(a_{k+1} - a_{k+2})}{a_k^4 + a_{k+1}^4 + a_{k+2}^4 + 1} < \frac{(\frac{1}{5})^3}{4 \times 3 \times 6^4} = \frac{1}{1944000} < \frac{1}{1500000}.$$

9. $a_{301} < 6, a_{313} \geqslant 5$. 此时我们有

$$1 > a_{301} - a_{313} = (a_{301} - a_{303}) + (a_{303} - a_{305}) + \cdots + (a_{311} - a_{313}).$$

若等号右边的 6 个括号中的值均不小于 $\frac{1}{6}$，则我们有

$$1 > a_{301} - a_{313} > 6 \times \frac{1}{6} = 1$$

矛盾。因此必存在 $k \in \{301, 303, \cdots, 311\}$ 使得

$$a_k - a_{k+2} < \frac{1}{6}.$$

取 $\{x, y, z\} = \{a_k, a_{k+1}, a_{k+2}\}$ 并用引理 1，我们有

$$\frac{(a_k - a_{k+1})(a_k - a_{k+2})(a_{k+1} - a_{k+2})}{a_k^4 + a_{k+1}^4 + a_{k+2}^4 + 1} < \frac{(\frac{1}{6})^3}{4 \times 3 \times 5^4} = \frac{1}{1620000} < \frac{1}{1500000}.$$

10. $a_{313} < 5, a_{329} \geqslant 4$. 此时我们有

$$1 > a_{313} - a_{329} = (a_{313} - a_{315}) + (a_{315} - a_{317}) + \cdots + (a_{327} - a_{329}).$$

若等号右边的 8 个括号中的值均不小于 $\frac{1}{8}$，则我们有

$$1 > a_{313} - a_{329} > 8 \times \frac{1}{8} = 1$$

矛盾。因此必存在 $k \in \{313, 315, \cdots, 327\}$ 使得

$$a_k - a_{k+2} < \frac{1}{8}.$$

取 $\{x, y, z\} = \{a_k, a_{k+1}, a_{k+2}\}$ 并用引理 1，我们有

$$\frac{(a_k - a_{k+1})(a_k - a_{k+2})(a_{k+1} - a_{k+2})}{a_k^4 + a_{k+1}^4 + a_{k+2}^4 + 1} < \frac{(\frac{1}{8})^3}{4 \times 3 \times 4^4} = \frac{1}{1572864} < \frac{1}{1500000}.$$

11. $a_{329} < 4, a_{353} \geqslant 3$. 此时我们有

$$1 > a_{329} - a_{353} = (a_{329} - a_{331}) + (a_{331} - a_{333}) + \cdots + (a_{351} - a_{353}).$$

若等号右边的 12 个括号中的值均不小于 $\frac{1}{12}$，则我们有

$$1 > a_{329} - a_{353} > 12 \times \frac{1}{12} = 1$$

矛盾。因此必存在 $k \in \{329, 331, \cdots, 351\}$ 使得

$$a_k - a_{k+2} < \frac{1}{12}.$$

取 $\{x, y, z\} = \{a_k, a_{k+1}, a_{k+2}\}$ 并用引理 1，我们有

$$\frac{(a_k - a_{k+1})(a_k - a_{k+2})(a_{k+1} - a_{k+2})}{a_k^4 + a_{k+1}^4 + a_{k+2}^4 + 1} < \frac{(\frac{1}{12})^3}{4 \times 3 \times 3^4} = \frac{1}{1679616} < \frac{1}{1500000}.$$

12. $a_{353} < 3, a_{537} \geqslant 1$. 此时我们有

$$2 > a_{353} - a_{537} = (a_{353} - a_{355}) + (a_{355} - a_{357}) + \cdots + (a_{535} - a_{537}).$$

若等号右边的 92 个括号中的值均不小于 $\frac{1}{46}$，则我们有

$$2 > a_{353} - a_{537} > 92 \times \frac{1}{46} = 2$$

矛盾。因此必存在 $k \in \{353, 355, \cdots, 535\}$ 使得

$$a_k - a_{k+2} < \frac{1}{46}.$$

取 $\{x, y, z\} = \{a_k, a_{k+1}, a_{k+2}\}$ 并用引理 1，我们有

$$\frac{(a_k - a_{k+1})(a_k - a_{k+2})(a_{k+1} - a_{k+2})}{a_k^4 + a_{k+1}^4 + a_{k+2}^4 + 1} < \frac{(\frac{1}{46})^3}{4 \times (1 + 1 + 1 + 1)} = \frac{1}{1557376} < \frac{1}{1500000}.$$

13. $a_{537} < 1$. 此时我们有

$$1 > a_{537} > a_{537} - a_{699} = (a_{537} - a_{539}) + (a_{539} - a_{541}) + \cdots + (a_{697} - a_{699}).$$

若等号右边的 81 个括号中的值均不小于 $\frac{1}{81}$，则我们有

$$1 > a_{537} - a_{699} > 81 \times \frac{1}{81} = 1$$

矛盾。因此必存在 $k \in \{537, 539, \cdots, 697\}$ 使得

$$a_k - a_{k+2} < \frac{1}{81}.$$

取 $\{x, y, z\} = \{a_k, a_{k+1}, a_{k+2}\}$ 并用引理 1，我们有

$$\frac{(a_k - a_{k+1})(a_k - a_{k+2})(a_{k+1} - a_{k+2})}{a_k^4 + a_{k+1}^4 + a_{k+2}^4 + 1} < \frac{(\frac{1}{81})^3}{4 \times (0 + 0 + 0 + 1)} = \frac{1}{2125764} < \frac{1}{1500000}.$$

综合上述 13 种情况，我们就完成了定理 1 的证明。

参考文献

[1] 龚固. “一道模拟题的二次加强”. In: 天空的数学小天地 (2024).

[2] 龚固. “我也来个学习意志”. In: 天空的数学小天地 (2025).

Advances and Challenges in Sensory Retraining and Neurorehabilitation for Post-Stroke Arm Dysfunction: Integrating Neuroplasticity and Personalized Approaches

Tailai Cong (从泰来)

High School Affiliated to Renmin University of China, Beijing, China

Abstract

This paper explores the efficacy of sensory retraining therapy (SRT) and advanced neurorehabilitation strategies, such as virtual reality (VR) and non-invasive brain stimulation (NIBS), in promoting neuroplasticity and functional recovery post-stroke. This highlights the critical role of personalized rehabilitation approaches, addressing gaps in current methodologies, and underscores the need for integrating emerging technologies with tailored therapeutic protocols to optimize recovery. Key challenges, including standardization and patient selection, are discussed, alongside future directions for research and clinical application.

1 Introduction

Stroke poses a formidable global health challenge, ranking as a leading cause of death and disability worldwide [42, 43]. Ischemic stroke, its most prevalent form, imposes substantial global health and economic burdens [42, 43]. Projections indicate a sustained increase in the global age-standardized incidence rate of ischemic stroke through 2030, suggesting an expanding affected population [43]. Nevertheless, overall death and disability-adjusted life years (DALYs) rates are anticipated to decline, potentially reflecting advancements in acute care and improved survival outcomes [43]. However, significant disparities in stroke burden persist. Countries with a low socio-demographic index (SDI) may continue to experience rising death and DALY rates due to persistent challenges in healthcare access, health literacy, and service quality [42, 43]. This highlights a critical tension between global health progress and persistent regional inequities [42, 43].

2 Post-Stroke Arm Dysfunction

A profound and highly prevalent consequence of stroke is post-stroke arm dysfunction, which encompasses a spectrum of severe motor and sensory deficits [24, 59]. Motor impairments, such as unilateral arm paresis, are observed in a high percentage of acute stroke cases, significantly impeding a survivor's ability to perform self-care and diminishing overall quality of life [59, 60]. Beyond overt motor

weakness, subtle proprioceptive deficits—a crucial sensory impairment—are also common, profoundly affecting motor performance and hindering functional recovery [24].

Contemporary understanding of motor recovery from stroke increasingly acknowledges its complexity, challenging the long-held "proportional recovery rule" by suggesting that recovery is not solely determined by initial motor function loss [3]. Instead, it is significantly influenced by spared function and a confluence of other demographic, clinical, imaging, and physiological factors, underscoring the need for more nuanced recovery models [3].

3 Rehabilitation Approaches

Given these pervasive functional challenges, effective post-stroke rehabilitation is paramount for improving upper limb function and facilitating a return to daily living activities [59]. Rehabilitation approaches encompass a range of interventions, from central strategies like repetitive transcranial magnetic stimulation (rTMS) to peripheral interventions, such as robotic therapy [59]. Nevertheless, a notable gap remains in identifying optimal, evidence-based rehabilitation strategies, particularly for patients with severe upper limb dysfunction [59].

While general sensory stimulation has been explored, specific interventions like proprioceptive training with visual feedback present a promising, yet under-researched, avenue to address the profound impact of sensory deficits on motor function and overall recovery [24]. This highlights a broader tension in stroke rehabilitation research, where enhanced methodological rigor, particularly in the design of control comparators, is essential to ensure the validity and generalizability of findings and ultimately accelerate the translation of effective interventions into widespread clinical practice [23].

4 Upper-Limb Dysfunction and Sensory Deficits

Stroke often results in significant upper-limb dysfunction, characterized by intricate neurological underpinnings involving damage to specific brain regions that disrupt both motor and sensory pathways, profoundly impacting an individual's self-care ability and overall quality of life [2, 6]. A critical aspect of post-stroke impairment is the high prevalence of somatosensory deficits, affecting a substantial proportion of survivors [8]. For instance, leg somatosensory impairment can be observed in up to 89% of cases [8].

These deficits are not confined to the contralesional side but are also frequently present in the ipsilesional hand, with tactile impairment reported in 83% of contralesional and 42% of ipsilesional hands [35]. Specific types of sensory impairments include proprioception, light touch, tactile discrimination, stereognosis, two-point discrimination, and temperature sensation [8, 35], encompassing superficial, deep, cortical, and subjective sensations [18]. The primary motor cortex (M1), conventionally associated with motor control, also plays a crucial role in somatosensation through its extensive connections with somatosensory cortices and the thalamus, making it a critical area where damage or dysfunction can con-

tribute to sensory loss [18].

5 Impact of Sensory Deficits

These pervasive sensory deficits directly impair motor control, fine motor skills, and the ability to perform daily activities. The loss of proprioception, for example, significantly hinders effective motor learning and balance training [36]. Furthermore, tactile sensory feedback is indispensable for precise initial force scaling and ongoing finger force control during gripping tasks [14].

Stroke survivors with sensory deficits frequently exhibit a greater phalanx force deviation during power grip, meaning forces are directed more tangentially to the object surface, consequently elevating the risk of finger slippage and object dropping [14]. This altered gripping strategy is often accompanied by aberrant muscle activation patterns, such as reduced activity in the first dorsal interosseous (FDI) and extensor digitorum communis (EDC) muscles relative to the flexor digitorum superficialis (FDS) [14]. Such observations highlight that sensory deficits independently and significantly contribute to impaired hand motor control post-stroke, extending beyond the impact of motor impairment alone [14].

While sensory retraining interventions have demonstrated improvements in somatosensory function and balance, their consistent impact on complex motor outcomes like gait remains less clear [8, 36], underscoring the multifaceted challenges in full functional recovery.

6 Neuroplasticity and Recovery

The brain's inherent capacity for neuroplasticity plays a pivotal role in both the manifestations of impairment and the potential for recovery of sensorimotor function post-stroke. Cortical reorganization is a dynamic process where damage to primary motor areas can induce compensatory sensory responses in adjacent premotor regions, such as the rostral forelimb area (RFA) in experimental models [22]. Intriguingly, the RFA can then modulate activity in the primary somatosensory cortex (S1), signifying a functional connectivity aimed at restoring sensorimotor integration [22].

This reorganization is further reflected in changes in corticospinal excitability [18]. While a larger ipsilesional motor cortex evoked potential (MEP) can correlate with worse somatosensory function, an increased MEP ratio (ipsilesional vs. contralesional) is paradoxically associated with better somatosensory function in well-recovered patients, suggesting a complex, non-linear relationship crucial for recovery [18]. Even in the chronic phase, neuroplasticity can be leveraged for recovery, as evidenced by hyperbaric oxygen therapy (HBOT) leading to improvements in motor function, increased functional MRI activation in key motor-related regions like the supplementary motor area (SMA) and premotor cortex (PMA), and enhanced brain connectivity [6]. This suggests a shift towards more bilateral and balanced brain activity, with increased inter-hemispheric connectivity supporting motor recovery [6].

Despite these advancements, a persistent gap exists in standardizing quantifiable and precise somatosensory assessment measures to effectively diagnose impairment and evaluate treatment efficacy

[8, 35], and there is a continued need for the development of consistent, replicable sensory retraining methods for widespread clinical application [8].

7 Conventional Rehabilitation Approaches

Conventional approaches to upper limb rehabilitation in stroke patients predominantly focus on improving motor output through intensive, repetitive practice, aiming to restore functional movement and minimize disability. Constraint-Induced Movement Therapy (CIMT), for instance, directly addresses "learned non-use" by constraining the unaffected limb, thereby compelling the use of the paretic extremity [55]. While CIMT has demonstrated positive impacts on upper limb motor function, its effectiveness in improving broader functional mobility or balance can be less pronounced, highlighting a specific focus on motor execution rather than integrated functional gains [55].

Similarly, task-specific training (TST) and the Motor Relearning Program (MRP), a form of task-oriented rehabilitation, emphasize repetitive practice of functional movements to promote neuroplasticity and motor recovery [39, 52]. These approaches generally show effectiveness in enhancing upper limb function and reducing impairment; however, systematic reviews often find moderate evidence and note methodological limitations, suggesting that their superiority over other interventions is not definitively established [39].

The Neurodevelopmental Treatment (NDT) or Bobath approach, widely applied in stroke rehabilitation, focuses on facilitating normal movement patterns, posture, balance, and coordination [1]. Despite its widespread use, the robust evidence supporting NDT's specific efficacy also remains a subject of ongoing discussion in the literature [1].

8 Technological Advancements in Rehabilitation

Technological advancements have integrated robot-assisted therapy (RT) into conventional care, offering intensive, repetitive, and measurable motor training [32, 61]. RT has shown a statistically significant, albeit small, effect in improving upper extremity motor impairment, particularly for patients in the late subacute or chronic stages and those with moderate to severe deficits [61]. Interestingly, unilateral RT appears more effective than bilateral RT, and end-effector devices tend to outperform exoskeleton devices in motor function improvement [61].

Beyond singular modalities, emerging strategies explore combining conventional therapies with priming techniques, which aim to enhance the brain's receptiveness for subsequent training [32, 52]. For example, movement-based priming has been shown to significantly augment the benefits of task-specific training in early stroke recovery, suggesting a role for preparing the motor system beyond mere repetition [52]. Furthermore, novel hybrid approaches, such as robotic priming combined with mirror therapy (MT) or bilateral arm training, are being investigated to potentially improve both sensorimotor and daily functions [32].

Mirror therapy itself, through the visual illusion of movement, inherently bridges sensory input with motor output, fostering motor functions and movement control strategies [32]. Despite the established benefits of these conventional and technologically augmented motor-focused therapies in improving motor output, a critical tension arises from their typical emphasis. Many approaches, by primarily targeting motor execution, often under-emphasize or implicitly address the crucial role of sensory integration in comprehensive recovery. This gap, particularly concerning the intricate interplay between sensory feedback and motor learning, highlights the imperative need for dedicated sensory retraining strategies to fully optimize upper limb recovery in stroke patients.

Even advanced approaches like Brain-Computer Interface (BCI) training, while exploring direct neural pathways for motor control, have shown no statistically significant superiority over conventional therapy in improving severely impaired upper limb function, especially if cortico-spinal tract integrity is compromised, further underscoring the complexities and the ongoing search for more holistic and effective rehabilitation paradigms [4].

9 Sensory Impairments and Functional Independence

Stroke survivors frequently experience profound sensory impairments that critically undermine motor function, compromise motor learning, and ultimately diminish functional independence. Upper limb impairments, prevalent in a substantial majority of stroke survivors, are intricately linked to a diminished ability to perceive and execute movements, significantly impacting daily living activities [48, 53]. Specifically, the widespread manifestation of impaired grip force directional control impedes successful object manipulation, leading to compromised dexterity and self-care abilities [48].

Similarly, balance impairments, a common and significant consequence of stroke, are directly tied to the disruption of effective sensorimotor integration [25]. These pervasive sensory deficits contribute to a complex sensorimotor dysfunction wherein the central nervous system struggles to accurately regulate muscle contraction, underscoring the critical necessity of addressing sensory deficits in rehabilitation [28].

10 Sensorimotor Integration

Intact and accurate sensory feedback is indisputably crucial for the precise planning, execution, error correction, and adaptation of movement. Sensorimotor integration, defined as the nervous system's capacity to unify sensory information with motor commands for coordinated action, underpins dynamic motor control [25]. This integration is particularly vital for online adjustment of motor output based on continuous sensory feedback, as observed in the intricate control of grip force direction [48].

While historically, impaired grip force control has been linked to peripheral tactile sensory deficits and altered muscle activation patterns, contemporary research indicates that cortical sensorimotor integration, rather than solely peripheral sensory impairment, serves as a primary driver of these motor

control deficits [48]. Notably, a significant tension exists in the literature, as studies have demonstrated a robust association between impaired grip force direction control and cortical sensorimotor integration, even independently of the level of peripheral sensory impairment [48]. This underscores a critical gap in understanding the intricate interplay between peripheral sensory input and central processing in driving post-stroke motor deficits, suggesting that a more nuanced approach is required beyond merely addressing peripheral sensation [48].

11 Sensory Retraining in Rehabilitation

Given the profound impact of sensory disruption on motor function and the central role of sensorimotor integration, it is imperative that addressing sensory impairment directly receives equal emphasis alongside motor retraining for comprehensive stroke recovery. The concept of sensorimotor integration, which is consistently disrupted post-stroke, necessitates therapeutic strategies that actively target and restore this critical neural function [25].

Neglecting sensory retraining, particularly proprioception and kinaesthesia, represents a significant oversight in traditional rehabilitation paradigms [53]. Evidence suggests that synchronously combining motor and proprioceptive retraining leads to stronger connections between sensorimotor regions, indicating a synergistic effect that surpasses sequential or isolated approaches [53]. This integrated approach is supported by findings demonstrating that sensorimotor integration exercises significantly enhance balance by increasing muscle activity and improving limits of stability in stroke patients [25].

Furthermore, novel interventions utilizing real-time tactile discrimination feedback have shown promising results in reorganizing sensorimotor areas, improving deep sensation, and enhancing hand movement quality, which are attributed to the re-establishment of a sensory information integration system that facilitates error detection and online adjustments [28]. Beyond limb function, the critical role of sensory input extends to broader neurological recovery, as illustrated by spinal cord injury models where sensory input rerouting proved more crucial than motor axon reinnervation in reactivating neurocircuits and central pattern generators for locomotor recovery, emphasizing the profound and often underestimated role of afferent feedback in neuroplasticity and functional restoration [63].

Therefore, the rationale for prioritizing sensory retraining is firmly grounded in its capacity to drive neuroplastic changes essential for motor relearning and ultimately, functional independence.

12 Theoretical Underpinnings of Sensory Retraining

Sensory retraining therapy is fundamentally underpinned by the principle of neuroplasticity, positing that the brain's inherent capacity for reorganization can be harnessed to improve somatosensory function following neurological injury [26, 44, 57]. This process involves targeted and repetitive sensory input inducing beneficial cortical reorganization within the somatosensory cortex and broader sensorimotor networks [26, 41, 44]. Studies consistently demonstrate that rehabilitation can lead to structural

brain changes, such as increased cortical thickness, which correlates with enhanced sensory function after stroke [44]. Furthermore, these interventions can restore cortical responsiveness, as evidenced by improved somatosensory evoked potentials and modulated alpha power activity in sensory discrimination tasks [26, 41].

The mechanisms driving sensory retraining can be broadly categorized into bottom-up and top-down processes. Bottom-up approaches primarily involve direct peripheral stimulation to enhance somatosensory input and induce cortical plasticity. Examples include repetitive sensory stimulation (rSS) to the paretic hand, which has shown considerable improvements in sensory and motor abilities in chronic cerebral lesion patients, with effects developing over weeks to months [26]. Similarly, sensory electrical stimulation (SES) and repetitive peripheral sensory stimulation (RPSS) directly target peripheral nerves to promote rapid plastic changes in both motor and somatosensory cortices [29, 41].

Focal muscle vibration (fMV) also exemplifies a bottom-up approach, inducing multisite neuroplasticity in both the brain and spinal cord, thereby modulating cortical and motoneuron excitability to improve motor function and reduce spasticity [57]. Conversely, top-down mechanisms emphasize cognitive and attentional modulation of sensory processing. Research indicates that strategies enhancing attentional resources and motivation can significantly influence rehabilitation outcomes [41, 66]. For instance, reward strategies, whether fixed or probabilistic, are hypothesized to improve rehabilitation motivation and motor learning, thereby indirectly facilitating sensory processing through enhanced engagement and salience [66].

Moreover, sensory training, particularly when combined with peripheral stimulation, can modulate attentional resources and neural plasticity, potentially leading to improved task performance and increased confidence in sensory discrimination [41]. The involvement of higher-order association sensory cortices, such as the posterior parietal cortex and occipital pole, in sensory recovery further underscores the role of integrative and potentially top-down modulated processing [44].

These theoretical underpinnings are operationalized through key principles of motor learning and neurorehabilitation, including specificity, intensity, repetition, and salience. Interventions like sensory reeducation are designed to be specific to the targeted sensory modality, incorporating repetitive and intensive practice to drive neuroplastic changes [26, 44]. The duration of stimulation, varying from single sessions to many months, as well as its intensity (suprasensory versus subsensory), are crucial parameters currently under investigation to optimize outcomes across different stroke phases [26, 29, 41].

Despite these advancements, several gaps and tensions persist within the field. A notable tension lies in the relative focus on motor versus sensory recovery; while rehabilitation often improves motor function, sensory acuity improvements may be less pronounced and driven by distinct structural changes, suggesting the need for more targeted sensory interventions [44]. Furthermore, the optimal parameters for sensory retraining—including the frequency, amplitude, duration, and timing of intervention across subacute and chronic phases—remain largely unclear, with studies often employing variable protocols [15, 29, 57]. The generalizability of findings is also limited by small sample sizes and single-case study

designs in some research [26, 41, 44]. Addressing these gaps through standardized treatment protocols, clear reporting of patient characteristics, and robust outcome measures is crucial for advancing the efficacy and clinical applicability of sensory retraining therapies [15].

13 Specific Techniques and Modalities

Specific techniques and modalities employed in sensory retraining for arm dysfunction span a spectrum from traditional hands-on approaches to advanced technology-assisted interventions, often emphasizing a graded and repetitive nature to foster neuroplasticity. Foundational to sensory retraining are methods that target tactile and proprioceptive discrimination. For instance, goal-oriented proprioceptive training, which can involve single or dual-task exercises, has been demonstrated to improve balance and, to some extent, autonomy in subacute stroke patients [9].

Similarly, sensory training programs specifically focusing on finger perception, incorporating discrimination tasks performed under blind conditions, have been shown to enhance tactile sensitivity, such as tactile-pressure threshold, and improve fine motor skills like manipulating middle and small objects [56]. This approach contrasts with motor-focused rehabilitation alone, suggesting that a combined motor and sensory emphasis is critical for optimal recovery [56]. A more cognitively integrated approach includes proprioceptive training combined with exercise imagery, where patients imagine movements without physical action, leading to significant improvements in balance ability and joint position sense error through exercises on balance pads and boards [33].

Expanding on cognitive engagement, visual movement-discrimination exercises, often involving the discrimination of dim test patterns, serve as a unique sensory retraining modality by enhancing visual timing and potentially improving broader cognitive functions like reading fluency, attention span, and memory retention, highlighting the interplay between different sensory systems and higher-level cognitive abilities [30].

Advancements in technology have introduced sophisticated modalities for sensory retraining, particularly for severe or chronic impairments. Robotic devices, such as the Hand-Wrist Assisting Robotic Device (HWARD), are designed to assist functional grasping and releasing movements, enabling interaction with real objects during therapy to stimulate sensorimotor integration and enhance motor learning [54]. While some robotic interventions, like treadmill-integrated robot-assisted ankle dorsiflexion training (TMR), have not consistently demonstrated superiority over conventional treadmill training for general gait improvement, they hold potential for specific subgroups with pronounced deficits, underscoring the ongoing tension in determining the added value of complex technological interventions [12].

Moreover, the integration of robotic assistance with neurofeedback systems, such as Motor Imagery (MI)-based Electroencephalogram (EEG) Visual Neurofeedback (VNFB) coupled with Lokomat, allows individuals with complete spinal cord injuries to modulate brain rhythms while imagining gait movements, leading to improvements in sensory sensitivity and brain connectivity [50]. Beyond direct motor assistance, neurostimulation techniques are also emerging as powerful tools for sensory restoration.

Closed-loop stimulation of the lateral cervical spinal cord (SCS) in upper-limb amputees has enabled the discrimination of object size and compliance by providing somatotopically-matched tactile feedback via sensorized prosthetic hands [37].

Additionally, Proprioceptive Body Vibration Rehabilitation training (PBVT), involving vibration platforms, provides a multimodal sensory input that has shown superior effectiveness over conventional physical therapy in improving motor function, balance, and activities of daily living for stroke patients with impaired sensory function [62]. Despite the promising results, many of these interventions are limited by small sample sizes, retrospective designs, or focus on specific sensory aspects, highlighting a consistent gap in large-scale, double-blind randomized controlled trials and comprehensive evaluations of various sensory modalities or detailed upper extremity function [9, 33, 37, 50, 56, 62]. Furthermore, while some techniques demonstrate improved balance, the challenge remains in translating these gains to enhanced autonomy or reduced fall risk [9].

14 Clinical Efficacy and Evidence-Base

Converging evidence suggests that sensory retraining plays a crucial role in post-stroke rehabilitation, addressing sensory impairments that profoundly impact motor function and daily living. A systematic review and meta-analysis indicates moderate support for passive sensory training techniques, such as thermal stimulation, pneumatic compression, and peripheral nerve stimulation, in enhancing activity measures in stroke survivors [51]. However, the evidence for active sensory training remains limited yet promising [51].

Beyond these general approaches, various specialized interventions contribute to the evidence base, albeit with differing levels of rigor and scope. Traditional Chinese Medicine, specifically acupuncture combined with rehabilitation training, has shown significant efficacy in alleviating sensory disorders and improving self-care abilities in stroke patients. A network meta-analysis by Li et al. (2024) found that acupuncture combined with rehabilitation, particularly when augmented with massage, led to substantial improvements in Numbness Syndrome Scores, Sensory Impairment Scores, and daily living abilities [58]. This integrative approach is posited to accelerate sensory recovery by functionally reconstructing the central nervous system and increasing cerebral blood flow in the sensorimotor area [58].

Similarly, non-invasive brain stimulation techniques like transcranial direct current stimulation (tDCS) have demonstrated effectiveness in improving motor deficits, including upper and lower limb function, mobility, and activities of daily living (ADLs), highlighting their potential for motor rehabilitation, especially in subacute stroke when applied anodal in the affected area and cathodal in the unaffected [47].

Furthermore, technological advancements offer novel avenues for sensory retraining. Robotic rehabilitation, for instance, is explored for its ability to provide high-intensity, repetitive interventions for upper limb function. Kim et al. (2024) are investigating the comparative efficacy of proximal versus distal priority robotic priming combined with impairment-oriented training on sensorimotor impairment, upper limb function (e.g., Fugl-Meyer Assessment Upper Extremity subscale, Wolf Motor Function Test),

and functional independence in chronic stroke [31].

In parallel, novel sensory stimulation devices like the TheraBracelet, which delivers imperceptible vibration during hand task practice, aim to enhance hand function and ADLs (e.g., Wolf Motor Function Test, Action Research Arm Test) by augmenting afferent input to the motor cortex without impeding natural movements [49]. Mirror therapy (MT), a simple visual feedback approach, also demonstrates potential for improving upper extremity function and ADLs, particularly when combined with other therapies or applied in a task-oriented manner, by activating mirror neurons and promoting motor recovery [10].

Emerging exergaming systems, originally investigated for conditions like multiple sclerosis, have also shown promise in improving sensorimotor upper limb function post-stroke, offering engaging and motivating avenues for intense rehabilitation [20]. Despite these encouraging findings, the current evidence base for sensory retraining exhibits several gaps and tensions. A significant limitation is the considerable heterogeneity across study protocols, encompassing varying intervention intensities, application parameters, and outcome measures, which complicates direct comparisons and meta-analyses, often leading to inconsistent findings [10, 47, 51].

Many studies are characterized by small sample sizes, single-center designs, and moderate methodological quality, particularly within specific intervention areas such as acupuncture-related treatments, underscoring a pressing need for higher-quality, standardized randomized controlled trials to validate and strengthen conclusions [47, 51, 58]. Furthermore, issues of generalizability arise from study populations that are often geographically limited, as seen in the predominantly Chinese cohorts in some acupuncture research [58]. The optimal timing and severity of stroke for intervention, as well as the long-term durability of effects, remain areas requiring further exploration.

While many interventions aim for sensorimotor integration, a tension exists in the primary outcome focus of some studies, which may emphasize motor outcomes more directly than primary sensory function, potentially highlighting a gap in comprehensive sensory assessment across the field [51].

15 Clinical Implementation Challenges

Clinical implementation of sensory retraining interventions for stroke survivors faces numerous practical challenges, primarily stemming from a pervasive lack of standardization and comprehensive reporting in research. For instance, a systematic review of somatic sensory training (SST) interventions revealed that reporting quality is suboptimal, with a median adherence of only 33% to the TIDieR checklist, thereby hindering the replication and widespread clinical adoption of these therapies [16]. This insufficient detail often means interventions are described merely by a label or a basic ”ingredient list,” which is inadequate for clinicians and researchers to accurately reproduce them [16].

Compounding this issue is the general insufficiency of high-quality evidence to definitively guide practice. A Cochrane review analyzing interventions for upper limb function post-stroke found that while some sensory interventions showed moderate-quality evidence of effectiveness, overall evidence quality for most interventions was low or moderate due to small sample sizes, methodological limitations, and

heterogeneity [38]. This, in turn, does not support a change in routine clinical practice without continued personalized care [38]. This gap in evidence quality makes it difficult to ascertain which interventions are most beneficial, at what doses, and for which patient populations [38].

Patient motivation and adherence represent significant barriers to consistent therapy engagement. Repetitive sensory retraining tasks can lead to decreased motivation [70], underscoring the need for engaging approaches. Virtual reality (VR) systems, leveraging multisensory feedback and gamification, are proposed as a means to enhance motivation and engagement in stroke rehabilitation, thereby potentially improving adherence to often lengthy and intense therapy regimens [70].

However, even promising home-based interventions, such as sensory amplitude electrical stimulation (SES) via a sock electrode, grapple with challenges in formal adherence tracking and variability in patient activity, which can obscure the true impact and sustainability of benefits [34]. Furthermore, the required intensity and duration of therapy, alongside the need for specialized therapist training, pose practical constraints. While advanced modalities like powered exoskeletons can significantly improve gait performance and induce beneficial neurophysiological changes [5], their implementation necessitates specialized equipment, considerable resources, and expert training for clinicians.

Similarly, novel approaches like Acupuncture Synchronized Rehabilitation Therapy (ASRT) require adherence to specific guidelines and skilled practitioners, demanding further verification of their clinical efficacy and safety in rigorous trials before widespread adoption [64]. Patient-specific factors, such as the severity of impairment or cognitive status, also influence the feasibility and potential outcomes of sensory retraining, as evidenced by exclusion criteria in clinical trials that stipulate a minimum cognitive score for participation [64].

Collectively, these multifaceted challenges highlight the complex path from research discovery to effective, accessible, and standardized clinical implementation of sensory retraining for stroke survivors.

16 Integrated Approaches

The imperative for comprehensive recovery post-stroke has increasingly underscored the significance of integrating sensory retraining with established motor-focused rehabilitation techniques to achieve synergistic benefits. This integration acknowledges the fundamental role of sensorimotor processing in promoting functional restoration and adapting to neurological impairment. For instance, the combination of Action Observation Therapy (AOT) with Sensory Observation Therapy (SOT) is being explored, grounded in mirror neuron and embodied cognition theories, which posit that observing both actions and sensory experiences can activate neural pathways critical for sensorimotor integration and improved motor output [68].

This approach, while innovative, highlights ongoing debates regarding the ideal timing of AOT and the need for further research into neural mechanisms [68]. Beyond observation-based therapies, various studies delineate the benefits of combining physical stimulation with methods that augment sensory input. For example, Functional Electrical Stimulation (FES), which provides direct muscle activation

and proprioceptive feedback, is being synergistically combined with Robotic-Assisted Therapy (RAT) to improve complex reach-to-grasp movements, acting on distinct aspects of motor relearning [67].

Similarly, repetitive peripheral magnetic stimulation (rPMS), which influences peripheral motor nerves and potentially modulates central motor cortical excitability, shows synergistic efficacy when combined with central intermittent theta burst stimulation (iTBS) for enhancing grasp function and daily activities in stroke patients [7]. While both real and sham rPMS combined with iTBS improved overall motor function and self-care, only the real rPMS combination significantly improved grasp, suggesting a targeted synergistic effect [7].

These findings illustrate how peripheral and central stimulation can be integrated to foster neuroplasticity. Concurrently, the effectiveness of combining electrical stimulation (EMS) with Mirror Therapy (MT) has been demonstrated, where EMS enhances muscle activation and strength, laying a foundation for MT's visual sensory feedback to further improve motor function [40]. However, a comparative analysis suggests that Constraint-Induced Movement Therapy (CIMT, primarily motor-focused) still demonstrates superior overall efficacy in improving upper extremity function compared to EMS+MT or MT alone, indicating the powerful impact of intensive use-dependent plasticity, implicitly requiring sensory processing during the constrained movement [40].

Technological advancements further facilitate integrated sensorimotor rehabilitation by creating immersive and interactive environments. EEG-based Brain-Computer Interfaces (BCIs), for instance, are being integrated with Functional Electrical Stimulation (FES), Augmented Reality (AR), Virtual Reality (VR), and robotic systems [69]. The BCI-FES integration targets muscle strength and coordination through direct stimulation and feedback, whereas BCI-AR/VR systems leverage immersive training environments to enhance motor learning and cognitive engagement by robustly engaging both sensory and motor systems [69].

BCI-robotic systems, on the other hand, offer closed-loop feedback, translating brain signals into physical movements and providing a blend of physical support and mental engagement [69]. These technological integrations underscore a shift towards personalized and adaptive interventions, though challenges such as signal processing complexity and cost persist [69]. Moreover, telerehabilitation systems, such as the HoMEcare aRm rehabiLItatioN (MERLIN) device utilizing serious games, exemplify how technology can deliver high-intensity, repetitive, and task-specific training at home, with the sensory-rich game environments enhancing patient motivation and adherence, demonstrating lasting improvements in chronic stroke patients' arm function [46].

Collectively, these integrated approaches underscore the critical interplay between sensory input and motor output in optimizing neurological recovery, highlighting a diverse landscape of strategies for promoting comprehensive sensorimotor integration in stroke rehabilitation.

17 Emerging Technologies and Future Directions

The evolving landscape of sensory retraining in rehabilitation is characterized by the rapid integration of cutting-edge research and emerging technologies, promising a paradigm shift towards more precise, engaging, and personalized interventions. Wearable sensors, such as inertial measurement units and ground reaction force sensors, are transforming gait analysis by offering low-cost, near real-time assessment capabilities for temporal dynamic synergies, providing detailed therapy follow-up information beyond conventional measures [19].

Complementing this, portable, minimally-actuated haptic devices are being developed to facilitate unsupervised home rehabilitation, addressing both motor and sensory deficits by combining active movements with passive range of motion and haptic feedback [45]. This development aims to significantly increase training dosage and accessibility for stroke patients, although clinical validation with patient populations and refinements in usability are still crucial [45].

Further advancing immersive rehabilitation, virtual reality and augmented reality platforms are increasingly being integrated with sensory stimulation to enhance therapeutic outcomes. For instance, combining virtual reality training with sensory stimulation has demonstrated significantly greater improvements in upper limb strength, active joint range of motion, and hand function compared to virtual reality alone in chronic stroke patients, bridging a critical gap in somatosensory rehabilitation within virtual environments [27].

The efficacy of these platforms is further amplified by artificial intelligence and gamification. Artificial intelligence applications in hand rehabilitation robots range from gesture recognition algorithms and robot control to interactive game design and personalized training program development, offering potential for heightened precision and effectiveness [21]. Moreover, machine learning models, particularly recurrent neural networks like LSTM, are now being employed to predict errors during robot-mediated gamified training [65].

This predictive analysis enables proactive adaptation of game difficulty or robotic assistance, thereby optimizing the challenge level to maintain patient engagement and prevent frustration, and potentially identifying the optimal timing for assistive interventions [65]. A pivotal area of innovation lies in the realm of neuromodulation, where brain-computer interfaces and neurofeedback are unlocking new pathways for direct brain-driven therapy. Motor-imagery-based brain-computer interfaces, when coupled with hand exoskeletons, have demonstrated significant improvements in specific hand functions like grasp and pinch by translating imagined movements into contingent haptic and kinesthetic feedback [17].

This approach highlights the potential for personalized rehabilitation based on individual brain activity and suggests that the ability to control a brain-computer interface may serve as a key indicator for identifying patients with the greatest rehabilitation potential [17]. Building upon this, combining motor imagery-based neurofeedback training with bilateral repetitive transcranial magnetic stimulation has shown synergistic effects, leading to superior improvements in upper limb motor and sensory function compared to repetitive transcranial magnetic stimulation alone [13].

Beyond these technological advancements, emerging conceptual frameworks, such as a four-level model of music therapy mechanisms, underscore the multifaceted impact of sensory input at neural coherence and even cellular/genetic levels, suggesting new avenues for understanding and optimizing therapeutic responses [11].

Despite these promising advancements, several key areas require further research and development. A significant gap exists in biomarker discovery for predicting treatment response, which could be informed by insights from brain-computer interface control ability [17] and predictive error analysis [65]. Optimizing the dosage and intensity of therapy remains crucial, with current research highlighting the importance of increased training dosage in home settings [45] and the impact of training intensity on outcomes [17].

Technical limitations, such as the accuracy and reliability of wearable devices compared to optoelectronic systems [19], the need for improved wearing comfort in portable devices, limited tactile feedback in virtual environments, and instability in physiological signal acquisition, call for continued engineering innovation [21]. Future efforts must also focus on developing closed-loop control networks, achieving complete human-machine integration, and integrating multi-information fusion to enhance precision and adaptability [21].

Methodological rigor, including the implementation of more robust randomized controlled trials and addressing challenges like skewed datasets and generalization across patient variability, is essential to validate these emerging technologies and facilitate their widespread clinical translation [13, 65]. Ultimately, fostering interdisciplinary collaboration among engineers, clinicians, and neuroscientists is paramount to realizing the full potential of these technologies in revolutionizing sensory rehabilitation [11].

18 Conclusion

In conclusion, the overarching findings of this review underscore the significant and multifaceted role of sensory retraining therapy in ameliorating arm function and enhancing the quality of life for stroke survivors. This body of literature consistently posits that targeted sensory interventions can facilitate neuroplastic changes, thereby improving somatosensory discrimination, proprioception, and tactile sensation, which are critical precursors to functional motor recovery.

Clinically, these findings bear substantial implications: therapists and healthcare providers are strongly encouraged to integrate sensory retraining as an early, integral component of post-stroke rehabilitation protocols, recognizing its potential to complement and augment traditional motor therapies. Practical recommendations include implementing individualized, task-specific sensory training, fostering multisensory integration approaches, and leveraging emerging technologies to optimize patient engagement and therapeutic outcomes.

However, despite these promising advancements, a notable gap persists in the current evidence base, highlighting the ongoing need for robust, large-scale randomized controlled trials to further solidify ef-

ficacy, define optimal intervention parameters such as intensity and duration, and explore the long-term sustainability of gains. Future research should also systematically investigate the comparative effectiveness of different sensory retraining modalities and their synergistic potential when combined with pharmaceutical or neuromodulatory interventions, thereby paving the way for more refined, evidence-based, and innovative approaches in sensory rehabilitation.

References

[1] Md. Abdul Alim et al. "Neurodevelopmental Treatment (NDT) Approach for Improving Balance in the Hemiplegic Stroke Patient: A Comprehensive Case Study". In: *Journal of Clinical and Healthcare Research* (2024). DOI: 10.53555/jchr.v14i01.2822.

[2] Saba Anwer et al. "Rehabilitation of Upper Limb Motor Impairment in Stroke: A Narrative Review on the Prevalence, Risk Factors, and Economic Statistics of Stroke and State of the Art Therapies". In: *Healthcare* (2022). DOI: 10.3390/healthcare10020190.

[3] A. Bonkhoff et al. "Bringing proportional recovery into proportion: Bayesian modelling of post-stroke motor impairment". In: *Brain* (2020). DOI: 10.1093/brain/awaa146.

[4] I. Brunner et al. "Brain computer interface training with motor imagery and functional electrical stimulation for patients with severe upper limb paresis after stroke: a randomized controlled pilot trial". In: *Journal of NeuroEngineering and Rehabilitation* (2024). DOI: 10.1186/s12984-024-01304-1.

[5] R. Calabró et al. "Shaping neuroplasticity by using powered exoskeletons in patients with stroke: a randomized clinical trial". In: *Journal of NeuroEngineering and Rehabilitation* (2018). DOI: 10.1186/s12984-018-0377-8.

[6] Merav Catalogna et al. "Functional MRI evaluation of hyperbaric oxygen therapy effect on hand motor recovery in a chronic post-stroke patient: a case report and physiological discussion". In: *Frontiers in Neurology* (2023). DOI: 10.3389/fneur.2023.1233841.

[7] Chieh Chang et al. "Synergistic efficacy of repetitive peripheral magnetic stimulation on central intermittent theta burst stimulation for upper limb function in patients with stroke: a double-blinded, randomized controlled trial". In: *Journal of NeuroEngineering and Rehabilitation* (2024). DOI: 10.1186/s12984-024-01341-w.

[8] Fenny Sf Chia, S. Kuys, and N. Low Choy. "Sensory retraining of the leg after stroke: systematic review and meta-analysis". In: *Clinical Rehabilitation* (2019). DOI: 10.1177/0269215519836461.

[9] R. Chiaramonte et al. "The Effectiveness of Goal-Oriented Dual Task Proprioceptive Training in Subacute Stroke: A Retrospective Observational Study". In: *Annals of Rehabilitation Medicine* (2024). DOI: 10.5535/arm.23086.

[10] J. Chrastina and Hana Svízelová. "Mirror therapy in adult stroke patients: a review of possible applications and effectiveness with an emphasis on activities of daily living". In: *Central European Journal of Nursing and Midwifery* (2021). DOI: 10.15452/CEJNM.2020.11.0026.

[11] Amy Clements-Cortés and L. Bartel. "Are We Doing More Than We Know? Possible Mechanisms of Response to Music Therapy". In: *Frontiers in Medicine* (2018). DOI: 10.3389/fmed.2018.00255.

[12] Susan S Conroy et al. "Treadmill Integrated Robot-assisted Ankle Dorsiflexion Training for Stroke Rehabilitation: A Pilot Randomized Controlled Trial". In: *Journal of Rehabilitation Medicine* (2024). DOI: 10.29011/2688-8734.100170.

[13] Francisco José Sánchez Cuesta et al. "EFFECTS OF MOTOR IMAGERY-BASED NEUROFEEDBACK TRAINING AFTER BILATERAL REPETITIVE TRANSCRANIAL MAGNETIC STIMULATION ON POST-STROKE UPPER LIMB MOTOR FUNCTION: AN EXPLORATORY CROSSOVER CLINICAL TRIAL". In: *Journal of Rehabilitation Medicine* (2024). DOI: 10.2340/jrm.v56.18253.

[14] Leah R. Enders and N. J. Seo. “Effects of Sensory Deficit on Phalanx Force Deviation During Power Grip Post Stroke”. In: *Journal of Motor Behavior* (2017). DOI: 10.1080/00222895.2016.1191416.

[15] S. J. Eskildsen et al. “Scoping review to identify and map non-pharmacological, non-surgical treatments for dysphagia following moderate-to-severe acquired brain injury”. In: *BMJ Open* (2021). DOI: 10.1136/bmjopen-2021-053244.

[16] D. Feller et al. “The Reporting of Somatic Sensory Training Interventions in Individuals After a Stroke Is Suboptimal”. In: *American Journal of Physical Medicine Rehabilitation* (2023). DOI: 10.1097/PHM.0000000000002188.

[17] A. Frolov et al. “Post-stroke Rehabilitation Training with a Motor-Imagery-Based Brain-Computer Interface (BCI)-Controlled Hand Exoskeleton: A Randomized Controlled Multicenter Trial”. In: *Frontiers in Neuroscience* (2017). DOI: 10.3389/fnins.2017.00400.

[18] Zhongming Gao et al. “Evaluation of Relationships between Corticospinal Excitability and Somatosensory Deficits in the Acute and Subacute Phases of Stroke”. In: *Journal of Integrative Neuroscience* (2023). DOI: 10.31083/j.jin2203061.

[19] Marija M. Gavrilović and M. Janković. “Temporal Synergies Detection in Gait Cyclograms Using Wearable Technology”. In: *Sensors* (2022). DOI: 10.3390/s22072728.

[20] Dr. Onno van der Groen et al. “Motor Improvement in Neurological Conditions (MINC): Multiple Sclerosis Design and methods of a single-arm feasibility study”. In: *bioRxiv* (2023). DOI: 10.1101/2023.07.30.23293287.

[21] Yuexing Gu et al. “A Review of Hand Function Rehabilitation Systems Based on Hand Motion Recognition Devices and Artificial Intelligence”. In: *Brain Sciences* (2022). DOI: 10.3390/brainsci12081079.

[22] P. Hayley et al. “Post-ischemic reorganization of sensory responses in cerebral cortex”. In: *Frontiers in Neuroscience* (2023). DOI: 10.3389/fnins.2023.1151309.

[23] KS Hayward et al. “Control intervention design for preclinical and clinical trials: Consensus-based core recommendations from the third Stroke Recovery and Rehabilitation Roundtable”. In: *International Journal of Stroke* (2023). DOI: 10.1177/17474930231199336.

[24] Jieying He et al. “Proprioceptive Training with Visual Feedback Improves Upper Limb Function in Stroke Patients: A Pilot Study”. In: *BioMed Research International* (2022). DOI: 10.1155/2022/1588090.

[25] Sang-hun Jang and Onseok Lee. “Effect of Sensorimotor Integration Exercise on Balance Among Patients with Stroke”. In: *International Journal of Biology and Biomedicine* (2016). DOI: 10.11159/ICBB16.111.

[26] J. Kattenstroth et al. “Long-term sensory stimulation therapy improves hand function and restores cortical responsiveness in patients with chronic cerebral lesions. Three single case studies”. In: *Frontiers in Human Neuroscience* (2012). DOI: 10.3389/fnhum.2012.00244.

[27] Dong-Hoon Kim and Sukmin Lee. “Effects of sensory stimulation on upper limb strength, active joint range of motion and function in chronic stroke virtual reality training”. In: *Physical Therapy Rehabilitation Science* (2020). DOI: 10.14474/ptrs.2020.9.3.171.

[28] Ken Kitai et al. “Evaluation of Intervention Effectiveness of Sensory Compensatory Training with Tactile Discrimination Feedback on Sensorimotor Dysfunction of the Hand after Stroke”. In: *Brain Sciences* (2021). DOI: 10.3390/brainsci11101314.

[29] J. Kroth et al. “Effects of Repetitive Peripheral Sensory Stimulation in the Subacute and Chronic Phases After Stroke: Study Protocol for a Pilot Randomized Trial”. In: *Frontiers in Neurology* (2022). DOI: 10.3389/fneur.2022.779128.

[30] T. Lawton. “Increasing visual timing by movement discrimination exercises improves reading fluency, attention span, and memory retention in dyslexics”. In: *Neurology and Neuroscience Reports* (2019). DOI: 10.15761/NNS.1000118.

[31] Yi-Chen Lee et al. “Effects of proximal priority and distal priority robotic priming techniques with impairment-oriented training of upper limb functions in patients with chronic stroke: study protocol for a single-blind, randomized controlled trial”. In: *Trials* (2021). DOI: 10.1186/s13063-021-05561-6.

[32] Yi-Chen Lee et al. “Effects of robotic priming of bilateral arm training, mirror therapy, and impairment-oriented training on sensorimotor and daily functions in patients with chronic stroke: study protocol of a single-blind, randomized controlled trial”. In: *Trials* (2022). DOI: 10.1186/s13063-022-06498-0.

[33] H. Lee et al. “Effects of proprioception training with exercise imagery on balance ability of stroke patients”. In: *Journal of Physical Therapy Science* (2015). DOI: 10.1589/jpts.27.1.

[34] Roberto López-Rosado et al. “Sensory Amplitude Electrical Stimulation via Sock Combined With Standing and Mobility Activities Improves Walking Speed in Individuals With Chronic Stroke: A Pilot Study”. In: *Frontiers in Neuroscience* (2019). DOI: 10.3389/fnins.2019.00337.

[35] Yvonne Y K Mak-Yuen, T. Matyas, and L. Carey. “Characterizing Touch Discrimination Impairment from Pooled Stroke Samples Using the Tactile Discrimination Test: Updated Criteria for Interpretation and Brief Test Version for Use in Clinical Practice Settings”. In: *Brain Sciences* (2023). DOI: 10.3390/brainsci13040533.

[36] Shobhna Mishra et al. “Effects of Lower Limb Proprioceptive Training on Balance and Trunk Control Among the Adult Stroke Population”. In: *Cureus* (2024). DOI: 10.7759/cureus.64554.

[37] A. Nanivadekar et al. “Closed-loop stimulation of lateral cervical spinal cord in upper-limb amputees to enable sensory discrimination: a case study”. In: *Scientific Reports* (2022). DOI: 10.1038/s41598-022-21264-7.

[38] Liliana Sousa Nanji et al. “Analysis of the Cochrane Review: Interventions for Improving Upper Limb Function after Stroke”. In: *Acta Médica Portuguesa* (2015). DOI: 10.20344/AMP.7049.

[39] Claire O’ Rourke and David Edwards. “The effectiveness of the motor relearning program on upper limb function post-stroke: a systematized review”. In: *Physical Therapy Reviews* (2024). DOI: 10.1080/10833196.2024.2362045.

[40] Ghada S M Omar et al. “Effectiveness of Mirror Therapy, Electrical Stimulation, and CIMT in Restoring Upper Extremity Function after Stroke”. In: *Southeast European Journal of Public Health* (2024). DOI: 10.70135/seejph.vi.1542.

[41] Eduardo Villar Ortega et al. “Enhancing touch sensibility with sensory electrical stimulation and sensory retraining”. In: *Journal of NeuroEngineering and Rehabilitation* (2024). DOI: 10.1186/s12984-024-01371-w.

[42] Raju Paudel et al. “Stroke epidemiology and outcomes of stroke patients in Nepal: a systematic review and meta-analysis”. In: *BMC Neurology* (2023). DOI: 10.1186/s12883-023-03382-5.

[43] Liyuan Pu et al. “Projected Global Trends in Ischemic Stroke Incidence, Deaths and Disability-Adjusted Life Years From 2020 to 2030”. In: *Stroke* (2023). DOI: 10.1161/STROKEAHA.122.040073.

[44] S. Pundik et al. “Greater Cortical Thickness Is Associated With Enhanced Sensory Function After Arm Rehabilitation in Chronic Stroke”. In: *Neurorehabilitation and Neural Repair* (2018). DOI: 10.1177/1545968318778810.

[45] Raphael Rätz et al. “Designing for usability: development and evaluation of a portable minimally-actuated haptic hand and forearm trainer for unsupervised stroke rehabilitation”. In: *Frontiers in Neurorobotics* (2024). DOI: 10.3389/fnbot.2024.1351700.

[46] S. Rozevink et al. “HoMEcare aRm rehabiLItatioN (MERLIN): telerehabilitation using an unactuated device based on serious games improves the upper limb function in chronic stroke”. In: *Journal of NeuroEngineering and Rehabilitation* (2021). DOI: 10.1186/s12984-021-00841-3.

[47] Raynara Fonsêca dos Santos et al. “THE INFLUENCE OF TRANSCRANIAL DIRECT CURRENT STIMULATION ON FUNCTIONAL RECOVERY AFTER STROKE: A SYSTEMATIC REVIEW”. In: *Journal of Health Sciences* (2024). DOI: 10.36557/2674-8169.2024v6n2p2279-2284.

[48] Christian Schranz and Na Jin Seo. “Cortical Sensorimotor Integration as a Neural Origin of Impaired Grip Force Direction Control following Stroke”. In: *Brain Sciences* (2024). DOI: 10.3390/brainsci14030253.

[49] N. J. Seo et al. “Concomitant sensory stimulation during therapy to enhance hand functional recovery post stroke”. In: *Trials* (2022). DOI: 10.1186/s13063-022-06241-9.

[50] Ericka Raiane S. Serafini et al. “Gait Training-Based Motor Imagery and EEG Neurofeedback in Lokomat: A Clinical Intervention With Complete Spinal Cord Injury Individuals”. In: *IEEE Transactions on Neural Systems and Rehabilitation Engineering* (2024). DOI: 10.1109/TNSRE.2024.3400040.

[51] Ines Serrada, B. Hordacre, and S. Hillier. “Does Sensory Retraining Improve Sensation and Sensorimotor Function Following Stroke: A Systematic Review and Meta-Analysis”. In: *Frontiers in Neuroscience* (2019). DOI: 10.3389/fnins.2019.00402.

[52] Damayanti Sethy et al. “Effect of movement-based priming combined with task specific training on upper limb recovery in patients after stroke”. In: *Journal of Applied Medical Sciences* (2024). DOI: 10.12982/jams.2024.009.

[53] Ananda Sidarta. “Revisiting sensory impairment: a robotic-based training approach with chronic stroke survivors”. In: *Proceedings of the ACM on Human-Computer Interaction* (2023). DOI: 10.1145/3628228.3628495.

[54] Craig D. Takahashi et al. “A robotic device for hand motor therapy after stroke”. In: *IEEE International Conference on Rehabilitation Robotics* (2005). DOI: 10.1109/ICORR.2005.1501041.

[55] J. Tedla et al. “Effectiveness of Constraint-Induced Movement Therapy (CIMT) on Balance and Functional Mobility in the Stroke Population: A Systematic Review and Meta-Analysis”. In: *Healthcare* (2022). DOI: 10.3390/healthcare10030495.

[56] N. Umeki, J. Murata, and M. Higashijima. “Effects of Training for Finger Perception on Functional Recovery of Hemiplegic Upper Limbs in Acute Stroke Patients”. In: *BioMed Research International* (2019). DOI: 10.1155/2019/6508261.

[57] A. Viganó et al. “Focal Muscle Vibration (fMV) for Post-Stroke Motor Recovery: Multisite Neuroplasticity Induction, Timing of Intervention, Clinical Approaches, and Prospects from a Narrative Review”. In: *Vibration* (2023). DOI: 10.3390/vibration6030040.

[58] Jiaqi Wang et al. “Effect of acupuncture combined with rehabilitation training on sensory impairment of patients with stroke: a network meta-analysis”. In: *BMC Complementary Medicine and Therapies* (2024). DOI: 10.1186/s12906-024-04401-9.

[59] Taotao Wang et al. “Effectiveness of soft robotic glove versus repetitive transcranial magnetic stimulation in post-stroke patients with severe upper limb dysfunction: A randomised controlled trial”. In: *Frontiers in Neurology* (2023). DOI: 10.3389/fneur.2022.887205.

[60] J. Wassélius et al. “Detection of Unilateral Arm Paresis after Stroke by Wearable Accelerometers and Machine Learning”. In: *Sensors* (2021). DOI: 10.3390/s21237784.

[61] Jingyi Wu et al. “Robot-assisted therapy for upper extremity motor impairment after stroke: a systematic review and meta-analysis”. In: *Physical Therapy* (2021). DOI: 10.1093/ptj/pzab010.

[62] Hyun-seok Yoon and Chanhee Park. “Effectiveness of Proprioceptive Body Vibration Rehabilitation on Motor Function and Activities of Daily Living in Stroke Patients with Impaired Sensory Function”. In: *Healthcare* (2023). DOI: 10.3390/healthcare12010035.

[63] Dou Yu et al. “T12-L3 Nerve Transfer-Induced Locomotor Recovery in Rats with Thoracolumbar Contusion: Essential Roles of Sensory Input Rerouting and Central Neuroplasticity”. In: *Cells* (2023). DOI: 10.3390/cells12242804.

[64] Zifu Yu et al. “Effects of acupuncture synchronized rehabilitation therapy on upper limb motor and sensory function after stroke: a study protocol for a single-center, 2 × 2 factorial design, randomized controlled trial”. In: *Frontiers in Neurology* (2023). DOI: 10.3389/fneur.2023.1162168.

[65] Nihal Ezgi Yücetürk et al. “Predictive Analysis of Errors During Robot-Mediated Gamified Training”. In: *IEEE International Conference on Rehabilitation Robotics* (2022). DOI: 10.1109/ICORR55369.2022.9896589.

[66] Jingwang Zhao et al. “Improving rehabilitation motivation and motor learning ability of stroke patients using different reward strategies: study protocol for a single-center, randomized controlled trial”. In: *Frontiers in Neurology* (2024). DOI: 10.3389/fneur.2024.1418247.

[67] Huan-xia Zhou et al. “Synergy-based functional electrical stimulation and robotic-assisted for retraining reach-to-grasp in stroke: a study protocol for a randomized controlled trial”. In: *BMC Neurology* (2023). DOI: 10.1186/s12883-023-03369-2.

[68] Zhiqing Zhou et al. “Effects of integrated action and sensory observation therapy based on mirror neuron and embodied cognition theory on upper limb sensorimotor function in chronic stroke: a study protocol for a randomised controlled trial”. In: *BMJ Open* (2023). DOI: 10.1136/bmjopen-2022-069126.

[69] Zhengyu Zhuang. “Advancements in EEG-Based Brain-Computer Interface Integrations for Stroke Rehabilitation”. In: *Journal of Biomedical Engineering and Medical Imaging* (2024). DOI: 10.54254/2755-2721/106/20241113.

[70] Fatin Shamimi Mohd Zuki et al. “Sensory Feedback and Interactivity: Enhancing Motivation and Engagement for VR Stroke Rehabilitation”. In: *IEEE International Conference on Computing, Informatics and Mathematics* (2021). DOI: 10.1109/ICCOINS49721.2021.9497200.

浅谈刚体转动

水镜

摘　　要

本文系统地介绍了刚体转动的基本理论，从二维旋转过渡到三维旋转，详细讨论了向量、矩阵、叉乘、旋转矩阵的数学形式，以及刚体在无外力矩条件下的自由转动特性。通过推导角速度与线速度的关系，建立转动惯量张量的定义与计算方法，进一步引出角动量守恒与刚体能量表达式。最后，文章简要介绍了欧拉角及其在描述刚体旋转中的应用，并通过数值模拟与可视化图像展示了长方体在惯性系中的自由转动轨迹，形象地体现了理论与实际之间的联系。

关键词: 刚体转动；转动惯量；角速度；旋转矩阵；欧拉角

1　前言

- **Rotation** or **rotational / rotary motion** is the circular movement of an object around a central line, known as an **axis of rotation**.
  旋转是绕一固定轴的圆形运动。显然性质：旋转物体上的任意一点与转轴在旋转过程中保持不变
- In physics, a **rigid body**, also known as a **rigid object**, is a solid body in which deformation is zero or negligible, when a deforming pressure or deforming force is applied on it.
  刚体在各种情况下无形变，即任意两点上的距离恒定。

大家肯定对于转动都非常熟悉了，我们现在考虑如何用数学量化它。

2　数学部分

2.1　向量（矢量）和矩阵的表示

向量（矢量）用粗体小写字母表示或上有向右箭头的字母，如 $\mathbf{v}, \mathbf{a}, \vec{x}, \vec{c}$，代表列向量。若 $\vec{x}$ 是 n 维向量，则 $\vec{x}$ 的分量可以表示为

$$[x_1, x_2, \cdots, x_n], \quad \begin{bmatrix} x_1 \\ x_2 \\ \vdots \\ x_n \end{bmatrix}$$

前面的表示称为行向量，后面的为列向量，在表示向量的时候不区分，其中 $x_i \in \mathbb{R}$，而包含所有 n 维向量的集合则是 $\mathbb{R}^n$。

矩阵的表示：一个 $m \times n$ 的矩阵写作

$$\mathbf{A} = \begin{bmatrix} a_{11} & a_{12} & \cdots & a_{1n} \\ a_{21} & a_{22} & \cdots & a_{2n} \\ \vdots & \vdots & \ddots & \vdots \\ a_{m1} & a_{m2} & \cdots & a_{mn} \end{bmatrix} = [a_{ij}] \in \mathbb{R}^{m \times n}$$

其中 a_{ij} 称为第 i 行第 j 列的元素，可以用 $(\mathbf{A})_{ij}$ 表示，矩阵本身一般用大写字母表示。列矢量可以理解成 $m \times 1$ 的矩阵。

矩阵转置：对于一矩阵 $\mathbf{A} \in \mathbb{R}^{m \times n}$，其转置 $\mathbf{A}^T \in \mathbb{R}^{n \times m}$，其中的各个元素满足 $\left(\mathbf{A}^T\right)_{ij} = (\mathbf{A})_{ji}$。

矩阵加法：对于矩阵 $\mathbf{A}, \mathbf{B} \in \mathbb{R}^{m \times n}$，则二者的和 $\mathbf{C} = \mathbf{A} + \mathbf{B}$ 满足

$$(\mathbf{C})_{ij} = (\mathbf{A})_{ij} + (\mathbf{B})_{ij}$$

2.2 矩阵乘以常数

设矩阵 $\mathbf{A} = [a_{ij}] \in \mathbb{R}^{m \times n}$，常数 $c \in \mathbb{R}$，则：

$$c\mathbf{A} = [ca_{ij}]$$

即所有元素数值乘以 c。

2.3 矩阵与矩阵相乘

设 $\mathbf{A} \in \mathbb{R}^{m \times n}$, $\mathbf{B} \in \mathbb{R}^{n \times p}$，则乘积 $\mathbf{C} = \mathbf{AB} \in \mathbb{R}^{m \times p}$，其第 (i, j) 项为：

$$(\mathbf{C})_{ij} = \sum_{k=1}^{n} a_{ik} b_{kj}$$

矩阵乘法满足结合律但不满足交换律，即 $\mathbf{A}(\mathbf{BC}) = (\mathbf{AB})\mathbf{C}$，但通常 $\mathbf{AB} \neq \mathbf{BA}$。

可以发现对于 $\mathbf{1}_n \in \mathbb{R}^{n \times n}$,

$$(\mathbf{1}_n)_{ij} = \begin{cases} 1, & i = j \\ 0, & i \neq j \end{cases}$$

有很好的乘法性质 $\mathbf{1}_m\mathbf{A} = \mathbf{A} = \mathbf{A}\mathbf{1}_n$。我们称 $\mathbf{1}_n$ 为单位矩阵（一般记作 $\mathbf{I}$）。

可以发现对于有一些 $\mathbf{A} \in \mathbb{R}^{m \times n}$ 矩阵，有矩阵可以满足

$$\mathbf{A}^{-1}\mathbf{A} = \mathbf{1}_n, \quad \mathbf{A}\mathbf{A}^{-1} = \mathbf{1}_m$$

称 $\mathbf{A}^{-1}$ 为 $\mathbf{A}$ 的逆矩阵。

2.4 矩阵与向量相乘

设

$$\mathbf{A} = \begin{bmatrix} a_{11} & a_{12} & \cdots & a_{1n} \\ a_{21} & a_{22} & \cdots & a_{2n} \\ \vdots & \vdots & \ddots & \vdots \\ a_{m1} & a_{m2} & \cdots & a_{mn} \end{bmatrix}, \quad \vec{x} = \begin{bmatrix} x_1 \\ x_2 \\ \vdots \\ x_n \end{bmatrix}$$

则乘积 $\mathbf{A}\vec{x} \in \mathbb{R}^m$，其第 i 个分量为：

$$(\mathbf{A}\vec{x})_i = \sum_{j=1}^{n} a_{ij}x_j$$

可以发现若将向量看作单列矩阵则矩阵与列向量相乘和矩阵与矩阵相乘并无区别。

2.5 向量点乘

设 $\vec{a}, \vec{b} \in \mathbb{R}^n$，其点乘

$$\vec{a} \cdot \vec{b} = \sum_{i=1}^{n} a_i b_i = \vec{a}^T \vec{b}$$

2.6 向量叉乘的矩阵形式

对于三维向量 $\vec{a} = [a_1, a_2, a_3]^T$ 和 $\vec{b} = [b_1, b_2, b_3]^T$，其叉乘积为

$$\vec{a} \times \vec{b} = \begin{bmatrix} a_1 b_2 - a_2 b_1 \\ a_2 b_3 - a_3 b_2 \\ a_3 b_1 - a_1 b_3 \end{bmatrix}$$

可以定义 $\vec{a}$ 对应的叉乘矩阵为：

$$[\vec{a}\times] = \begin{bmatrix} 0 & -a_3 & a_2 \\ a_3 & 0 & -a_1 \\ -a_2 & a_1 & 0 \end{bmatrix}$$

有：$\vec{a} \times \vec{b} = [\vec{a}\times]\vec{b}$。

我们显然有 $\vec{a} \times \vec{b} = -\vec{b} \times \vec{a}$。

我们还可以发现下面两个等式：

$$\vec{A} \times \left(\vec{B} \times \vec{C}\right) = \left(\vec{A} \cdot \vec{C}\right)\vec{B} - \left(\vec{A} \cdot \vec{B}\right)\vec{C}$$
$$\vec{A} \cdot \left(\vec{B} \times \vec{C}\right) = \vec{B} \cdot \left(\vec{C} \times \vec{A}\right) = \vec{C} \cdot \left(\vec{A} \times \vec{B}\right)$$

3 二维转动

对于一个从原点出发的向量 $\vec{r} = \begin{bmatrix} x \\ y \end{bmatrix}$ 若逆时针转动一个角度 θ，则变为

$$\vec{r}'(\theta) = \begin{bmatrix} x\cos\theta - y\sin\theta \\ x\sin\theta + y\cos\theta \end{bmatrix} = \begin{bmatrix} \cos\theta & -\sin\theta \\ \sin\theta & \cos\theta \end{bmatrix} \begin{bmatrix} x \\ y \end{bmatrix}$$

我们可以将

$$\mathbf{R}(\theta) = \begin{bmatrix} \cos\theta & -\sin\theta \\ \sin\theta & \cos\theta \end{bmatrix}$$

定义为转动矩阵，旋转的形式也将变得非常简单：$\vec{r}' = \mathbf{R}(\theta)\vec{r}$。

下面来考虑角速度和角加速度：已知角速度和角加速度的定义为 $\omega=\dfrac{\mathrm{d}\theta}{\mathrm{d}t},\beta=\dfrac{\mathrm{d}\omega}{\mathrm{d}t}$，可以得出角速度和线速度的关系

$$\vec{v}=\frac{\mathrm{d}\vec{r}}{\mathrm{d}t}=\lim_{\Delta\theta=\omega\Delta t\to 0}\frac{\vec{r}'(\theta)-\vec{r}}{\Delta t}=\lim_{\Delta t\to 0}\frac{\mathbf{R}(\omega\Delta t)-\mathbf{1}_2}{\Delta t}\vec{r}=\omega\begin{bmatrix}0&-1\\1&0\end{bmatrix}\vec{r} \tag{1}$$

$$\vec{a}=\frac{\mathrm{d}\vec{v}}{\mathrm{d}t}=\frac{\mathrm{d}}{\mathrm{d}t}\left(\omega\begin{bmatrix}0&-1\\1&0\end{bmatrix}\vec{r}\right)=\frac{\mathrm{d}\omega}{\mathrm{d}t}\begin{bmatrix}0&-1\\1&0\end{bmatrix}\vec{r}=\beta\begin{bmatrix}0&-1\\1&0\end{bmatrix}\vec{r} \tag{2}$$

4 三维转动

先分析自由度：自由度从 1 个变成了 3 个，因为 $C_2^2\to C_3^2$。另外，三维中的旋转不满足交换律，即先绕 x 轴转再绕 y 轴转和先绕 y 轴转再绕 x 轴转会得出两个完全不同的结果。

类似于二维转动，我们考虑写出分别沿 x,y,z 轴的转动矩阵

$$\mathbf{R}_x(\theta)=\begin{bmatrix}1&0&0\\0&\cos\theta&-\sin\theta\\0&\sin\theta&\cos\theta\end{bmatrix},\quad \mathbf{R}_y(\theta)=\begin{bmatrix}\cos\theta&0&\sin\theta\\0&1&0\\-\sin\theta&0&\cos\theta\end{bmatrix},\quad \mathbf{R}_z(\theta)=\begin{bmatrix}\cos\theta&-\sin\theta&0\\\sin\theta&\cos\theta&0\\0&0&1\end{bmatrix}$$

由于矩阵乘法没有交换律，可以证明在上述例子中，即一般情况下

$$\mathbf{R}_x(\theta_1)\mathbf{R}_y(\theta_2)\neq\mathbf{R}_y(\theta_2)\mathbf{R}_x(\theta_1)$$

对于更普遍的任意轴转动，用单位向量 $\hat{n}=\begin{bmatrix}n_x,n_y,n_z\end{bmatrix}^T$ 表示转轴，θ 表示转角，可以采用一些变换操作。更具体的，可以先将 x 轴变换至 $\vec{n}$ 方向，y 和 z 分别与 $\vec{n}$ 垂直，进行 $\mathbf{R}_x(\theta)$ 变换，并再做前面的逆变换。数学上可以有正交基底

$$\{\hat{e}_1=\hat{n},\hat{u},\hat{v}\}$$

而前面描述的初变换和末变换分别为

$$\mathbf{P}^{-1}=\mathbf{P}^T=\begin{bmatrix}\hat{e}_1&\hat{u}&\hat{v}\end{bmatrix}^T\quad \mathbf{P}=\begin{bmatrix}\hat{e}_1&\hat{u}&\hat{v}\end{bmatrix}$$

经过组合可得

$$\begin{aligned}\mathbf{R}(\hat{n},\theta)&=\mathbf{P}\mathbf{R}_x(\theta)\mathbf{P}^T\\&=\hat{e}_1\hat{e}_1^T+\cos\theta\left(\hat{u}\hat{u}^T+\hat{v}\hat{v}^T\right)+\sin\theta\left(\hat{v}\hat{u}^T-\hat{u}\hat{v}^T\right)\\&=\cos\theta\mathbf{1}_3+(1-\cos\theta)\hat{n}\hat{n}^T+\sin\theta[\hat{n}\times]\\&=\cos\theta\mathbf{1}_3+(1-\cos\theta)[\hat{n}\times]^2+\sin\theta[\hat{n}\times]\end{aligned}$$

其中，可以证明 $\hat{u}\hat{u}^T+\hat{v}\hat{v}^T=\mathbf{1}_3-\hat{n}\hat{n}^T$，$\hat{n}\hat{n}^T=[\hat{n}\times]^2$ 和

$$\hat{v}\hat{u}^T-\hat{u}\hat{v}^T=[\hat{n}\times]=\begin{bmatrix}0&-n_z&n_y\\n_z&0&-n_x\\-n_y&n_x&0\end{bmatrix}$$

这就是旋转矩阵的 Rodrigues 形式。

重复二维中计算角速度和线速度的过程可得

$$\begin{aligned}\vec{v}&=\frac{\mathrm{d}\vec{r}}{\mathrm{d}t}=\lim_{\Delta\theta=\omega\Delta t\to 0}\frac{\vec{r}'(\theta)-\vec{r}}{\Delta t}=\omega\lim_{\Delta\theta\to 0}\frac{\mathbf{R}(\hat{n},\Delta\theta)-\mathbf{1}_3}{\Delta\theta}\vec{r}\\&=\omega\lim_{\Delta\theta\to 0}\frac{(\cos\Delta\theta-1)\mathbf{1}_3+(1-\cos\Delta\theta)[\hat{n}\times]^2+\sin\Delta\theta[\hat{n}\times]}{\Delta\theta}\\&=\omega\frac{\mathrm{d}}{\mathrm{d}\theta}\bigg((\cos\theta-1)\mathbf{1}_3+(1-\cos\theta)[\hat{n}\times]^2+\sin\theta[\hat{n}\times]\bigg)\vec{r}\\&=\omega\bigg(\sin\theta\mathbf{1}_3+\sin\theta[\hat{n}\times]^2+\cos\theta[\hat{n}\times]\bigg)_{\theta=0}\vec{r}=\omega[\hat{n}\times]\vec{r}=\vec{\omega}\times\vec{r}\\\vec{a}&=\frac{\mathrm{d}\vec{v}}{\mathrm{d}t}=\frac{\mathrm{d}}{\mathrm{d}t}(\omega[\hat{n}\times]\vec{r})=\frac{\mathrm{d}\omega}{\mathrm{d}t}[\hat{n}\times]\vec{r}=\beta[\hat{n}\times]\vec{r}=\vec{\beta}\times\vec{r}\end{aligned}$$

其中 $\vec{\omega}=\omega\hat{n}$，$\vec{\beta}=\beta\hat{n}$，分别称为角速度（矢量）和角加速度（矢量）。可以简单的证明角速度矢量具有可加性：

$$\frac{\mathrm{d}}{\mathrm{d}t}[\mathbf{R}_1(\hat{n}_1,\theta_1)\mathbf{R}_2(\hat{n}_2,\theta_2)]=\omega_1[\hat{n}_1\times]\mathbf{R}_1(\hat{n}_1,0)+\omega_2\mathbf{R}_2(\hat{n}_2,0)[\hat{n}_2\times]=[(\vec{\omega}_1+\vec{\omega}_2)\times]$$

5 角动量、力矩、转动惯量（张量）

定理 5.1. *诺特定理（Noether's Theorem）：每一个物理系统的连续对称性，对应着一个守恒量。*

动量守恒来源于空间的平移对称性，能量守恒来源于时间的平移对称性，角动量守恒则来源于空间的旋转对称性。这里我们不讨论如何通过变分由这些对称性和拉格朗日量推导守恒量的形式，而是直接给出角动量的形式。

对于质点系统：$\vec{L}_i=\vec{r}_i\times\vec{p}_i$，总角动量有形式 $\vec{L}=\sum_i\vec{L}_i$。下面将开始讨论刚体 / 刚性的系统，注意在下面的讨论中两两质点 / 质量元的距离都在运动过程中保持不变。

对于刚性的质点系统在旋转时 $\vec{p}=m\vec{v}=m(\vec{\omega}\times\vec{r})$，总角动量有变形

$$\begin{aligned}\vec{L}&=\sum_i m_i\vec{r}_i\times(\vec{\omega}\times\vec{r}_i)\\&=\sum_i[m_i(\vec{r}_i\cdot\vec{r}_i)\vec{\omega}-m_i\vec{r}_i(\vec{r}_i\cdot\vec{\omega})]\\&=\sum_i m_i\left(r_i^2\mathbf{1}_3-\vec{r}_i\vec{r}_i^T\right)\vec{\omega},\end{aligned}$$

因此，我们定义矩阵 $\mathbf{I}=\sum_i m_i\left(r_i^2\mathbf{1}_3-\vec{r}_i\vec{r}_i^T\right)$ 为转动惯量矩阵（张量），满足 $\vec{L}=\mathbf{I}\vec{\omega}$。

这个系统的能量也可以进行变形：

$$\begin{aligned}E&=\sum_i\frac{1}{2}mv_i^2=\sum_i\frac{1}{2}m_i\vec{v}_i\cdot\vec{v}_i\\&=\sum_i\frac{1}{2}m_i(\vec{\omega}\times\vec{r}_i)^2\\&=\sum_i\frac{1}{2}m_i\vec{r}_i\cdot[(\vec{\omega}\times\vec{r}_i)\times\vec{\omega}]\\&=\sum_i\frac{1}{2}m_i[\omega^2r_i^2-(\vec{\omega}\cdot\vec{r}_i)^2]\\&=\frac{1}{2}\vec{\omega}^T\mathbf{I}\vec{\omega}.\end{aligned}$$

对于连续系统有类似的 $\mathrm{d}\vec{L}=\vec{r}\times\mathrm{d}\vec{p}$，$\vec{L}=\int_V\mathrm{d}\vec{L}$，$\mathbf{I}=\int_V\mathrm{d}m\left(r^2\mathbf{1}_3-\vec{r}\vec{r}^T\right)$，$\vec{L}=\mathbf{I}\vec{\omega}$，$E=\frac{1}{2}\vec{\omega}^T\mathbf{I}\vec{\omega}$。（后续将只讨论离散情况，使用代换 $m_i\to\mathrm{d}m,\vec{r}_i\to\vec{r},\sum_i\to\int_V$）

下面我们将考虑转动惯量张量的一些性质：对于质心系 O'（原点在系统质心，有约束 $\sum_i m_i\vec{r}_i=0$），可以将上面 $\vec{r}=\vec{r}'+\vec{R}$，可以发现 $\mathbf{I}=\mathbf{I}_0+\left(R^2\sum_i m_i\right)\mathbf{1}_3$，即角动量有柯尼希定理。

$$\mathbf{I}=\sum_i m_i\left(r_i^2\mathbf{1}_3-\vec{r}_i\vec{r}_i^T\right)=\begin{bmatrix}\sum_i m_i\left(y_i^2+z_i^2\right) & -\sum_i m_i x_i y_i & -\sum_i m_i z_i x_i\\ -\sum_i m_i x_i y_i & \sum_i m_i\left(z_i^2+x_i^2\right) & -\sum_i m_i y_i z_i\\ -\sum_i m_i z_i x_i & -\sum_i m_i y_i z_i & \sum_i m_i\left(x_i^2+y_i^2\right)\end{bmatrix}$$

当系统对称性较高时，非对角元素消失，这种情况下对于绕 x 轴的转动即可用 $I_x=\sum_i m_i\left(y_i^2+z_i^2\right)$ 求解。

可以证明在有外力矩 $\vec{M}$ 的情况下满足 $\vec{M}=\frac{\mathrm{d}}{\mathrm{d}t}\vec{L}$。

6 转动参考系的矢量变换

对于两个参考系，$S-XYZ$ 和 $S'-X'Y'Z'$，其中 S' 绕 S 系原点以角速度 ω 转动。对于一个矢量

$$\vec{A}=A_x\hat{e}_x+A_y\hat{e}_y+A_z\hat{e}_z=A'_x\hat{e}_{x'}+A'_y\hat{e}_{y'}+A'_z\hat{e}_{z'}$$

我们知道单位矢量的导数可以用

$$\frac{\mathrm{d}}{\mathrm{d}t}\hat{e}_{x'}=\omega\times\hat{e}_{y'},\quad\frac{\mathrm{d}}{\mathrm{d}t}\hat{e}_{y'}=\omega\times\hat{e}_{z'},\frac{\mathrm{d}}{\mathrm{d}t}\hat{e}_{z'}=\omega\times\hat{e}_{x'}$$

而 $\vec{A}$ 对时间的导数也可以得出

$$\frac{\mathrm{d}A}{\mathrm{d}t}=\frac{\mathrm{d}A'_x}{\mathrm{d}t}\hat{e}_{x'}+\frac{\mathrm{d}A'_y}{\mathrm{d}t}\hat{e}_{y'}+\frac{\mathrm{d}A'_z}{\mathrm{d}t}\hat{e}_{z'}+\vec{\omega}\times\vec{A}=\frac{\mathrm{d}'\vec{A}}{\mathrm{d}t}+\vec{\omega}\times\vec{A}$$

7 欧拉角与欧拉方程

在实际解决问题的过程中，我们会发现刚体的转动会导致转动惯量张量的各个分量发生改变，导致较为复杂的计算。为了简化计算，将在空间中惯性坐标系写作 XYZ，固连于刚体的坐标系写作 $x_1x_2x_3$ 以便于区分。

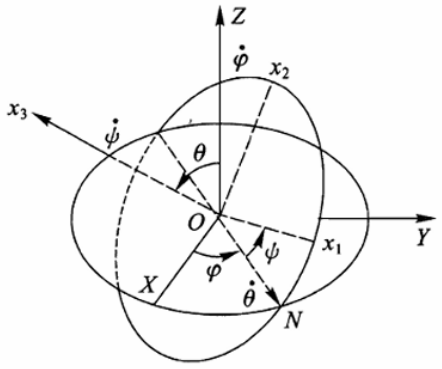

如图，ON 为 x_1x_2 与 XY 的交线，φ 为 ON 与 X 的夹角，ψ 为 ON 与 x_1 的夹角，θ 为 Z 与 z_3 的夹角，$x_1x_2x_3$ 与 XYZ 的关系可以完全由 (φ, ψ, θ) 描述。角速度则可以其中的几何关系描述：

$$\omega_1 = \dot{\varphi}\sin\theta\sin\psi + \dot{\theta}\cos\psi$$
$$\omega_2 = \dot{\varphi}\sin\theta\cos\psi - \dot{\theta}\sin\psi$$
$$\omega_3 = \dot{\varphi}\cos\theta + \dot{\psi}$$

这套描述方式称为欧拉角。欧拉角在机器人方向有着许多应用。

8 例题：长方体自由转动问题

一个质量均匀分布为 m 的长方体，其边长为 a, b, c，考虑其在初始时刻绕其空间对角线以角速度 $\vec{\omega}_0 = \omega_0\hat{n}$ 的自由转动（无外力和外力矩作用）。

Hint: 有角动量守恒

$$\vec{L} = \mathbf{I}(t)\omega(t) = \mathbf{I}\vec{\omega}_0$$

和能量守恒

$$E = \frac{1}{2}\vec{\omega}(t)^T\mathbf{I}(t)\vec{\omega}(t) = \frac{1}{2}\vec{\omega}_0^T\mathbf{I}_0\vec{\omega}_0$$

可以参考 / 使用前面各节的方法和结论。

8.1 解 1

我们可以让 $\mathbf{I}$ 先以 φ, ψ, θ 为参数，直接确定其姿态并积分得到长方体对地面的转动惯量张量。最后在地面系中联立上面两个（算分量的话实际上是四个）式子并解出角速度，积分得其姿态（实际上并不推荐这种方法）。

8.2 解 2

对于解 1 的改进，我们发现正方体还是存在很强的对称性，可以辨认出其主轴为通过相对两面正中心的直线，可以先利用第五节中介绍的转动惯量张量计算方法计算出主轴张量为

$$I_{11} = \frac{1}{12}m(b^2 + c^2)$$
$$I_{22} = \frac{1}{12}m(c^2 + a^2)$$
$$I_{33} = \frac{1}{12}m(a^2 + b^2)$$

其中 x_1, x_2, x_3 分别对应平行于 a, b, c 的方向。然后用第三节中变换基底的方法计算出变换矩阵为

$$\mathbf{P} = \mathbf{R}\left(\hat{e}_3, \psi\right)\mathbf{R}\left(\hat{e}_{ON}, \theta\right)\mathbf{R}\left(\hat{e}_{OZ}, \varphi\right)$$

并计算出相对于地面的惯量张量为

$$\mathbf{I} = \mathbf{P}\mathbf{I}_d\mathbf{P}^T$$

其中 $\mathbf{I}_d = \begin{bmatrix} I_{11} & & \\ & I_{22} & \\ & & I_{33} \end{bmatrix}$，后续计算同解 1。

8.3 解 3

发现角速度也有变换

$$\vec{\omega}_{123} = \mathbf{P}^T\vec{\omega}_{xyz}$$

这里用 $\vec{\omega}_{xyz}$ 和 $\vec{\omega}_{123}$ 区分 XYZ 和 $x_1x_2x_3$ 系下的各个分量，实际上 $\vec{\omega}_{xyz}$ 和 $\vec{\omega}_{123}$ 表示了同一个物理量，实际相等，只是因为基底不同导致分量形式不同。经过这样基底的变换，有

$$\begin{aligned} 2E &= \vec{\omega}_{xyz}^T\mathbf{I}\vec{\omega}_{xyz} = \vec{\omega}_{xyz}^T\mathbf{P}\mathbf{P}^T\mathbf{I}\mathbf{P}\mathbf{P}^T\vec{\omega}_{xyz} = \vec{\omega}_{123}^T\mathbf{I}_d\vec{\omega}_{123} \\ &= I_{11}\omega_1^2 + I_{22}\omega_2^2 + I_{33}\omega_3^2 \end{aligned}$$

$$\begin{aligned} \vec{L} &= \mathbf{I}\vec{\omega}_{xyz} = \mathbf{P}\mathbf{P}^T\mathbf{I}\mathbf{P}\mathbf{P}^T\vec{\omega}_{xyz} = \mathbf{P}\mathbf{I}_d\vec{\omega}_{123} \\ \Rightarrow L^2 &= \vec{L}\cdot\vec{L} = \vec{\omega}_{123}^T\mathbf{I}_d^T\mathbf{P}^T\mathbf{P}\mathbf{I}_d\vec{\omega}_{123} = \vec{\omega}_{123}^T\mathbf{I}_d^T\mathbf{I}_d\vec{\omega}_{123} \\ &= I_{11}^2\omega_1^2 + I_{22}^2\omega_2^2 + I_{33}^2\omega_3^2 \end{aligned}$$

可以解得 ω_1, ω_3 和 ω_2 的关系：

$$\begin{aligned} \omega_1^2 &= \frac{(2E - I_{22}\omega_2^2)I_{33} - (L^2 - I_{22}^2\omega_2^2)}{I_{11}(I_{33} - I_{11})} \\ \omega_3^2 &= \frac{(2E - I_{22}\omega_2^2)I_{11} - (L^2 - I_{22}^2\omega_2^2)}{I_{11}(I_{11} - I_{33})} \end{aligned}$$

并将第六节中所提到的公式中 $\vec{A}$ 换成 $\vec{L}$：

$$\frac{\mathrm{d}\vec{L}}{\mathrm{d}t} = \mathbf{I}_d\frac{\mathrm{d}\vec{\omega}_{123}}{\mathrm{d}t} + \vec{\omega}_{123}\times\mathbf{I}_d\vec{\omega}_{123} = 0$$

其中 x_2 的分量为

$$I_{22}\frac{\mathrm{d}\omega_2}{\mathrm{d}t} + (I_{11} - I_{33})\omega_3\omega_1 = 0$$

最终得到一个 ω_2 对 t 的微分式

$$\begin{aligned} \frac{\mathrm{d}\omega_2}{\mathrm{d}t} &= -\frac{I_{11} - I_{33}}{I_{22}}\omega_1\omega_3 \\ &= \frac{1}{I_{22}\sqrt{I_{11}I_{33}}}\sqrt{-[(2E - I_{22}\omega_2^2)I_{33} - (L^2 - I_{22}^2\omega_2^2)][(2E - I_{22}\omega_2^2)I_{11} - (L^2 - I_{22}^2\omega_2^2)]} \end{aligned}$$

后续可通过椭圆积分或数值求解（下面是用 python 跑出来的一个 demo，代码参见附录 A，注意代码不是用的这个解法）。

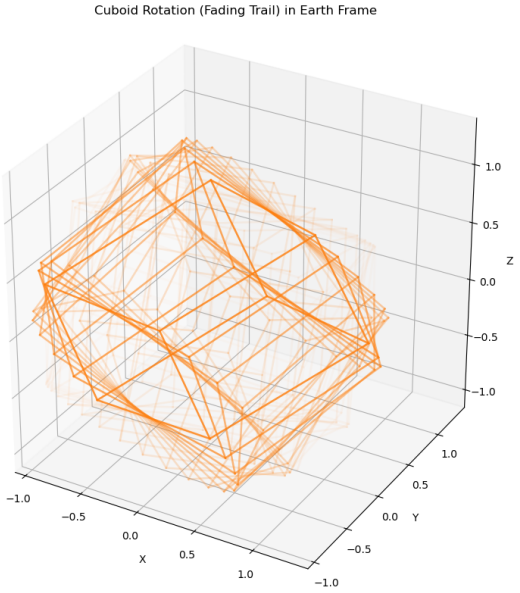

参考文献

[1] L. D. Landau and E. M. Lifshitz. *Mechanics*. 3rd. Vol. 1. Course of Theoretical Physics. Translated from the Russian by J. B. Sykes and J. S. Bell. Pergamon Press, 1976.

[2] Wikipedia contributors. *Rotation matrix — Wikipedia, The Free Encyclopedia*. Accessed: 2025-06-26. 2024. URL: https://en.wikipedia.org/wiki/Rotation_matrix.

A 附录

```python
import numpy as np
import matplotlib.pyplot as plt

a, b, c = 2.0, 1.5, 1.0
m = 1.0

I1 = (m / 12) * (b**2 + c**2)
I2 = (m / 12) * (c**2 + a**2)
I3 = (m / 12) * (a**2 + b**2)
I = np.array([I1, I2, I3])

omega0 = np.array([1, 1, 1]) / np.sqrt(3)

def euler_eqs(t, omega):
    domega = np.zeros(3)
```

```
    domega[0] = ((I2 - I3) / I1) * omega[1] * omega[2]
    domega[1] = ((I3 - I1) / I2) * omega[2] * omega[0]
    domega[2] = ((I1 - I2) / I3) * omega[0] * omega[1]
    return domega

from scipy.integrate import solve_ivp

t_span = (0, 5)
t_eval = np.linspace(*t_span, 20)  # fewer frames
sol = solve_ivp(euler_eqs, t_span, omega0, t_eval=t_eval)

def skew(omega):
    return np.array([[0, -omega[2], omega[1]],
                     [omega[2], 0, -omega[0]],
                     [-omega[1], omega[0], 0]])

def dRdt(t, R_flat):
    omega_t = np.array([np.interp(t, sol.t, sol.y[i]) for i in range(3)])
    R = R_flat.reshape(3,3)
    return (R @ skew(omega_t)).flatten()

R0 = np.eye(3).flatten()
sol_R = solve_ivp(dRdt, t_span, R0, t_eval=t_eval)

x, y, z = a/2, b/2, c/2
vertices_body = np.array([
    [ x,  y,  z],
    [ x,  y, -z],
    [ x, -y,  z],
    [ x, -y, -z],
    [-x,  y,  z],
    [-x,  y, -z],
    [-x, -y,  z],
    [-x, -y, -z],
])
edges = [
    (0,1),(0,2),(0,4),
    (1,3),(1,5),
```

```
    (2,3),(2,6),
    (3,7),
    (4,5),(4,6),
    (5,7),
    (6,7)
]

fig = plt.figure(figsize=(8,8))
ax = fig.add_subplot(111, projection='3d')

lim = max(a, b, c)
ax.set_xlim(-lim, lim)
ax.set_ylim(-lim, lim)
ax.set_zlim(-lim, lim)
ax.set_box_aspect([1,1,1])
ax.set_title("Cuboid Rotation (Fading Trail) in Earth Frame")
ax.set_xlabel("X")
ax.set_ylabel("Y")
ax.set_zlabel("Z")

for i, t in enumerate(t_eval):
    fade_factor = np.exp((i - len(t_eval)) / 5.0)
    alpha = min(1.0, fade_factor)
    R = sol_R.y[:, i].reshape(3,3)
    verts = (R @ vertices_body.T).T
    for e in edges:
        xline = [verts[e[0], 0], verts[e[1], 0]]
        yline = [verts[e[0], 1], verts[e[1], 1]]
        zline = [verts[e[0], 2], verts[e[1], 2]]
        ax.plot(xline, yline, zline, color='C1', alpha=alpha, linewidth=1.8)

plt.tight_layout()
plt.show()
```

电磁漫谈—从毕奥萨伐尔定律到相对论

Guozhi Ji (姬国智)

High School Affiliated to Renmin University of China, Beijing, China

摘　　要

本篇文章从高中课内电磁学内容讲起，在回顾对于电磁的认识历程基础上提出了在相对论尺度下的协变量和非协变量的概念。接着从最简单的平行电流元模型出发，借助库仑定律和尺缩效应推导出了该情况下的磁力表达式并利用小量近似导出了毕奥萨伐尔定律。最后给出了三维形式洛伦兹力的洛伦兹变换，更加全面地阐释了电与磁之间的内在联系。

在高中的时候，我们学电磁学时常常把电和磁拆成不同的部分学。我们对于电磁场的初步认识来自于库仑定律和毕奥萨伐尔定律，即静电场和静磁场。等到我们学的更多时，我们可以认识到电磁感应，并能感性理解电磁波。如果我们再进一步，或许会知道麦克斯韦方程组，了解了电磁互作的基本方式。但是，电与磁的本质究竟是什么？这引人深思。

首先，我问一个问题：库仑定律和毕奥萨伐尔定律

$$\vec{E} = \frac{q\vec{r}}{4\pi\epsilon_0 r^3}, \tag{1}$$

$$\vec{B} = \frac{\mu_0}{4\pi}\int \frac{Id\vec{l}\times\vec{r}}{r^3} \tag{2}$$

和洛伦兹力的公式

$$F = q\vec{v}\times\vec{B} + q\vec{E} \tag{3}$$

这三个公式哪些是普遍适用的公式？大部分人可能认为都普遍适用，然而，事实并非如此。(1) 和 (2) 本质上都是实验定律，并非符合所有情况，而 (3) 则是普遍满足的，通过其洛伦兹协变的性质，可以推导出普遍的电场和磁场表达式，我将会在后续给出论证。但是，这里提到的所有的情况又是什么呢？实际上，正是大家都了解过的时空理论——相对论。

这个时候有人就要问了，相对论不是只有高速情况下才应该考虑吗？这个观点是对的，低速情况下两个定律与用相对论方法处理后的结果是一样的。但是我们忽略了一个重要的事情：磁场本身就来自于电流的相对论效应，如果忽略相对论效应，磁力也不复存在。在这一部分，我将使用两平行电流元作为特例，半定量地分析磁场的产生，并进行讨论。

由于我们考虑的仅仅是电流的相对论效应，因此满足单位长度总电荷为 0。于是我们能画出以下的物理图像：

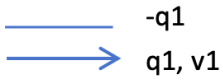

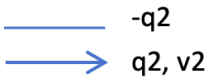

这是两个平行电流元，大小等于 qv，对于每个电流元可以分成“运动元”和“不动元”，我们可以考虑另外一个电流元对其相对论效应并进行累加。我们不妨计算电流元 1 对电流元 2 的力。对于所有子电流元，根据相对论尺缩效应，有

$$l' = l\sqrt{1-\frac{u^2}{c^2}}. \tag{4}$$

又由于电荷守恒，因此电荷线密度有

$$\lambda' = \frac{\lambda}{\sqrt{1-\frac{u^2}{c^2}}}. \tag{5}$$

考虑电流元长度不变，因此有

$$q' = \frac{q}{\sqrt{1-\frac{u^2}{c^2}}}. \tag{6}$$

这个时候我们运用库仑定律表示出其总受力，有

$$F = \frac{1}{4\pi\epsilon_0 r^2}(q_2\frac{-q_1}{\sqrt{1-\frac{v_2^2}{c^2}}} + q_2\frac{q_1}{\sqrt{1-\frac{(v_1-v_2)^2}{c^2}}} + (-q_2)(-q_1) + (-q_2)\frac{q_1}{\sqrt{1-\frac{v_1^2}{c^2}}}). \tag{7}$$

这个时候读者也许会疑惑，这表达式与磁力相差甚远啊。别急，我们还需要再做一步小量近似。运用近似公式，

$$(1+x)^n \approx 1+nx\ (when\ x \ll 1) \tag{8}$$

得到

$$F = \frac{q_1 q_2}{4\pi\epsilon_0 r^2 c^2}(-c^2 - \frac{v_2^2}{2} + c^2 + \frac{(v_1-v_2)^2}{2} + c^2 - c^2 - \frac{v_1^2}{2}). \tag{9}$$

化简得

$$F = \frac{q_1 v_1 q_2 v_2}{4\pi\epsilon_0 r^2 c^2}. \tag{10}$$

这与 (2) 式很像了，只要我们注意到恒等式

$$c^2 = \frac{1}{\epsilon_0\mu_0}, \tag{11}$$

就推导出了特殊情况下的 (2) 式了。实际上，(11) 式的特例证明正可以用 (10) 和 (2) 联合得到。这种方式下，我们能感性地理解磁力的本质。

实际上，我们还可以把事情变得更普遍一些。运用相对论的基本假设和洛伦兹力的普遍性，

我们可以对其进行相对论变换，得到以下：

$$\begin{cases} E'_x = E_x, \\ E'_y = \gamma(E_y - vB_z), \\ E'_z = \gamma(E_z + vB_y), \\ B'_x = B_x, \\ B'_y = \gamma(B_y + \frac{v^2}{c^2}E_z), \\ B'_z = \gamma(B_z - \frac{v^2}{c^2}E_y), \\ \gamma = (1 - \frac{v^2}{c^2})^{-\frac{1}{2}} \end{cases} \tag{12}$$

即为点电荷的相对论电磁场变换，我们利用这些结论，可以更普遍地推导电磁场中的现象。这个时候，我们会发现电磁现象与相对论息息相关，电磁这种协调下的统一正诠释了宇宙的美丽。

最后，我想用牛顿的一句话结束这篇探讨较为浅显的文章，“我不知道世人怎样看我，但我自己以为我不过像一个在海边玩耍的孩子，不时为发现比寻常更为美丽的一块卵石或一片贝壳而沾沾自喜，至于展现在我面前的浩瀚的真理海洋，却全然没有发现。”我们在探索物理学的过程中，不应仅仅局限于唯象的理论，更应该不断深入，去了解事物运作的内在关系。这才是物理学真正震撼人心之处。

漫谈 2024 诺贝尔物理学奖

Guozhi Ji (姬国智)

High School Affiliated to Renmin University of China, Beijing, China

摘　　要

本文转载微信公众号 RDFZPhysics 发布的推文《漫谈 2024 诺贝尔物理学奖》。

本文属于科普向短文，浅显易懂，因此对诺奖具体原理和机制以及例子中的公式描述较少，感兴趣的可以搜索文献，本文旨在通过探讨 AI 与物理的关系让大家更深入了解统计物理这门学科的精髓。

如果大家关注物理的话，看到今年的诺贝尔物理学奖是这个时（如图）

第一眼：machine？这是什么机械吗？

第二眼：自主学习？神经网络？

第三眼：不对，这不 AI 吗！

不知道大家有没有这样的疑惑：一个看似信息学的事情，为什么会得诺贝尔物理学奖？此刻，粒子和凝聚态的都默默落泪了。。。

书归正传，其实这和统计力学有关，像是一些基本公式比如 $S = K \ln W$（**玻尔兹曼公式**）、$\Delta G = T\Delta S + \Delta H$（**吉布斯自由能公式**）大家都应该是耳熟能详了。但是这些确实看似与这种神经网络图（如图）相差甚远。

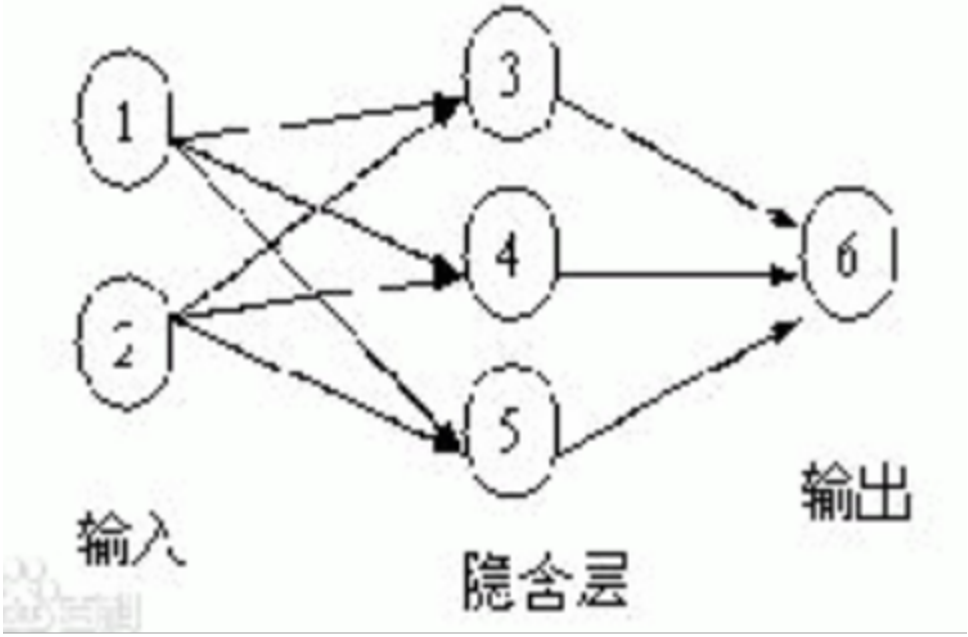

先看看统计物理为什么脱颖而出吧。

首先，不如先做一个**思维实验**：一个木块从粗糙斜面上滑下，到达地面上某一点停止。牛顿老先生告诉我们，根据**牛顿可逆性**原理，它势必能从下面划上去。乍一看，诶，是不是发现新物理了？木块吸热，不就可以上去了吗？But，谁说牛顿老先生就一定对了？这正是**第二类永动机**的原理，而一物降一物，**热力学第二定律**刚好降伏这第二类永动机。好，我们现在从一个简单的思维实验和前人的研究中证明了**牛顿可逆性原理在是"错误"的**。

其次，再看**牛顿决定性原理**，看似没问题，实则没啥用。出了比较简单的模型，真实物理世界的情况总是存在**混沌**的现象，所以面对大量质点，只能通过耗能极大的分子模拟实现，而且还不准。

现在，我们可能差不多认识到了经典力学的无力，也知道了物理不止一堆太空中的小球来回绕圈那回事。我们也许能稍微理解了，但是还不够，毕竟 AI 也不是通过物理实现的，完完全全是计算机模拟啊。

关于为什么统计力学和 AI 有关系，首先咱们要理解一个重要的概念：**相空间**。什么是相空间呢？通俗定义，就是一个系统所有物理量的维度组成的空间。举个简单的例子，小编在高一年级，会一点物理，有两个眼睛等这些特征就能描绘出一个现实版的"相空间"。（为便于理解，物理研究中不是这样子的）

AI 为什么能自我学习？大部分人认为 AI 不会思考，实际上确实我们认为它不能像人类一样思考。本质上，AI 是在模仿，它模仿什么都大同小异，都是通过图二实现的，而图二最重要的**隐含层**就是通过统计力学实现的。

拿玻尔兹曼公式来举例，它不同于列亿堆哈密顿方程（经典力学的计算方法），用 Ω 来表示可能的微观态数，然后就非常简洁地表达出来了。这体现了统计力学中"降维"的一种方法。而 AI 也是一样的样子，中间隐含层就是构建相空间的一个过程，输出则是进行"降维"的一种操作，而通过两个操作，输出变会与原先产生偏差，这时候便通过迭代重新优化"降维"算法，这也就是**训练 AI** 的原理。

有人会说，道理我都懂，只能说是有物理思想，但是它凭啥是物理？先看实例，华为的盘古模型，没有运用任何物理引擎，只是通过这种算法，就能高精度预测天气。这体现了把一些物理相**数据化**，并对数据进行统计力学分析，大大提高了效率。

大家注意到了我提到了**数据**这个词。粗略地讲，本质上，世界只存在三种组成部分：**物质**、**能量**、还有**信息**。而数据化就是把一些物质和能量变成信息。自然，对于物理学，传统只是研究物质和能量，而如今的物理则用物质和能量的方式更加简洁美妙的方式研究了信息。这次物理不一定是反常，有可能只是对这方面的研究开了一个好头。

其实，物理通俗解释就是事物的道理。而当我们一步又一步踏向未知的世界时，或许可能某一天就会出现最简洁最美妙物质能量信息三位一体的大一统理论。让我们拭目以待吧。